P · A · R · T · 4

OPTICAL AND PHYSICAL PROPERTIES OF MATERIALS

CHAPTER 33
PROPERTIES OF CRYSTALS AND GLASSES

William J. Tropf, Michael E. Thomas, and Terry J. Harris
Applied Physics Laboratory
Johns Hopkins University
Laurel, Maryland

33.1 GLOSSARY

A_i, B, C, D, E, G	constants
a, b, c	crystal axes
B	inverse dielectric constant
B	bulk modulus
C	heat capacity
c	speed of light
$\mathbf{c}$	elastic stiffness
$\mathbf{D}$	electric displacement
d	piezoelectric coefficient
$d_{ij}^{(2)}$	nonlinear optical coefficient
E	Young's modulus
E	energy
$\mathbf{E}$	electric field
$\mathbf{e}$	strain
G	shear modulus
g	degeneracy
Hi	Hilbert transform
h	heat flow
k	extinction coefficient
k_B	Boltzmann constant
ℓ	phonon mean free path
MW	molecular weight
m	integer
$N(\ )$	occupation density

n	refractive index
$\tilde{n}$	complex refractive index $= n + ik$
$\mathbf{P}$	electric polarization
$P_{x,y}$	relative partial dispersion
$\mathbf{p}$	elasto-optic tensor
p	elasto-optic compliance
p	pyroelectric constant
$\mathbf{q}$	piezo-optic tensor
r	electro-optic coefficient
r	amplitude reflection coefficient
r_{ij}	electro-optic coefficient
$S(\ )$	line strength
$\mathbf{s}$	elastic compliance
T	temperature
t	amplitude transmission coefficient
U	enthalpy
u	atomic mass unit
V	volume
v	velocity of sound
x	displacement
x	variable of integration
Z	formulas per unit
α	linear expansion coefficient
α	intensity absorption
α	thermal expansion
α_m	macroscopic polarizability
α, β, γ	crystal angles
β	power absorption coefficient
$\gamma(\ )$	line width
γ	Gruneisen parameter
ϵ	dielectric constant, permittivity
ϵ	emittance
θ_D	Debye temperature
κ	thermal conductivity
$\Lambda(\ )$	complex function
μ	permeability
ν	wave number $(\omega/2\pi c)$
ρ	density
ρ	intensity reflectivity
σ	stress
τ	intensity transmission
τ	power transmittance

χ	susceptibility
$\chi^{(2)}$	second-order susceptibility
Ω	solid angle
ω	radian frequency

Subscripts

ABS	absorptance
bb	blackbody
c	656.3 nm
d	587.6 nm
EXT	extinctance
F	486.1 nm
i	integers
0	vacuum, $T = 0$, or constant terms
P	constant pressure
p, **s**	polarization component
r	relative
SCA	scatterance
V	constant volume

33.2 INTRODUCTION

Nearly every nonmetallic crystalline and glassy material has a potential use in optics. If a nonmetal is sufficiently dense and homogeneous, it will have good optical properties. Generally, a combination of desirable optical properties, good thermal and mechanical properties, and cost and ease of manufacture dictate the number of readily available materials for any application. In practice, glasses dominate the available optical materials for several important reasons. Glasses are easily made of inexpensive materials, and glass manufacturing technology is mature and well-established. The resultant glass products can have very high optical quality and meet most optical needs.

Crystalline solids are used for a wide variety of specialized applications. Common glasses are composed of low-atomic-weight oxides and therefore will not transmit beyond about 2.5 μm. Some crystalline materials transmit at wavelengths longer (e.g., heavy-metal halides and chalcogenides) or shorter (e.g., fluorides) than common glasses. Crystalline materials may also be used for situations that require the material to have very low scatter, high thermal conductivity, or high hardness and strength, especially at high temperature. Other applications of crystalline optical materials make use of their directional properties, particularly those of noncubic (i.e., uni- or biaxial) crystals. Phasematching (e.g., in wave mixing) and polarization (e.g., in wave plates) are example applications.

This chapter gives the physical, mechanical, thermal, and optical properties of selected crystalline and glassy materials. Crystals are chosen based on availability of property data and usefulness of the material. Unfortunately, for many materials, property data are imprecise, incomplete, or not applicable to optical-quality material. Glasses are more accurately and uniformly characterized, but their optical property data are usually limited to wavelengths below 1.06 μm. Owing to the preponderance of glasses, only a representative

small fraction of available glasses are included below. SI derived units, as commonly applied in material characterization, are used.

Property data are accompanied with brief explanations and useful functional relationships. We have extracted property data from past compilations[1–11] as well as recent literature. Unfortunately, property data are somewhat sparse. For example, index data may be available for only a portion of the transparent region or the temperature dependence of the index may not be known. Strength of many materials is poorly characterized. Thermal conductivity is frequently unavailable and other thermal properties are usually sketchy.

33.3 OPTICAL MATERIALS

Crystalline and amorphous (including glass) materials are differentiated by their structural (crystallographic) order. The distinguishing structural characteristic of amorphous substances is the absence of long-range order; the distinguishing characteristics of crystals are the presence of long-range order. This order, in the form of a periodic structure, can cause directional-dependent (anisotropic) properties that require a more complex description than needed for isotropic, amorphous materials. The periodic features of crystals are used to classify them into six crystal systems,* and further arrange them into 14 (Bravais) space lattices, 32 point groups, and 230 space groups based on the characteristic symmetries found in a crystal.

Glass is by far the most widely used optical material, accounting for more than 90 percent of all optical elements manufactured. Traditionally, glass has been the material of choice for optical systems designers, owing to its high transmittance in the visible-wavelength region, high degree of homogeneity, ease of molding, shaping, and machining, relatively low cost, and the wide variety of index and dispersion characteristics available.

Under the proper conditions, glass can be formed from many different inorganic mixtures. Hundreds of different optical glasses are available commercially. Primary glass-forming compounds include oxides, halides, and chalcogenides with the most common mixtures being the oxides of silicon, boron, and phosphorous used for glasses transmitting in the visible spectrum. By varying the chemical composition of glasses (glasses are not fixed stoichiometrically), the properties of the glass can be varied. Most notably for optical applications, glass compositions are altered to vary the refractive index, dispersion, and thermo-optic coefficient.

Early glass technologists found that adding BaO offered a high-refractive-index glass with lower than normal dispersion, B_2O_3 offered low index and very low dispersion, and by replacing oxides with fluorides, glasses could be obtained with very low index and very low dispersion. Later, others developed very high index glasses with relatively low dispersions by introducing rare-earth elements, especially lanthanum, to glass compositions. Other compounds are added to silica-based glass mixtures to help with chemical stabilization, typically the alkaline earth oxides and in particular Al_2O_3 to improve the resistance of glasses to attack by water.

To extend the transmission range of glasses into the ultraviolet, a number of fluoride and fluorophosphate glasses have been developed. Nonoxide glasses are used for infrared applications requiring transmission beyond the transmission limit of typical optical glasses (2.4 to 2.7 μm for an absorption coefficient of 1 cm^{-1}). These materials include chalcogenides such as As_2S_3 glass and heavy-metal fluorides such as ZrF_4-based glasses.

Crystalline materials include naturally occurring minerals and manufactured crystals. Both single crystals and polycrystalline forms are available for many materials. Polycrystalline optical materials are typically composed of many small (cf., 50 μm) individual

* Cubic (or isometric), hexagonal (including rhombohedral), tetragonal, orthorhombic, monoclinic, and triclinic are the crystallographic systems.

crystals with random orientations and *grain boundaries* between them. These grain boundaries are a form of material defect arising from the lattice mismatch between individual grains. Polycrystalline materials are made by diverse means such as pressing powders (usually with heat applied), sintering, or chemical vapor deposition. Single crystals are typically grown from dissolved or molten material using a variety of techniques. Usually, polycrystalline materials offer greater hardness and strength at the expense of increased scatter.

Uniformity of the refractive index throughout an optical element is a prime consideration in selecting materials for high-performance lenses, elements for coherent optics, laser harmonic generation, and acousto-optical devices. In general, highly pure, single crystals achieve the best uniformity, followed by glasses (especially those selected by the manufacturer for homogeneity), and lastly polycrystalline materials. Similarly, high-quality single crystals have very low scatter, typically one-tenth that of glasses.

Applications requiring optical elements with direction-dependent properties, such as polarizers and index-matching materials for harmonic generation, frequently use single crystals.

Purity of starting materials is a prime factor in determining the quality of the final product. High material quality and uniformity of processing is required to avoid impurity absorption, index nonuniformity, voids, cracks, and bubbles, and excess scatter. Practical manufacturing techniques limit the size of optics of a given material (glasses are typically limited by the moduli, i.e., deformation caused the weight of the piece). Some manufacturing methods, such as hot pressing, also produce significantly lower quality material when size becomes large (especially when the thinnest dimension is significantly increased). Cost of finished optical elements is a function of size, raw material cost, and the difficulty of machining, polishing, and coating the material. Any one of these factors can dominate cost.

General information on the manufacturing methods for glasses and crystalline materials is available in several sources.[9–11] Information on cutting and polishing of optical elements can be found in the literature.[2,12,13]

33.4 PROPERTIES OF MATERIALS

Symmetry Properties

The description of the properties of solids depends on structural symmetry. The structural symmetry crystalline materials dictate the number of appropriate directional-dependent terms that describe a property.[14] *Neumann's principle* states that physical properties of a crystal must possess at least the symmetry of the point group of the crystal. Amorphous (glassy) materials, having no long-range symmetry, are generally considered isotropic,* and require the least number of property terms. Macroscopic material properties are best described in tensor notation; the rank of the property tensors can range from zero (scalar property) up to large rank. Table 1 summarizes common material properties and the rank of the tensor that describes them.

The rank of the property tensor and the symmetry of the material (as determined by the point group for crystals) determines the number of terms needed to describe a property. Table 2 summarizes both the number of terms needed to describe a property and the number of unique terms as a function of property tensor rank and point group. Another important term in the definition of tensor characteristics is the *principal values* of

* Glass properties are dependent on cooling rate. Nonuniform cooling will result in density variation and residual stress which cause anisotropy in all properties. Such nonisotropic behavior is different from that of crystals in that it arises from thermal gradients rather than periodic structure order. Hence, the nature of anisotropy in glasses varies from sample to sample.

TABLE 1 Tensor Characteristics and Definitions of Properties

Tensor rank	Property	Symbol	Units	Relationship
0	Enthalpy (energy)	U	J/mole	—
	Temperature	T	K	—
	Heat capacity	C	J/(mole · K)	$C = \partial U/\partial T$
1	Displacement	x	m	—
	Heat flow	h	W/m^2	—
	Electric field	$\mathbf{E}$	V/m	—
	Electric polarization	$\mathbf{P}$	C/m^2	$\mathbf{P} = \epsilon_0\chi\mathbf{E}$
	Electric displacement	$\mathbf{D}$	C/m^2	$\mathbf{D} = \epsilon_0\mathbf{E} + \mathbf{P}$
	Pyroelectric constant	p	C/(m^2 · K)	$\Delta\mathbf{P} = p\,\Delta T$
2	Stress	σ	Pa	—
	Strain	e	—	—
	Thermal expansion	α	K^{-1}	$e = \alpha T$
	Thermal conductivity	κ	W/(m · K)	$h = -\kappa(\partial T/\partial x)$
	Dielectric constant (relative permittivity)	ϵ_r	—	$\mathbf{D} = \epsilon_0\epsilon_r\mathbf{E}$
	Inverse dielectric tensor	$\mathbf{B}$	—	$\mathbf{B} = \epsilon_r^{-1}$
	Susceptibility	χ	—	$\epsilon_r = \chi + 1$
3	Piezoelectric coefficient (modulus)	d	m/V ≡ C/N	$\mathbf{P} = d \cdot \sigma$
	(converse piezoelectric effect)	d	m/V ≡ C/N	$e = d \cdot \mathbf{E}$
	Electro-optic coefficient (linear)	r	m/V	$\Delta\mathbf{B} = r \cdot \mathbf{E}$
	Second-order susceptibility	$\chi^{(2)}$	m/V	$\mathbf{P} = \epsilon_0\chi^{(2)}\mathbf{E}_1\mathbf{E}_2$
4	Elastic stiffness	$\mathbf{c}$	Pa	$\sigma = c \cdot e; c = 1/\mathbf{s}$
	Elastic compliance	$\mathbf{s}$	Pa^{-1}	$e = \mathbf{s} \cdot \sigma; \mathbf{s} = 1/c$
	Elasto-optic tensor	$\mathbf{p}$	—	$\Delta\mathbf{B} = \mathbf{p} \cdot e; \mathbf{p} = \mathbf{q} \cdot c$
	Piezo-optic tensor	$\mathbf{q}$	Pa^{-1}	$\Delta\mathbf{B} = \mathbf{q} \cdot \sigma; \mathbf{q} = \mathbf{p} \cdot \mathbf{s}$

a second-rank tensor property. The principal values of a property are those values referenced to (measured along) the crystal axes as defined in Table 2. For example, a second-rank tensor of a triclinic crystal has nine nonzero coefficients, and because of symmetry, six independent coefficients. These six coefficients can be separated into (1) three principal values of the quantity (e.g., thermal expansion coefficient, dielectric constant, refractive index, and stress), and (2) the three angles describing the orientation of the crystal axes (α, β, γ).

Properties of materials depend on several fundamental constants that are listed in Table 3.[15] These constants are defined as follows.

Optical Properties: Introduction

Refractive Index. Important optical properties, definitions, formulas, and basic concepts are derived from a classical description of propagation based on the macroscopic Maxwell's equations. The standard wave equation for the electric field $\mathbf{E}$ is obtained from the Faraday, Gauss, and Ampere Laws in Maxwell's form:*

$$\nabla^2\mathbf{E} = (-i\omega\mu\sigma - \omega^2\mu\epsilon)\mathbf{E} \tag{1}$$

* The definition of the dielectric constant and refractive index in this section is based on a harmonic field of the form $\exp(-i\omega t)$. Other definitions lead to different sign conventions (e.g., $\bar{n} = n - ik$) and care must be taken to insure consistency.

TABLE 2 Crystal Classes and Symmetries

Crystal system	Crystal axes	Space lattice		Point group		Space group nos.	Tensor coefficients*			
		Types	Symmetry	Schönflies	Internat'l		Rank 1	Rank 2	Rank 3	Rank 4
Triclinic	$a \neq b \neq c$	P	$\bar{1}$	C_1	1	1	3 (3)	9 (6)	18(18)	36 (21)
(—)	$\alpha \neq \beta \neq \gamma$			C_i	$\bar{1}$	2	0	9 (6)	0	36 (21)
Monoclinic	$a \neq b \neq c$	P,	2/m	C_2	2	3–5	1 (1)	5 (4)	8(8)	20 (13)
(2-fold axis)	$\alpha = \beta = 90°$	I (or C)		C_s	m	6–9	2 (2)	5 (4)	10(10)	20 (13)
	$\gamma \neq 90°$			C_{2h}	2/m	10–15	0	5 (4)	0	20 (13)
Orthorhombic	$a \neq b \neq c$	P, I,	mmm	D_2	222	16–24	0	3 (3)	3(3)	12 (9)
(3 ⊥ 2-fold	$\alpha = \beta = \gamma = 90°$	C, F		C_{2v}	2mm	25–46	1 (1)	3 (3)	5(5)	12 (9)
axes)				D_{2h}	mmm	47–74	0	3 (3)	0	12 (9)
Tetragonal	$a = b \neq c$	P, I	4/mmm	C_4	4	75–80	1 (1)	3 (2)	7(4)	16 (7)
(4-fold axis)	$\alpha = \beta = \gamma = 90°$			S_4	$\bar{4}$	81–82	0	3 (2)	7(4)	16 (7)
				C_{4h}	4/m	83–88	0	3 (2)	0	16 (7)
				D_4	422	89–98	0	3 (2)	2(1)	12 (6)
				C_{4v}	4mm	99–110	1 (1)	3 (2)	5(3)	12 (6)
				D_{2d}	$\bar{4}$2m	111–122	0	3 (2)	3(2)	12 (6)
				D_{4h}	4/mmm	123–142	0	3 (2)	0	12 (6)
Hexagonal	$a = b \neq c$	P, R	$\bar{3}$	C_3	3	143–146	1 (1)	3 (2)	13 (6)	24 (7)
(3-fold axis)	$\alpha = \beta = 90°$			C_{3i}	$\bar{3}$	147–148	0	3 (2)	0	24 (7)
	$\gamma = 120°$		$\bar{3}$m	D_3	32	149–155	0	3 (2)	5 (2)	18 (6)
				C_{3v}	3m	156–161	1 (1)	3 (2)	8 (4)	18 (6)
				D_{3h}	$\bar{3}$m	162–167	0	3 (2)	0	18 (6)
(6-fold axis)		P	6/m	C_6	6	168–173	1 (1)	3 (2)	7 (4)	12 (5)
				C_{3h}	$\bar{6}$	174	0	3 (2)	6 (2)	12 (5)
				C_{6h}	6/m	175–176	0	3 (2)	0	12 (5)
			6/mmm	D_6	622	177–182	0	3 (2)	2 (1)	12 (5)
				C_{6v}	6mm	183–186	1 (1)	3 (2)	5 (3)	12 (5)
				D_{3h}	$\bar{6}$2m	187–190	0	3 (2)	3 (1)	12 (5)
				D_{6h}	6/mmm	191–194	0	3 (2)	0	12 (5)
Cubic	$a = b = c$	P, I, F	m3	T	23	195–199	0	3 (1)	3 (1)	12 (3)
(isometric)	$\alpha = \beta = \gamma = 90°$			T_h	m3	200–206	0	3 (1)	0	12 (3)
(4 3-fold axes)			m3m	O	432	207–224	0	3 (1)	0	12 (3)
				T_d	$\bar{4}$3m	215–220	0	3 (1)	3 (1)	12 (3)
				O_h	m3m	221–230	0	3 (1)	0	12 (3)
Isotropic	Amorphous	—	—	—	—	—	0	3 (1)	0	12 (2)

* Values are the number of nonzero coefficients in (equilibrium) property tensors and the values in parentheses are the numbers of independent coefficients in the tensor. Note that the elasto-optic and piezo-optic tensors have lower symmetry than the rank-4 tensors defined in this table and therefore have more independent coefficients than shown. Second-, third-, and fourth-rank tensors are given in the usual reduced index format (see text).

TABLE 3 Fundamental Physical Constants (1986 CODATA Values)

Constant	Symbol	Value	Unit
Atomic mass unit (amu)	u	$1.660\,540\,2 \cdot 10^{-27}$	kg
Avogadro constant	N_A	$6.022\,136\,7 \cdot 10^{23}$	mole^{-1}
Boltzmann constant	k_B	$1.380\,658 \cdot 10^{-23}$	J/K
Elementary charge	$\mathbf{e}$	$1.602\,177\,33 \cdot 10^{-19}$	C
Permeability of vacuum	μ_0	$4\pi \cdot 10^{-7} = 12.566\,370\,614 \cdot 10^{-7}$	N/A^2 or H/m
Permittivity of vacuum	ϵ_0	$8.854\,187\,187 \cdot 10^{-12}$	F/m
Planck constant	h	$6.626\,075\,5 \cdot 10^{-34}$	J · s
Speed of light	c	299 792 458	m/s

where σ, ϵ, and μ are the frequency-dependent conductivity, permeability, and permittivity, respectively. These quantities are scalars in an isotropic medium. To simplify notation, a generalized permittivity is sometimes defined as:

$$\epsilon_c(\omega) = \epsilon_r(\omega)\left[1 + i\frac{\sigma(\omega)}{\omega\varepsilon(\omega)}\right] \tag{2}$$

where $\epsilon_c(\omega)$ is a generalized relative permittivity of dielectric constant (i.e., with ε_0 removed from $\epsilon = \epsilon_0\epsilon_c$) that includes contributions from free charges [via the conductivity $\sigma(\omega)$] and bound charges [via the relative permittivity, $\epsilon_r(\omega)$]. Assuming a nonmagnetic material ($\mu_r = 1$), and using the preceding generalized dielectric constant, the plane-wave solution to the wave equation is

$$\mathbf{E}(z, \omega) = \mathbf{E}(0)\exp\left[i(\omega z/c)\sqrt{\varepsilon_c(\omega)}\right] \tag{3}$$

In optics, it is frequently convenient to define a *complex refractive index* $\bar{n}$ the square root of the complex dielectric constant (henceforth, the symbol ϵ will be used for the relative complex dielectric constant):

$$\begin{aligned} \bar{n} &= n + ik = \sqrt{\epsilon} = \sqrt{\epsilon' + i\epsilon''} \\ \epsilon' &= n^2 - k^2; \qquad \epsilon'' = 2nk \\ n^2 &= \tfrac{1}{2}\left[\epsilon' + \sqrt{\epsilon'^2 + \epsilon''^2}\right] \\ k^2 &= \tfrac{1}{2}\left[-\epsilon' + \sqrt{\epsilon'^2 + \epsilon''^2}\right] \end{aligned} \tag{4}$$

where n is the (real) *index of refraction* and k is the *index of absorption* (or imaginary part of the complex refractive index). (The index of absorption is also called the absorption constant, index of extinction, or some other combination of these terms.) Using this definition of the complex index of refraction and the solution of the wave equation [Eq. (3)], the optical power density (proportional to $\frac{1}{2}|\mathbf{E}|^2$ from Poynting's vector) is

$$\text{Power density} = \tfrac{1}{2}\sqrt{\mu_0/\epsilon_0}\,|\mathbf{E}(z)|^2 = \tfrac{1}{2}\sqrt{\mu_0/\epsilon_0}\,|\mathbf{E}(0)|^2\exp\left(-2\omega k z/c\right) \tag{5}$$

where the exponential function represents the attenuation of the wave. The meanings of n and k are clear: n contributes to phase effects (time delay or variable velocity) and k contributes to attenuation by absorption. In practice, attenuation is conveniently described by a power absorption coefficient, β_{ABS}, which describes the internal transmittance over a distance z, i.e.,

$$\tau = \frac{|\mathbf{E}(z)|^2}{|\mathbf{E}(z=0)|^2} = e^{-2\omega k z/c} = e^{-\beta_{\text{ABS}} z} \tag{6a}$$

and β_{ABS} (with units of reciprocal length, usually cm^{-1}) is

$$\beta_{ABS} = 2\omega k/c = 4\pi\nu k \tag{6b}$$

Kramers–Krönig and Sum Rule Relationships. The principal of causality—that a material cannot respond until acted upon—when applied to optics, produces important symmetry properties and relationships that are very useful in modeling and analyzing optical properties. As a consequence of these symmetry properties, the real and imaginary parts of the dielectric constant (and of the complex index of refraction) are Hilbert transforms of each other. The Hilbert transform, Hi[$\Lambda(\omega)$], of the complex function $\Lambda(\omega)$ is defined as (the symbol P denotes the principal value of the integral)

$$\text{Hi}\,[\Lambda(\omega)] = \frac{i}{\pi} P \int_{-\infty}^{\infty} \frac{\Lambda(\omega')}{\omega - \omega'} d\omega' \tag{7}$$

and the relationships between the components of the dielectric constant or index of refraction are

$$\begin{aligned} \epsilon' - 1 &= \text{Hi}\,[\epsilon''] \\ \epsilon'' &= \text{Hi}^{-1}\,[\epsilon' - 1] \\ n - 1 &= \text{Hi}\,[k] \\ k &= \text{Hi}^{-1}\,[n - 1] \end{aligned} \tag{8}$$

These are the *Kramers–Krönig relationships* (abbreviated KK). Usually the Hilbert transforms for the refractive index are written in single-sided form:

$$n(\omega) - 1 = \frac{2}{\pi} P \int_0^{\infty} \frac{\omega' k(\omega')}{\omega'^2 - \omega^2} d\omega' \tag{9a}$$

with the inverse transform given by

$$k(\omega) = \frac{2\omega}{\pi} P \int_0^{\infty} \frac{n(\omega') - 1}{\omega^2 - \omega'^2} d\omega' \tag{9b}$$

These are fundamental relationships of any causal system.

A number of useful integral relationships, or *sum rules* result from Fourier transforms and the Kramers–Krönig relationship.[16] For example, the real part of the refractive index satisfies

$$\int_0^{\infty} [n(\omega) - 1]\, d\omega = 0 \tag{10a}$$

and

$$\begin{aligned} n(\omega = 0) - 1 &= \frac{2}{\pi} \int_0^{\infty} \frac{k(\omega')}{\omega'} d\omega' \\ &= \frac{c}{\pi} \int_0^{\infty} \frac{\beta_{ABS}(\omega')}{\omega'^2} d\omega' \end{aligned} \tag{10b}$$

The dielectric constant and the refractive index also have the following symmetry properties:

$$\begin{aligned} \epsilon(\omega) &= \epsilon^*(-\omega) \\ \bar{n}(\omega) &= \bar{n}^*(-\omega) \end{aligned} \tag{10c}$$

Practical models of the dielectric constant or refractive index must satisfy these fundamental symmetry properties and integral relationships.

Optical Properties: Origin and Models

Intrinsic optical properties of a material are determined by three basic physical processes: electronic transitions, lattice vibrations, and free-carrier effects.[5,6,17,18] However, the dominant physical process depends on the material and spectral region of interest. All materials have contributions to the complex index of refraction from electronic transitions. Insulators and semiconductors also require the characterization of the lattice vibrations (or phonons) to fully understand the optical properties. Transparency of semiconductors, particularly those with small band gaps, are additionally influenced by free-carrier effects. The strength of free-carrier influence on transmission and absorption depends on the free-carrier concentration; thus free-carrier effects dominate the optical properties of metals in the visible and infrared.

In the range of transparency of a bulk material, more subtle effects such as multiphonon processes (see later discussion), impurity and defect absorption, and scattering become the important loss mechanisms. Intrinsic atomic (Rayleigh) scattering is a very weak effect, but is important in long-path optical fibers and ultraviolet materials. Extrinsic scattering, caused by density (local composition) variations, defects, or grains in polycrystalline solids, is typically much larger than intrinsic scattering in the visible and infrared spectral regions. Impurity and defect (electronic or vibrational) absorption features can be of great concern depending on the spectral region, incident radiation intensity, or material temperature required by the application.

Figure 1 illustrates the frequency dependence of n and k for an insulating polar crystal.[19] The value of $n(\omega, T)$ is essentially the sum of the contributions of all electronic and lattice vibration resonances, and is dominated by those with fundamental oscillation frequencies above ω. Figure 1*a* indicates regions of validity for the popular Sellmeier model (see discussion under ''Electronic Transitions''). Frequency dependence of the imaginary part of the index of refraction $k(\omega, T)$ requires consideration of not only the dominant physical processes but also higher-order processes, impurities, and defects as illustrated in Fig. 1*b*. The spectral regions of the fundamental resonances are opaque. The infrared edge of transparency is controlled by multiphonon transitions. Transparent regions for insulators are divided in two regions: microwave and visible/infrared.

Lattice Vibrations. Atomic motion, or lattice vibrations, accounts for many material properties, including heat capacity, thermal conductivity, elastic constants, and optical and dielectric properties. Lattice vibrations are quantized; the quantum of lattice vibration is called a *phonon.* In crystals, the number of lattice vibrations is equal to three times the number of atoms in the primitive unit cell (see further discussion); three of these are acoustic vibrations (translational modes in the form of sound waves), the remainder are termed optical vibrations (or modes of phonons). For most practical temperatures, only the acoustic phonons are thermally excited because optical phonons are typically of much higher frequency, hence acoustic modes play a dominant role in thermal and elastic properties. There are three types of optical modes: infrared-active, Raman-active, and optically inactive. Infrared-active modes, typically occurring in the region from 100 to 1000 cm^{-1}, are those that (elastically) absorb light (photon converted to phonon) through an interaction between the electric field and the light and the dipole moment of the crystal. Raman modes* (caused by phonons that modulate the polarizability of the crystal to induce a dipole moment) weakly absorb light through an inelastic mechanism (photon converted to phonon and scattered photon) and are best observed with intense (e.g.,

* Brillouin scattering is a term applied to inelastic scattering of photons by acoustic phonons.

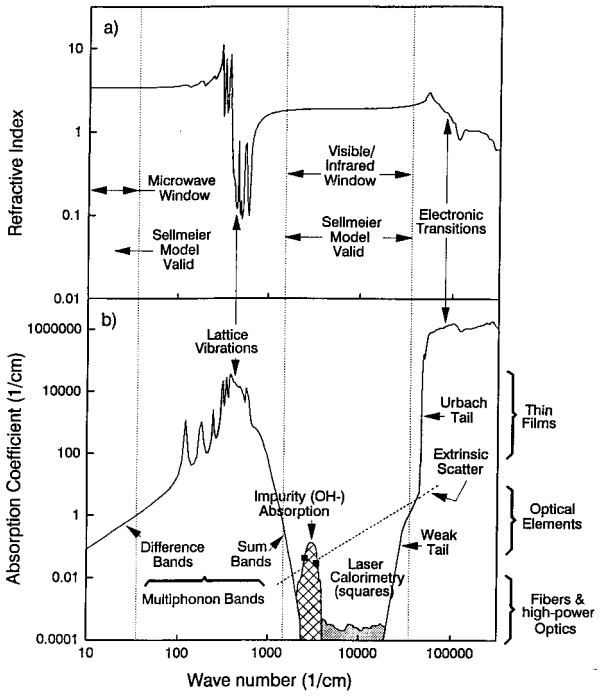

FIGURE 1 The wave number (frequency) dependence of the complex refractive index of Yttria:[19] (*a*) shows the real part of the refractive index, $n(\omega)$. The real part is high at low frequency and monotonically increases, becomes oscillatory in the lattice vibration (phonon) absorption bands, increases monotonically (normal dispersion) in the optical transparent region, and again becomes oscillatory in the electronic absorption region; (*b*) shows the imaginary part of the refractive index, in terms of the absorption coefficient, $\beta(\nu) = 4\pi\nu k(\nu)$. The absorption coefficient is small in the transparent regions and very high in the electronic and vibrational (phonon) absorption bands. The optical transparent region is bounded by the "Urbach tail" absorption at high frequency and by multiphonon absorption at low frequency (wave number). In between, loss is primarily due to impurities and scatter. (*Reprinted by permission of McGraw-Hill, Inc.*)

laser) light. Optically inactive modes have no permanent or induced dipole moment and therefore do not interact with light. Optical modes can be both infrared- and Raman-active and are experimentally observed by infrared or Raman spectroscopy, as well as by x-ray or neutron scattering.

Crystal symmetries reduce the number of unique lattice vibrations (i.e., introduce vibrational degeneracies). A group theory analysis will determine the number of optical modes of each type for an ideal material. Defects and impurities will increase the number of observed infrared-active and Raman modes in a real material. As structural disorder increases (nonstoichiometry, defects, variable composition), the optical modes broaden and additional modes appear. Optical modes in noncrystalline (amorphous) materials such as glasses are very broad compared to those of crystals.

Lattice vibration contributions to the static dielectric constant, $\epsilon(0)$, are determined from the longitudinal- (LO) and transverse-mode (TO) frequencies of the optical modes

using the Lyddane-Sachs-Teller (LST) relationship[20] as extended by Cochran and Cowley[21] for materials with multiple optical modes:

$$\epsilon(0) = \epsilon(\infty) \prod_{j}^{j_{\max}} \frac{\omega_j^2(\mathrm{LO})}{\omega_j^2(\mathrm{TO})} \tag{11}$$

where ω is frequency (usually in wave numbers) and $\epsilon(\infty)$ is the high-frequency (electronic transition) contribution to the dielectric constant (not the dielectric constant at infinite frequency). This relationship holds individually for each principal axis. The index j denotes infrared-active lattice vibrations with minimum value usually found from group theory (discussed later). This LST relationship has been extended to include the frequency dependence of the dielectric constant:

$$\epsilon(\omega) = \epsilon(\infty) \prod_{j} \frac{\omega_j^2(\mathrm{LO}) - \omega^2}{\omega_j^2(\mathrm{TO}) - \omega^2} \tag{12a}$$

A modified form of this fundamental equation is used by Gervais and Piriou[22] and others to model the dielectric constant in the infrared:

$$\epsilon(\omega) = \epsilon(\infty) \prod_{j}^{j_{\max}} \frac{\omega_j^2(\mathrm{LO}) - \omega^2 - i\omega\gamma_j(\mathrm{LO})}{\omega_j^2(\mathrm{TO}) - \omega^2 - i\omega\gamma_j(\mathrm{TO})} \tag{12b}$$

where γ is the line width of the longitudinal and transverse modes as denoted by the symbol in parentheses. This form of the dielectric constant is known as the *semiquantum* four-parameter model.

Frequently, the infrared dielectric constant is modeled in a three-parameter classical oscillator form (or Maxwell–Helmholtz–Drude[23] dispersion formula), namely

$$\epsilon(\omega) = \epsilon(\infty) + \sum_{j}^{j_{\max}} \frac{S_j \omega_j^2(\mathrm{TO})}{\omega_j^2(\mathrm{TO}) - \omega^2 - i\omega\gamma_j} \tag{13}$$

where $S_j (= \Delta\epsilon_j)$ is the strength and γ_j is the full width of the jth mode. This model assumes no coupling between modes and provides a good representation of the dielectric constant, especially if the modes are weak [small separation between $\omega(\mathrm{TO})$ and $\omega(\mathrm{LO})$] and uncoupled. The static dielectric constant $\epsilon(0)$ is merely the sum of the high-frequency dielectric constant $\epsilon(\infty)$ and strengths S_j of the individual, IR-active modes. This formulation has been widely used to model infrared dispersion. This model can also be used to represent the high-frequency dielectric constant using additional models (i.e., $\epsilon(\infty)$ is replaced by 1, the dielectric constant of free space, plus additional modes, see later discussion). Strengths and line widths for the classical dispersion model can be derived from the values of the four-parameter model.[24]

Both the classical and four-parameter dispersion models satisfy the Kramers–Krönig relationship [Eqs. (7) and (8)] and are therefore physically realizable. The frequencies $\omega(\mathrm{TO})$ and $\omega(\mathrm{LO})$ arise from the interaction of light with the material, correspond to solutions of the Maxwell wave equation, $\nabla \cdot \mathbf{D} = 0$ (no free charges), and are obtained from measurements. The transverse frequency corresponds to an electromagnetic wave with $\mathbf{E}$ perpendicular to the wave vector or $\mathbf{E} = 0$. At higher frequencies [$\omega > \omega(\mathrm{TO})$], the external electric field counters the internal polarization field of the material until the real part of the dielectric constant is zero, hence $\mathbf{D} = 0$ at $\omega(\mathrm{LO})$ [when $\gamma_j = 0$, i.e., case of Eq. (12*a*)]. The longitudinal frequency $\omega(\mathrm{LO})$ is always greater than the transverse frequency

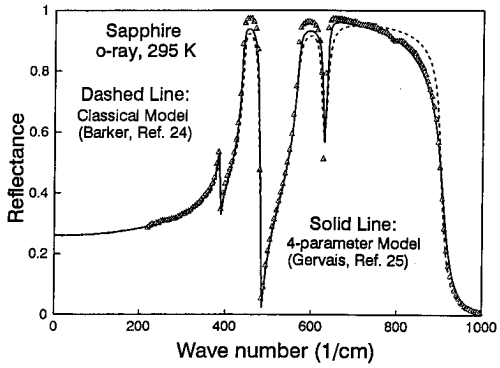

FIGURE 2 The infrared spectrum of sapphire (Al_2O_3) showing the fit to data of the three-parameter classic oscillator model of Barker (dashed line[25]) and the four-parameter model of Gervais (solid line[26]). The four-parameter model better fits experimental data (triangles) in the 650–900 cm^{-1} region.

ω(TO). The separation of ω(LO) and ω(TO) is a measure of the strength (S_j or $\Delta\epsilon_j$) of the optical mode. Raman modes are, by their nature, very weak and therefore $\omega(\text{LO}) \approx \omega(\text{TO})$, hence Raman modes do not appreciably contribute to dielectric properties.

In Eq. (12*a*), the ω(TO) frequencies correspond to the poles and the ω(LO) frequencies correspond to the zeros of the dielectric constant. The dielectric constant continuously rises with frequency [except for a discontinuity at ω(TO)] and the dielectric constant is real and negative [i.e., highly absorbing, Eq. (3)] between the transverse and longitudinal frequencies. When damping is added to the dielectric constant model to represent the response of real materials [e.g., Eq. (12*b*) or (13)], the transverse and longitudinal frequencies become the maxima and minima of the dielectric constant. With damping, a negative dielectric constant is not a necessary condition for absorption, and the material will also absorb outside the region bounded by ω(TO) and ω(LO). Furthermore, damping allows the real part of the dielectric constant (and also the refractive index) to decrease with frequency near ω(TO). This dispersive condition is called *anomalous dispersion* and can only occur in absorptive regions.

Figure 2 shows a typical crystal infrared spectrum and the corresponding classical oscillator[25] and four parameter model[26] fits to the data.

As an example of lattice vibrations, consider the simple case of crystalline sodium chloride (NaCl) which has four molecules (eight atoms) per unit cell. Since the sodium chloride structure is face-centered cubic, a primitive cell has one molecule or two atoms. The number of unique vibrations is further reduced by symmetry: for sodium chloride, the lattice vibrations consist of one (triply degenerate) acoustic mode and one (triply degenerate) optical mode. Many metals have one atom per primitive unit cell and therefore have no optical modes. Group IV cubic materials (diamond, silicon, germanium) have two atoms per unit cell with one (triply degenerate) optical mode that is Raman-active only. Therefore, to first order, these nonpolar materials are transparent from their band gap to very low frequencies. In practice, multiphonon vibrations, defects, impurities, and free carriers can introduce significant absorption.

Electronic Transitions. Electronic transitions in a solid begin at the material's band gap. This point generally marks the end of a material's useful transparency. Above the band gap, the material is highly reflective. The large number of possible electronic transitions

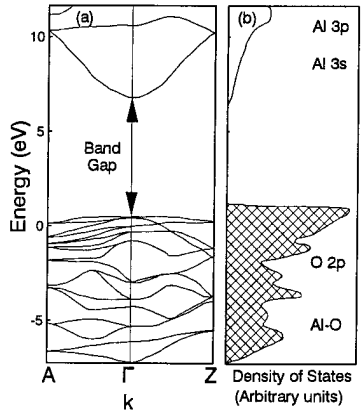

FIGURE 3 Electronic energy band diagram for sapphire at room temperature:[27] (*a*) shows the complex k-space energy levels of the electrons of sapphire. The arrow denotes the direct band gap transition; (*b*) shows the density of electronic states as a function of energy level. The many direct and indirect electronic transitions give rise to a broad electronic absorption with few features. (*Reprinted by permission of the American Ceramic Society.*)

produces broad-featured spectra. However, electronic structure is fundamental to understanding the nature of the bonds forming the solid and thus many of the material properties. In three dimensions, the band structure becomes more complicated, because it varies with direction just as lattice vibrations do. This point is illustrated in Fig. 3 for the case of the electronic k-space diagram for sapphire.[27] Also included in this figure is the corresponding electronic density of states that determines the strength of the absorption.

In polar insulators, no intraband electronic transitions are allowed, and the lowest frequency electronic absorption is frequently caused by creation of an *exciton,* a bound electron-hole pair. The photon energy required to create this bound pair is lower than the band-gap energy. Other lower-frequency transitions are caused by interband transitions between the anion valence band and the cation conduction band. For sapphire (see Fig. 3), the lowest energy transitions are from the upper valence band of oxygen ($2p^6$) to the conduction band of aluminum ($3s + 3p$). There are typically many of these transitions which appear as a strong, broad absorption feature. Higher energy absorption is caused by surface and bulk plasmons (quanta of collective electronic waves), and still higher energy absorption is attributable to promotion of inner electrons to the conduction band and ultimately liberation of electrons from the material (photoemission).

Excitons have many properties similar to that of a hydrogen atom. The absorption spectra of an exciton is similar to that of hydrogen and occurs near the band gap of the host material. The bond length between the electron-hole pair, hence the energy required to create the exciton, depends on the host medium. Long bond lengths are found in semiconductors (low-energy exciton) and short bond lengths are found in insulating materials.

Classical electronic polarization theory produces a model of the real part of the dielectric constant similar to the model used for the real dielectric constant of lattice vibrations [Eq. (13)]. General properties of the real dielectric constant (and real refractive index) can be deduced from this model. Bound electrons oscillate at a frequency proportional to the square root of the binding energy divided by the electronic mass.

Oscillator strength is proportional to the inverse of binding energy. This means that insulators with light atoms and strong bonding have large band gaps, hence good UV transmission (cf., LiF). Furthermore, high bonding energy (hence high-energy band gap) means low refractive index (e.g., fluorides).

When both electronic and lattice vibrational contributions to the dielectric constant are modeled as oscillations, the dielectric constant in the transparent region between electronic and vibrational absorption is (mostly) real and the real part takes the form

$$\epsilon'(\omega) - 1 = n^2(\omega) - 1 = \sum_j \frac{S_j \omega_j^2}{\omega_j^2 - \omega^2} \tag{14}$$

which is the widely-used *Sellmeier dispersion formula.* The sum includes both electronic (*UV*) and vibrational (IR or *ionic*) contributions. Most other dispersion formulas (such as the Schott glass power series) are recast or simplified forms of the Sellmeier model. The refractive index of most materials with good homogeneity can be modeled to a few parts in 10^5 over their entire transparent region with a Sellmeier fit of a few terms. The frequency (ω_j) term(s) in a Sellmeier fit are not necessarily TO modes, but are correlated to the strong TOs nearest the transparent region, with adjustments to the constants made to account for weaker modes, multiphonon effects, and impurities. The Sellmeier model works well because it is (1) based on a reasonable physical model and (2) adjusts constants to match data. The relationship between the Sellmeier equation and other dispersion formulas is discussed later.

The *Urbach tail* model is successfully applied to model the frequency and temperature dependence of the ultraviolet absorption edge in a number of materials, particularly those with a direct band gap, over several orders of magnitude in absorption. Urbach[28] observed an exponential absorption edge in silver halide materials (which have an indirect band gap). Further development added temperature dependence in the form:

$$\beta_{\text{ABS}}(E, T) = \beta_0 \exp\left[-\sigma(T)\frac{(E_0 - E)}{k_B T}\right] \tag{15a}$$

where

$$\sigma(T) = \sigma_0(T)\frac{2k_B T}{E_p}\tanh\frac{E_p}{2k_B T} \tag{15b}$$

where E_0 is the band gap energy at $T = 0\,\text{K}$ (typically the energy of an exciton), T temperature in Kelvins, and E_p a characteristic phonon energy. The interpretation of the Urbach tail is a broadening of the electronic band gap by phonon interactions, and several detailed theories have been proposed.[18,29]

Below the Urbach tail, absorption continues to decrease exponentially, albeit much slower than predicted by the Urbach formula. This region of slowly decreasing absorption is sometimes called the ''weak tail,'' and has been observed in both semiconductor[30] and crystalline materials.[31,32] Typically, the weak tail begins at the point when the absorption coefficient falls to $0.1\ \text{cm}^{-1}$.

Free Carriers. Free carriers, such as electrons in metals, or electrons or holes in semiconductors, also affect the optical properties of materials. For insulators or wide-band-gap semiconductors (i.e., band gap greater than 0.5 eV) with a low number of free carriers at room temperature (low conductivity), the effect of free carriers on optical absorption is small [see Eq. (2)]. For nonmetals, the free-carrier concentration grows with temperature so that even an ''insulator'' has measurable conductivity (and free-carrier absorption) at very high temperature. Commonly used optical materials such as silicon and germanium

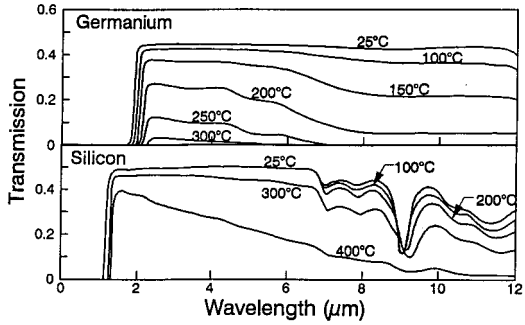

FIGURE 4 Decreased transmission of germanium and silicon with temperature is attributable to an increase in free-carrier concentration resulting in increased absorption.[33] The absorption is greater at longer wavelengths; see Eq. (16). (*Reprinted by permission of the Optical Society of America.*)

have a significant increase in free-carrier absorption at moderately high temperature as illustrated in Fig. 4.[33]

Free-carrier effects can be modeled as an additional contribution to the dielectric constant model. For example, the classical model [Eq. (13)] takes the form

$$\epsilon(\omega) = \epsilon(\infty) + \sum_{j}^{j_{\max}} \frac{S_j \omega_j^2(\mathrm{TO})}{\omega_j^2(\mathrm{TO}) - \omega^2 - i\omega\gamma_j} - \frac{\omega_p^2}{\omega^2 + i\omega\gamma_c} \tag{16}$$

where ω_p is the plasma frequency, proportional to the square root of the free-carrier density, and γ_c is the damping frequency (i.e., determines the effective width of the free-carrier influence). Such a model is well known to accurately predict the far-infrared ($\geq$10 μm) refractive index of metals[34] and also has been used to model the free-carrier contribution to optical properties of semiconductors.

Multiphonon Absorption and Refraction. Absorption at the infrared edge of insulators is principally caused by anharmonic terms in the lattice potential leading to higher harmonics of the lattice resonances. This phenomenon is called multiphonon absorption because the frequencies are harmonics of the characteristic lattice phonons (vibrations). For absorption in the infrared, each successively higher multiple of the fundamental frequency is weaker (and broader) leading to decreasing absorption beyond the highest fundamental absorption frequency (maximum transverse optical frequency). At about three times ω(TO) the absorption coefficient becomes small and a material with thickness of 1 to 10 mm is reasonably transparent. The infrared absorption coefficient of materials (especially highly ionic insulators) can be characterized by an exponential absorption coefficient[35] β_{ABS} of the form

$$\beta_{\mathrm{ABS}} = \beta_0 \exp\left(-\gamma \frac{\omega}{\omega_o}\right) \tag{17a}$$

where β_0 is a constant (dimensions same as the absorption coefficient, typically cm^{-1}), γ is a dimensionless constant (typically found to be near 4), ω_o is frequency or wave number of the maximum transverse optical frequency (units are cm^{-1} for wave numbers; values are given in the property data tables), and ω is the frequency or wave number of interest (units are cm^{-1} for wave numbers). This formula works reasonably well for ionic materials at room temperature for the range of absorption coefficients from 0.001 to 10 cm^{-1}.

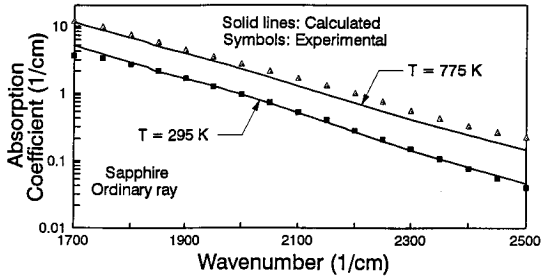

FIGURE 5 Temperature-dependent change of absorption in insulators is principally confined to the absorption edges, especially the infrared multiphonon absorption edge. This figure shows measured and predicted absorption coefficients at the infrared edge of transparency for the ordinary ray of crystalline sapphire. Increasing temperature activates higher multiphonon processes, resulting in a rapid increase in absorption. The multiphonon model of Thomas et al.,[38] accurately predicts the frequency- and temperature-dependence of infrared absorption in highly ionic materials such as oxides and halides.

In the classical (continuum) limit, the temperature dependence of multiphonon absorption has T^{n-1} dependence where n is the order of the multiphonon process,[36] i.e., $n \approx \omega/\omega_o$. At low temperature, there is no temperature dependence since only transitions from the ground state occur. Once the temperature is sufficiently high (e.g., approaching the Debye temperature), transitions that originate from excited states become important and the classical temperature dependence is observed. Bendow[37] has developed a simple model of the temperature dependence of multiphonon absorption based on a Bose–Einstein distribution of states:

$$\beta_{\mathrm{ABS}}(\omega, T) = \beta_0 \frac{[N(\omega_o, T) + 1]^{\omega/\omega_o}}{N(\omega, T) + 1} \exp(-A\omega/\omega_o) \tag{17b}$$

where $N(\omega, T)$ is phonon occupation density from Bose–Einstein statistics.

Thomas et al.,[38] have successfully developed a semiempirical, quantum mechanical model of (sum band) multiphonon absorption based on the Morse interatomic potential and a Gaussian function for the phonon density of states. Use of the Morse potential leads to an exact solution to the Schrödinger equation and includes anharmonic effects to all orders. The model contains parameters derived from room-temperature measurements of absorption, is computationally efficient, and has been applied to many ionic substances. Figure 5 shows a typical result compared to experimental data.

Multiphonon absorption modeling also contributes to the real refractive index. Although multiphonon contributions to the real index are small compared to one-phonon contributions, they are important for two cases in the infrared: (1) when the refractive index must be known beyond two decimal places, or (2) at high temperature. In the first case, multiphonon contributions to the index are significant over a large spectral region. In the second case, the contribution of multiphonon modes to real refractive index grows rapidly at high temperature because of the T^{n-1} dependence of the nth mode strength.

Absorption in the Transparent Region. In the transparent region, away from the electronic and vibrational resonances, absorption is governed by impurities and defects. The level of absorption is highly dependent on the purity of the starting materials, conditions of manufacture, and subsequent machining and polishing. For example, OH

impurities are common in oxides,* occurring at frequencies below the fundamental (nonbonded) OH vibration at 3735 cm^{-1}. OH can be removed by appropriate treatment.

Low-level absorption coefficient measurements are typically made by laser calorimetry or photoacoustic techniques. Data are available for a number of materials in the visible,[31,39] at 1.3 μm,[40] and at 2.7 and 3.8 μm.[41]

Optical Properties: Applications

Dielectric Tensor and Optical Indicatrix. Many important materials are nonisotropic (i.e., crystals Al_2O_3, SiO_2, and MgF_2) and their optical properties are described by tensor relationships (see earlier section, "Symmetry Properties"). The dielectric constant ϵ, a second-rank tensor, relates the electric field **E** to the electric displacement **D**:

$$\begin{vmatrix} \mathbf{D}_x \\ \mathbf{D}_y \\ \mathbf{D}_z \end{vmatrix} = \epsilon_0 \cdot \begin{vmatrix} \epsilon_{xx} & \epsilon_{xy} & \epsilon_{xz} \\ \epsilon_{yx} & \epsilon_{yy} & \epsilon_{yz} \\ \epsilon_{zx} & \epsilon_{zy} & \epsilon_{zz} \end{vmatrix} \cdot \begin{vmatrix} \mathbf{E}_x \\ \mathbf{E}_y \\ \mathbf{E}_z \end{vmatrix} \tag{18a}$$

From the symmetry of properties, this is a symmetric tensor with $\epsilon_{ab} = \epsilon_{ba}$. Usually, the dielectric constant components are given as principal values, i.e., those values along the unit cell of the appropriate crystal class. In this case, the principal dielectric constants are

$$\begin{aligned} \epsilon_{x'x'} &\equiv \epsilon_1 \\ \epsilon_{y'y'} &\equiv \epsilon_2 \\ \epsilon_{z'z'} &\equiv \epsilon_3 \end{aligned} \tag{18b}$$

where the primes on the subscripts denote principal values (i.e., along the crystallographic axes, possible in a nonorthogonal coordinate system) and the subscripts 1, 2, and 3 denote reduced notation for these values (see "Elastic Properties"). The relationship between dielectric constant and refractive index, Eq. (4), means there are similarly three principal values for the (complex) refractive index. Also, the components of the dielectric tensor are individually related to the corresponding components of the refractive index. (Subscripts *a, b,* and *c* or *x, y,* and *z* as well as others may be used for the principal values of the dielectric constant or refractive index.)

Three important cases arise:

1. Isotropic and cubic materials have only one dielectric constant, ϵ, (hence one refractive index, $\bar{n}$). Therefore $\epsilon_1 = \epsilon_2 = \epsilon_3 = \epsilon = \bar{n}^2$.

2. Hexagonal (including trigonal) and tetragonal crystals have two principal dielectric constants, ϵ_1 and ϵ_3 (hence two refractive indices, $\bar{n}_1$ and $\bar{n}_3$). Therefore $\epsilon_1 = \epsilon_2 \neq \epsilon_3$. Such materials are called *uniaxial*; the unique crystallographic axis is the *c* axis, which is also called the *optical axis.* One method of denoting the two unique principal axes is to state the orientation of the electric field relative to the optical axis. The dielectric constant for $\mathbf{E} \perp c$ situation is ϵ_1 or $\epsilon_\perp$. This circumstance is also called the *ordinary ray,* and the corresponding symbol for the refractive index is $\bar{n}_1$, $\bar{n}_\perp$, $\bar{n}_o$ (for ordinary ray), and $\bar{n}_\omega$ or ω

* The OH vibrational impurity absorption in oxides is known for Al_2O_3, ALON, $MgAl_2O_4$, MgO, SiO_2, Y_2O_3, and Yb_2O_3.

(primarily in the older literature). The dielectric constant for $\mathbf{E} \parallel c$ situation is ϵ_3 or $\epsilon_\parallel$. This condition is called the *extraordinary ray,* and the corresponding symbol for the refractive index is $\bar{n}_3$, $\bar{n}_\parallel$, $\bar{n}_e$ (for extraordinary ray), and $\bar{n}_\epsilon$ or ϵ (again, primarily in the older literature). Crystals are called *positive uniaxial* when $n_e - n_o > 0$, and *negative uniaxial* otherwise. Since the dispersions of the ordinary and extraordinary wave are different, a crystal can be positive uniaxial in one wavelength region and negative uniaxial in another ($AgGaS_2$ is an example).

3. Orthorhombic, monoclinic, and triclinic crystals have three principal dielectric constants, ϵ_1, ϵ_2, and ϵ_3 (hence, three refractive indices, $\bar{n}_1$, $\bar{n}_2$, and $\bar{n}_3$). Therefore $\epsilon_1 \neq \epsilon_2 \neq \epsilon_3 \neq \epsilon_1$. These crystals are called *biaxial.* Confusion sometimes arises from the correlation of the principal dielectric constants with the crystallographic orientation owing to several conventions in selecting the crystal axes. [The optical indicatrix (see following discussion) of a biaxial material has two circular sections that define optical axes. The orientation of these axes are then used to assign a positive- or negative-biaxial designation.]

The existence of more than one dielectric constant or refractive index means that, for radiation with arbitrary orientation with respect to the crystal axes, two plane-polarized waves, of different speed, propagate in the crystal. Hence, for light propagating at a random orientation to the principal axes, a uniaxial or biaxial crystal exhibits two effective refractive indices different from the individual principal values. The refractive index of the two waves is determined from the *optical indicatrix* or *index ellipsoid,* a triaxial ellipsoidal surface defined by

$$\frac{x_1^2}{n_1^2} + \frac{x_2^2}{n_2^2} + \frac{x_3^2}{n_3^2} = 1 \tag{19a}$$

where the x_1, x_2, and x_3 are the principal axes of the dielectric constant. The indicatrix is illustrated in Fig. 6: for a wave normal in an arbitrary direction (OP), the two waves have

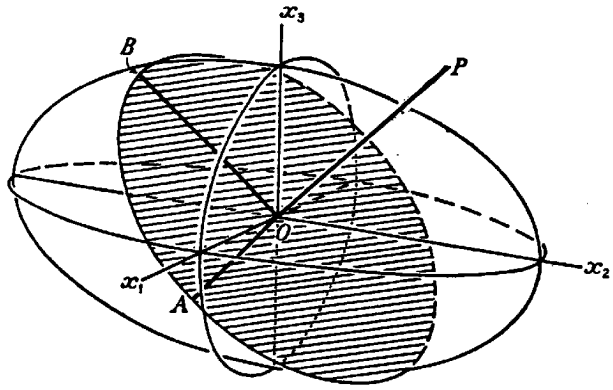

FIGURE 6 The *optical indicatrix* or *index ellipsoid* used to determine the effective refractive index for an arbitrary wave normal in a crystal. The axes of the ellipsoid correspond to the principal axes of the crystal, and the radii of the ellipsoid along the axes are the principal values of the refractive indices. For propagation along an arbitrary wave normal (OP), the effective refractive indices are the axes of the ellipse whose normal is parallel to the wave normal. In the illustrated case, the directions OA and OB define the effective refractive indices.[14] (*Reprinted by permission of Oxford University Press.*)

refraction indices equal to the axes of the ellipse perpendicular to the wave normal (OA and OB). The directions represented by OA and OB are the vibrational planes of the electric displacement vector **D** of the two waves. When the wave normal is parallel to an optic axis, the two waves propagate with principal refractive indices. For uniaxial material and the wave normal parallel to the x_3 (or z or c crystallographic or optical) axis, the vibrational ellipsoid is circular and the two waves have the same refractive index (n_o), and there is no double refraction. Equation (19*a*) can also be written

$$B_1x_1^2 + B_2x_2^2 + B_3x_3^2 = 1 \tag{19b}$$

where $B_i = 1/\bar{n}_1^2 = 1/\epsilon_i$ is called the *inverse dielectric tensor.* The inverse dielectric tensor is used in defining the electro-optic, piezo-optic, and elasto-optic effects.

***Reflection*: *Fresnel Formulas*.** Fresnel formulas for reflection and transmission at an interface are presented here. Results for two cases are given. The first is for cubic materials, and the second is for uniaxial (tetragonal and hexagonal) that have the crystallographic c axis normal to the interface surface. Orientation of the electric field in the plane of incidence is the case of *vertical polarization* or ***p*-polarization**; the electric field perpendicular to the plane of incidence is the case of *horizontal polarization* or ***s*-polarization.**

For a cubic medium $\epsilon_{xx} = \epsilon_{yy} = \epsilon_{zz} = \bar{n}^2$, and the field (amplitude) reflection r_{12} and transmission t_{12} (Fresnel) coefficients are, for **p**-polarization propagating from medium 1 to medium 2,

$$r_{p12} = \frac{\dfrac{\bar{n}_2}{\cos\theta_t} - \dfrac{\bar{n}_1}{\cos\theta_i}}{\dfrac{\bar{n}_2}{\cos\theta_t} + \dfrac{\bar{n}_1}{\cos\theta_i}} = \frac{\bar{n}^2\cos\theta_i - \sqrt{\bar{n}^2 - \sin^2\theta_i}}{\bar{n}^2\cos\theta_i + \sqrt{\bar{n}^2 - \sin^2\theta_i}} = -r_{p21} \tag{20a}$$

and

$$t_{p12} = \frac{2\bar{n}_1\cos\theta_1}{\bar{n}_1\cos\theta_i + \bar{n}_2\cos\theta_t} = \frac{\bar{n}_1\cos\theta_i}{\bar{n}_2\cos\theta_t}\,t_{p21} \tag{20b}$$

and the corresponding formulas for **s**-polarization are

$$r_{s12} = \frac{\bar{n}_1\cos\theta_i - \bar{n}_2\cos\theta_t}{\bar{n}_1\cos\theta_i + \bar{n}_2\cos\theta_t} = \frac{\cos\theta_i - \sqrt{\bar{n}^2 - \sin^2\theta_i}}{\cos\theta_i + \sqrt{\bar{n}^2 - \sin^2\theta_i}} = -r_{s21} \tag{20c}$$

and

$$t_{s12} = \frac{2\bar{n}_1\cos\theta_i}{(\bar{n}_1\cos\theta_i + \bar{n}_2\cos\theta_t)} = \frac{\bar{n}_1\cos\theta_i}{\bar{n}_2\cos\theta_t}\,t_{s21} \tag{20d}$$

where $\bar{n} = \bar{n}_2/n_1$ for n_1 real. Snell's law is then given by

$$n_1\sin\theta_1 = \bar{n}_2\sin\theta_2 \tag{20e}$$

where θ_1 is real and θ_2 is complex. The terms r_{21} and t_{21} are the field reflection and transmission coefficients for propagation from medium 2 to medium 1, respectively. The relationships between r_{12} and r_{21} and between t_{12} and t_{21} are governed by the *principle of*

reversibility. The single-surface (Fresnel) *power* coefficients for reflection (R) and transmission (T) are directly obtained from the field coefficients:

$$R_{p,s} = |r_{p,s}|^2 \tag{20f}$$

and

$$T_{p,s} = \frac{\bar{n}_2 \cos \theta_t}{\bar{n}_1 \cos \theta_i} |t_{p,s}| \tag{20g}$$

Using the formulas of Eq. (20), and assuming medium 1 is vacuum ($n_1 = 1$) and medium 2 is absorbing ($\bar{n}_2 = n + ik$), the power coefficients become

$$R_s = \frac{(a - \cos \theta_i)^2 + b^2}{(a + \cos \theta_i)^2 + b^2} \tag{21a}$$

and

$$R_p = R_s \left[\frac{(a - \sin \theta_i \tan \theta_i)^2 + b^2}{(a + \sin \theta_i \tan \theta_i)^2 + b^2} \right] \tag{21b}$$

where the terms a and b are

$$a^2 = \tfrac{1}{2}([(n^2 - k^2 - \sin^2 \theta_1)^2 + 4n^2k^2]^{1/2} + (n^2 - k^2 - \sin^2 \theta_i)) \tag{21c}$$

and

$$b^2 = \tfrac{1}{2}([(n^2 - k^2 - \sin^2 \theta_1)^2 + 4n^2k^2]^{1/2} - (n^2 - k^2 - \sin^2 \theta_i)) \tag{21d}$$

The principle of reversibility and Snell's law require that

$$R_{12} = R_{21} \qquad \text{and} \qquad T_{12} = T_{21} \tag{22a}$$

Also, from the preceding definitions, it can be shown that

$$R_{s,p} + T_{s,p} = 1 \tag{22b}$$

For unpolarized light, the single-surface reflection coefficient becomes

$$R = \tfrac{1}{2}(R_s + R_p) \tag{22c}$$

For uniaxial media, $\epsilon_{xx} = \epsilon_{yy} = \bar{n}_1^2 = \bar{n}_2^2 = \bar{n}_o^2$ and $\epsilon_{zz} = \bar{n}_3^2 = \bar{n}_e^2$. For the special case with the surface normal parallel to the crystallographic c axis (optical axis), the Fresnel formula becomes

$$R_p = \left| \frac{n_1 n_3 \cos \theta_i - [n_3^2 - \sin^2 \theta_i]^{1/2}}{n_1 n_3 \cos \theta_i + [n_3^2 - \sin^2 \theta_i]^{1/2}} \right|^2 \tag{23a}$$

and

$$R_s = \left| \frac{\cos \theta_i - (n_1^2 - \sin^2 \theta_i)^{1/2}}{\cos \theta_i + (n_1^2 - \sin^2 \theta_i)^{1/2}} \right|^2 \tag{23b}$$

If $n_1 = n_3 = n$, the isotropic results are obtained.

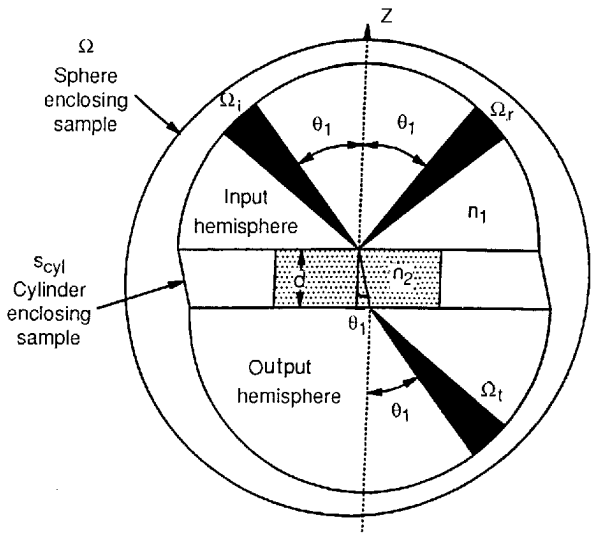

FIGURE 7 Geometry of incident, transmitted, and reflected beams for a plane transparent slab of thickness *d*. The power equals the reflected, refracted, and absorbed, assuming no scatter.

Total Power Law. Incident light on a material is reflected, transmitted, or absorbed. Scattering is a term used to describe diffuse reflectance (surface scatter) and diffuse transmittance (bulk scatter). Conservation of energy dictates that the fractional amount reflected ρ, absorbed α_{ABS}, transmitted τ, and scattered α_{SCA} total to unity, hence

$$1 = \rho(\Omega_i, \omega) + \alpha_{\text{SCA}}(\Omega_i, \omega) + \alpha_{\text{ABS}}(\Omega_i, \omega) + \tau(\Omega_i, \omega) \tag{24}$$

where these time-averaged quantities, illustrated in Fig. 7, are

$$\rho(\Omega_i, \omega) = \frac{\Phi_r(\Omega_i, \omega)}{\Phi_i(\omega)} = \text{total integrated reflectance}, \tag{25a}$$

$$\alpha_{\text{SCA}}(\Omega_i, \omega) = \frac{\Phi_s(\Omega_i, \omega)}{\Phi_i(\omega)} = \text{total integrated scatterance}, \tag{25b}$$

$$\alpha_{\text{ABS}}(\Omega_i, \omega) = \frac{\Phi_s(\Omega_i, \omega)}{\Phi_i(\omega)} = \text{total integrated absorptance}, \tag{25c}$$

and

$$\tau(\Omega_i, \omega) = \frac{\Phi_t(\Omega_i, \omega)}{\Phi_i(\omega)} = \text{total integrated transmittance} \tag{25d}$$

Notice that these quantities are functions of the angle of incidence and frequency only.

The sum of total integrated scatterance and total integrated absorptance can be defined as the total integrated extinctance α_{EXT},

$$\alpha_{\text{EXT}}(\Omega_i, \omega) = \alpha_{\text{ABS}}(\Omega_i, \omega) + \alpha_{\text{SCA}}(\Omega_i, \omega) \tag{26}$$

and the total power law becomes

$$1 = \rho(\Omega_i, \omega) + \alpha_{\text{EXT}}(\Omega_i, \omega) + \tau(\Omega_i, \omega) \tag{27}$$

Another useful quantity is emittance, which is defined as

$$\epsilon(\Omega_i, \omega) = \frac{\Phi_e(\Omega_i, \omega)}{\Phi_{\text{bb}}(\omega)} = \text{total integrated emittance} \tag{28a}$$

where Φ_{bb} is the blackbody function representing the spectral emission of a medium which totally absorbs all light at all frequencies. When $\Phi_i(\omega) = \Phi_{\text{bb}}(\omega)$, then the total integrated emittance equals the total integrated absorptance:

$$\varepsilon(\Omega_i, \omega) = \alpha_{\text{ABS}}(\Omega_i, \omega) \tag{28b}$$

Dispersion Formulas for Refractive Index. The dielectric constant and refractive index are functions of frequency, hence wavelength. The frequency or wavelength variation of refractive index is called *dispersion.* Disperson is an important property for optical design (i.e., correction of chromatic aberration) and in the transmission of information (i.e., pulse spreading). Other optical properties are derived from the change in refractive index with other properties such as temperature (*thermo-optic* coefficient), stress or strain (*piezo-optic* or *elasto-optic* coefficients), or applied field (*electro-optic* or *piezo-electric coefficients*). Since the dielectric constant is a second-order tensor with three principal values, the coefficients defined here are also tensor properties (see Table 1).

Precise refractive index measurements give values as functions of wavelength. Frequently, it is desirable to have a functional form for the dispersion of the refractive index (i.e., for calculations and value interpolation). There are many formulas used for representing the refractive index. One of the most widely used is the Sellmeier (or Drude or Maxwell-Helmholtz-Drude) dispersion model [Eq. (14)], which arises from treating the absorption like simple mechanical or electrical resonances. Sellmeier proposed the following dispersion formula in 1871 (although Maxwell had also considered the same derivation in 1869). The usual form of this equation for optical applications gives refractive index as a function of wavelength rather than wave number, frequency, or energy. In this form, the Sellmeier equation is:

$$n^2(\lambda) - 1 = \sum_{i=1} \frac{A_i \cdot \lambda^2}{\lambda^2 - \lambda_i^2} \tag{29a}$$

An often-used, slight modification of this formula puts the wavelength of the shortest wavelength resonance at zero ($\lambda_1 = 0$), i.e., the first term is a constant. This constant term represents contributions to refractive index from electronic transitions at energies far above the band gap. Sellmeier terms with small λ_i (representing electronic transitions) can be expanded as a power series,

$$\begin{aligned} \frac{A_i \cdot \lambda^2}{\lambda^2 - \lambda_i^2} &= A_i \cdot \sum_{j=0}^{\infty} \cdot (\lambda_i^2/\lambda^2)^j \\ &= A_i + \frac{A_i \cdot \lambda_i^2}{\lambda^2} + \frac{A_i \cdot \lambda_i^4}{\lambda^4} + \cdots \end{aligned} \tag{29b}$$

and the terms with large λ_i (representing vibrational transitions) are expanded as:

$$\begin{aligned} \frac{A_i \cdot \lambda^2}{\lambda^2 - \lambda_i^2} &= -A_i \cdot \sum_{j=1}^{\infty} (\lambda^2/\lambda_i^2)^j \\ &= -A_i \cdot \frac{\lambda^2}{\lambda_i^2} - A_i \cdot \frac{\lambda^4}{\lambda_i^4} - \cdots \end{aligned} \tag{29c}$$

The first term of this expansion is occasionally used to represent the long-wavelength contributions to the index of refraction (see Schott dispersion formula, following).

A generalized form of the short-wavelength approximation to the Sellmeier equation is the Cauchy formula, developed in 1836. This was the first successful attempt to represent dispersion by an equation:

$$n = A_0 + \sum_{i=1} \frac{A_i}{\lambda^{2i}} \qquad \text{or} \qquad n^2 = A_0' + \sum_{i=1} \frac{A_i'}{\lambda^{2i}} \tag{30}$$

Power series approximations to the Sellmeier equation are expressed in many forms. One common form is the Schott glass formula used for glasses:

$$n^2 = A_0 + A_1\lambda^2 + A_2\lambda^{-2} + A_3\lambda^{-4} + A_4\lambda^{-6} + A_5\lambda^{-8} \tag{31}$$

For typical high-quality glasses, this equation is accurate to $\pm 3 \cdot 10^{-6}$ in the visible (400 to 765 nm) and within $\pm 5 \cdot 10^{-6}$ from 365 to 1014 nm. A comparison of the Schott power series formula with a three-term Sellmeier formula showed equivalent accuracy of the range of the Schott fit, but that the Sellmeier model was accurate over a much wider wavelength range.[42] A number of other power series dispersion formulas (e.g., Ketteler–Neumann[43]) are occasionally used.

Frequently, Sellmeier terms are written in altered fashion such as this form used by Li:[44]

$$\frac{A_i}{(\lambda^2 - \lambda_i^2)} = \frac{A_i(\lambda^2/\lambda_i^2)}{(\lambda^2 - \lambda_i^2)} - \frac{A_i}{\lambda_i^2} \tag{32a}$$

which is the combination of two Sellmeier terms, one located at zero wavelength and the other at λ_i. The Zernike formula[45] also uses a term in this form. Another way to modify Sellmeier terms is to convert the wavelength of the resonances to wave number or energy [see Eq. (14)].

Another common formula for the index of refraction is the Hartmann or Cornu equation:

$$n = A + \frac{B}{\lambda - \lambda_0} \tag{32b}$$

This equation is more distantly related to the Sellmeier formulation. Note that a two-term Sellmeier formula (with $\lambda_1 = 0$) can be written as

$$(n^2 - n_0^2) \cdot (\lambda^2 - \lambda_0^2) = (n - n_0) \cdot (\lambda - \lambda_0) \cdot (n + n_0) \cdot (\lambda + \lambda_0) = \text{constant} \tag{32c}$$

and the Hartmann formula can be written as a hyperbola:

$$(n - n_0) \cdot (\lambda - \lambda_0) = \text{constant} \tag{32d}$$

Note that in a limited spectral region, the difference terms of the Sellmeier formula of Eq. (33*c*) vary much more rapidly than do the sum terms, hence the Hartmann and Sellmeier forms will have the same shape in this limited spectral range.

Other equations that combine Sellmeier and power series tersms (cf., Wemple formula) are often used. One such formulation is the Herzberger equation, first developed for glasses[46] and later applied to infrared crystalline materials:[47]

$$n = A + \frac{B}{(\lambda^2 - 0.028)} + \frac{C}{(\lambda^2 - 0.028)^2} + D\lambda^2 + E\lambda^4 \tag{32e}$$

where the choice of the constant $\lambda_o^2 = 0.028$ is arbitrary in that it is applied to all materials.

The Pikhtin-Yas'kov formula[48] is nearly the same as the Sellmeier form with the addition of another term representing a broadband electronic contribution to index:

$$n^2 - 1 = \frac{A}{\pi} \ln \frac{E_1^2 - (\hbar\omega)^2}{E_0^2 - (\hbar\omega)^2} + \sum_i \frac{G_i}{E_i^2 - (\hbar\omega)^2} \tag{32f}$$

This formulation has been applied to some semiconductor materials. The unique term arises from assuming that the imaginary part of the dielectric constant is a constant between energies $\mathbf{E}_0$ and $\mathbf{E}_1$ and that infinitely narrow resonances occur at $\mathbf{E}_i$. The formula is then derived by applying the Kramers–Krönig relationship to this model.

Typically for glasses, the *Abbe number,* or constringence ν_d, is also given. The Abbe number is a measure of dispersion in the visible and is defined as $\nu_d = (n_d - 1)/(n_F - n_C)$ where n_d, n_F, and n_C are refractive indices at 587.6 nm, 486.1 nm, and 656.3 nm. The quantity $(n_F - n_C)$ is known as the *principle dispersion.* A relative partial dispersion $P_{x,y}$ can be calculated at any wavelengths x and y from

$$P_{x,y} = \frac{(n_x - n_y)}{(n_F - n_C)} \tag{33a}$$

For so-called "normal" glasses, the partial dispersions obey a linear relationship, namely

$$P_{x,y} = a_{x,y} + b_{x,y}\nu_d \tag{33b}$$

where $a_{x,y}$ and $b_{x,y}$ are empirical constants characteristic of normal glasses. However, for correction of secondary spectrum in an optical system (that is, achromatization for more than two wavelengths), it is necessary to employ a glass that does not follow the glass line. Glass manufacturers usually list $\Delta P_{x,y}$ for a number of wavelength pairs as defined by:

$$P_{x,y} = a_{x,y} + b_{x,y}\nu_d + \Delta P_{x,y} \tag{33c}$$

The deviation term $\Delta P_{x,y}$ is a measure of the dispersion characteristics differing from the normal glasses. Schott glasses F2 and K7 define the normal glass line.

The Sellmeier formula has the appropriate physical basis to accurately represent the refractive index throughout the transparent region in the simplest manner. The Sellmeier constants have physical meaning, particularly for simple substances. Most other dispersion formulas are closely related to (or are a disguised form of) the Sellmeier equation. Many of these other dispersion formulas are unable to cover a wide spectral region, and unlike the Sellmeier form, do not lend themselves to extrapolation outside the region of available measurements. For these reasons, we strongly urge that the Sellmeier model be universally used as the standard representation of the refractive index.

Modifications of the Sellmeier terms that include composition variation[49,50] and temperature dependence[51] have been applied to successfully model refractive index. The variation of the Sellmeier A_i and λ_i constants is usually modeled as linearly dependent on the mole fraction of the components and temperature.

In the transparent region, refractive index decreases with wavelength, and the magnitude of $dn/d\lambda$ is a minimum between the electronic and vibrational absorptions. The wavelength of minimum $dn/d\lambda$, called the zero-dispersion point, is given by

$$\frac{d^2n}{d\lambda^2} = 0 \tag{34}$$

which is the desired operating point for high-bandwidth, information-carrying optical

fibers as well as the optimum wavelength for single-element refractive optical systems. For glassy silica fibers, the zero dispersion point is 1.272 μm. One approach to reducing both dispersion and loss is to use a material with a wide transparent region, i.e., widely separated electronic and vibrational absorptions, hence the interest in materials such as heavy-metal fluoride glasses for fiber applications.

Thermo-optic and Photoelastic Coefficients. Temperature is one of the main factors influencing the refractive index of solids. The thermo-optical coefficients $\partial n/\partial T$ (or $\partial \epsilon/\partial T$) can be estimated from a derivation of the Clausius-Mossotti relationship:[52]

$$\frac{1}{(\epsilon-1)(\epsilon+2)}\left(\frac{\partial \epsilon}{\partial T}\right) = -\alpha\left[1-\frac{V}{\alpha_m}\left(\frac{\partial \alpha_m}{\partial V}\right)_T\right]+\frac{1}{3\alpha_m}\left(\frac{\partial \alpha_m}{\partial T}\right)_v \tag{35}$$

where α_m is the macroscopic polarizability. The first two terms are the principal contributors in ionic materials: a positive thermal expansion coefficient α results in a negative thermo-optic coefficient and a positive change in polarizability with volume results in a positive thermo-optic coefficient. In ionic materials with a low melting point, thermal expansion is high and the thermo-optic coefficient is negative (typical of alkali halides); when thermal expansion is small (indicated by high melting point, hardness, and high elastic moduli), the thermo-optic coefficient is positive, dominated by the volume change in polarizability (typical of the high-temperature oxides).

Thermal expansion has no frequency dependence but polarizability does. At frequencies (wavelengths) near the edge of transparency, the polarizability (and $\partial \alpha_m/\partial V$) rises, and $\partial n/\partial T$ becomes more positive (or less negative). Figure 8 shows the variation of refractive index for sodium chloride as a function of frequency and temperature.

A formalism similar to the preceding for the thermo-optic coefficient can be used to estimate the photoelastic constants of a material. The simplest photoelastic constant is that produced by uniform pressure, i.e., dn/dP. More complex photoelastic constants are tensors whose components define the effect of individual strain (elasto-optic coefficients) or stress (piezo-optic coefficients) tensor terms. Bendow et al.,[53] calculate dn/dP and the

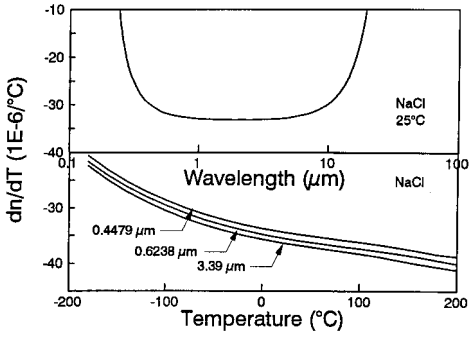

FIGURE 8 The thermo-optic coefficient (dn/dT) of sodium chloride (NaCl): (*a*) shows the wavelength dependence of room-temperature thermo-optic coefficient. The thermo-optic coefficient is nearly constant in the transparent region, but increases significantly at the edges of the transparent region; (*b*) illustrates the temperature dependence of the thermo-optic coefficient. The thermo-optic coefficient decreases (becomes more negative) with increasing temperature, primarily as the density decreases.

elasto-optic coefficients for a number of cubic crystals and compare the results to experiment.

Nonlinear Optical Coefficients. One of the most important higher-order optical coefficients is the nonlinear (or second-order) susceptibility. With the high electric fields generated by lasers, the nonlinear susceptibility gives rise to important processes such as second-harmonic generation, optical rectification, parametric mixing, and the linear electro-optic (Pockels) effect. The second-order susceptibility, $\chi^{(2)}$, is related to the polarization vector **P** by

$$\mathbf{P}_i(\omega) = \epsilon_0[\chi_{ij}\mathbf{E}_j + g\chi^{(2)}_{ijk}\mathbf{E}_j(\omega_1)\mathbf{E}_k(\omega_2)] \tag{36}$$

where g is a degeneracy factor arising from the nature of the electric fields applied. If the two frequencies are equal, the condition of optical rectification and second-harmonic generation (SHG) arises, and $g = \frac{1}{2}$. When the frequencies of $\mathbf{E}_j$ and $\mathbf{E}_k$ are different, parametric mixing occurs and $g = 1$. If $\mathbf{E}_k$ is a dc field, the situation is the same as the linear electro-optic (or Pockels) effect, and $g = 2$. The value of nonlinear susceptibility is a function of the frequencies of both the input fields and the output polarization ($\omega = \omega_1 \pm \omega_2$).

The nonlinear susceptibility is a third-order (3 by 3 by 3) tensor. A nonlinear optical coefficient $d^{(2)}$, frequently used to describe these nonlinear properties, is equal to one-half of the second-order nonlinear susceptibility, i.e., $d^{(2)} = \frac{1}{2}\chi^{(2)}$. Nonlinear optical coefficients are universally written in reduced (matrix) notation, d_{ij}, where the index $i = 1, 2,$ or 3 and the index j runs from 1 to 6.[54] (Both the piezo-electric coefficient and the nonlinear optical coefficient are given the symbol d, and the resulting confusion is enhanced because both coefficients have the same units.) The relationship between the electro-optic coefficient r and the nonlinear optical coefficient $d^{(2)}$ is

$$r_{ij} = \frac{2gd^{(2)}_{ji}}{\epsilon^2} \tag{37}$$

Units of the second-order nonlinear optical coefficient are m/V (or pm/V, where $\text{pm} = 10^{-12}$ m) in mks units.

Typical values of the nonlinear optical coefficients are listed in Table 4.[55] Additional nonlinear optical coefficients are given in reviews.[54,56,57]

Scatter. Scatter is both an intrinsic and extrinsic property. Rayleigh, Brillouin, Raman,

TABLE 4 Typical Nonlinear Optical Coefficients

Crystal	Nonlinear optical coefficient (pm/V)
β-BaB_2O_4	$d_{11} = 1.60$
KH_2PO_4	$d_{36} = 0.39$
LiB_3O_5	$d_{32} = 1.21$
$LiNbO_3$	$d_{31} = 5.07$
$LiIO_3$	$d_{31} = 3.90$
$KTiOPO_4$	$d_{31} = 5.85$
Urea	$d_{14} = 1.17$

and stoichiometric (index variation) contributions to scatter have been derived in simple form and used to estimate scatter loss in several fiber-optic materials.[58] Rayleigh scattering refers to elastic scatter from features small compared to the wavelength of light. In highly pure and defect-free optical crystals, Rayleigh scatter is caused by atomic scale inhomogeneities (much smaller than the wavelength) in analog to Rayleigh scatter from molecules in the atmosphere. In most materials, including glasses, Rayleigh scatter is augmented by extrinsic contributions arising from localized density variations (which also limit the uniformity of the refractive index). Attenuation in high-quality optical materials is frequently limited by Rayleigh scatter rather than absorption.

Brillouin and Raman scatter are forms of inelastic scattering from acoustic and optical phonons (vibrations). The frequency of the scattered light is shifted by the phonon frequency. Creation of phonons results in longer-wavelength (low-frequency) scattered light (Stokes case) and annihilation of phonons results in higher-frequency scattered light (anti-Stokes case). Rayleigh, Brillouin, and Raman scatter all have a λ^{-4} wavelength dependence. Polycrystalline and translucent materials have features such as grain boundaries and voids whose size is larger than the wavelength of light. This type of scatter is often called Mie scatter because the scattering features are larger than the wavelength of the light. Mie scatter typically has a measured λ^{-m} dependence where the parameter m typically lies between 1 and 2.[59,60] Rayleigh and Mie scatter may arise from either surface roughness or bulk nonuniformities.

Other Properties of Materials

Characterization of Crystals and Glasses. All materials are characterized by name(s) for identification, a chemical formula (crystalline materials) or approximate composition (glasses, amorphous substances), and a density (ρ, in kg/m^3). Crystalline materials are further identified by crystal class, space group, unit-cell lattice parameters, molecular weight (of a formula unit in atomic mass units, amu), and number of formula units per unit cell (Z). (See standard compilations of crystallographic data.[61,62])

Material Designation and Composition. Crystals are completely identified by both the chemical formulation and the space group. Chemical formulation alone is insufficient for identification because many substances have several structures (called polymorphs) with different properties. Properties in the data tables pertain only to the specific structure listed. Materials in the data tables having several stable polymorphs at room temperature include SiO_2 (eight polymorphs), C (diamond, graphite, and amorphous forms), and SiC and ZnS (both have cubic and hexagonal forms).

The space group also identifies the appropriate number of independent terms (see Tables 1 and 2) that describe a physical quantity. Noncubic crystals require two or more values to fully describe thermal expansion, thermal conductivity, refractive index, and other properties. Often, scalar quantities are given in the literature when a tensor characterization is needed. Such a characterization may be adequate for polycrystalline materials, but is unsatisfactory for single crystals that require knowledge of directional properties.

Optical glasses have been identified by traditional names derived from their composition and their dispersion relative to their index of refraction. Crown glasses have low dispersion (typically with Abbe number $\nu_d > 50$) and flint glasses have higher dispersion (typically, $\nu_d < 50$). More than a century ago, the crown and flint designations evolved to indicate primarily the difference between a standard soda-lime crown glass and that of flint glass which had a higher index and higher dispersion because of the addition of PbO to a silica base.

A more specific glass identifier is a six-digit number (defined in military standard

MIL-G-174) representing the first three digits of $(n_d - 1)$ and the first three digits of v_d. Each manufacturer also has its own designator, usually based on traditional names, that uniquely identifies each glass. For example, the glass with code 517624 has the following manufacturer's designations:

Manufacturer	Designation for glass 517624
Schott	BK-7
Corning	B-16-64
Pilkington	BSC-517642
Hoya	BSC-7
Ohara	BSL-7 (glass 516624)

Properties of glass are primarily determined from the compositions, but also depend on the manufacturing process, specifically the thermal history. In fact, refractive index specifications in a glass catalog should be interpreted as those obtained with a particular annealing schedule. Annealing removes stress (and minimizes stress-induced birefringence) and minimizes the effect of thermal history, producing high refractive-index uniformity. Special (*precision*) annealing designed to maximize refractive index homogeneity may, however, increase refractive index slightly above a nominal (catalog) value.

In general, both glass composition and thermal processing are proprietary (so the compositions given are only illustrative). However, manufacturers' data sheets on individual glasses can provide detailed and specific information on optical and mechanical properties. Also, the data sheets supply useful details on index homogeneity, climate resistance, stain resistance, and chemical (acid and alkaline) resistance for a particular glass type. For very detailed work or demanding applications, a glass manufacturer can supply a *melt data sheet* providing accurate optical properties for a specific glass lot.

Unit Cell Parameters, Molecular Weight, and Density. The structure and composition of crystals can be used to calculate density. This calculated (theoretical or x-ray) density should closely match that of optical-quality materials. Density ρ is mass divided by volume:

$$\rho = \frac{Z \cdot (\mathrm{MW}) \cdot u}{a \cdot b \cdot c \cdot \sqrt{\sin^2 \alpha + \sin^2 \beta + \sin^2 \gamma - 2(1 - \cos \alpha \cdot \cos \beta \cdot \cos \gamma)}} \tag{38}$$

where Z is the number of formula units in a crystal unit cell, MW is the molecular weight of a formula unit in amu, u is weight of an amu (Table 3), a, b, and c are unit cell axes lengths, and α, β, and γ are unit cell axes angles.

Typically, pure amorphous materials have lower density than the corresponding crystalline materials. Density of glasses and other amorphous materials is derived from measurements.

Elastic Properties. Elastic properties of materials can be described with a hierarchy of terms. On the atomic scale, interatomic force constants or potential energies can be used to predict the vibrational modes, thermal expansion, and elastic properties of a material. On the macroscopic scale, elastic properties are described using elastic moduli (or

constants) related to the directional properties of a material. The tensor relationships between stress (σ, a second-order tensor) and strain (**e**, a second-order tensor) are

$$\sigma_{ij} = \mathbf{c}_{ijkl} \cdot e_{kl}$$
$$e_{ij} = \mathbf{s}_{ijkl} \cdot \sigma_{kl} \tag{39a}$$

where the fourth-rank tensors $\mathbf{c}_{ijkl}$ and $\mathbf{s}_{ijkl}$ are named elastic stiffness **c** and elastic compliance **s**, respectively. This is the tensor form of Hooke's Law. Each index ($i, j, k,$ and l) has three values (i.e., $x, y,$ and z), hence the **c** and **s** tensors have 81 terms.

The stiffness and compliance tensors are usually written in a matrix notation made possible by the symmetry relationship of the stress and strain tensors. Symmetry reduces the number of independent terms in the stiffness and compliance tensors from 81 to 36. The usual notation for the reduced (matrix) notation form of the stiffness and compliance tensors is

$$\sigma_i = \mathbf{c}_{ij} \cdot e_j$$
$$e_i = \mathbf{s}_{ij} \cdot \sigma_j \tag{39b}$$

where the indices, an abbreviation of the ij or kl components, run from 1 to 6. Table 5 shows the conversion from tensor to matrix notation. Thus, the stiffness and compliance tensors are written as 6 by 6 matrices which can again be shown to be symmetric, given 21 independent terms. Virtually all data will be found in matrix notation. These tensors (matrices) that relate stress and strain are sometimes called *second-order* stiffness and compliance. Higher-order tensors are used to describe nonlinear elastic behavior (i.e., third-order stiffness determines the stress tensor from the square of the strain tensor).

Stiffness and compliance tensors are needed to completely describe the linear elastic properties of a crystal. Even a completely amorphous material has two independent constants that describe the relationship between stress and strain. Usually, the elastic properties of materials are expressed in terms of engineering (or technical) moduli: Young's modulus (E), shear modulus (or modulus of rigidity G), bulk modulus (B, compressibility^{-1}), and Poisson's ratio (ν). For example, Young's modulus is defined as the ratio of the longitudinal tension to the longitudinal strain for tension, a quantity which is anisotropic (i.e., directionally dependent) for all crystal classes (but is isotropic for amorphous materials). Therefore the engineering moduli only accurately describe the elastic behavior of isotropic materials. The engineering moduli also approximately describe the elastic behavior of polycrystalline materials (assuming small, randomly distributed grains). Various methods are available to estimate the engineering moduli of crystals.

TABLE 5 Matrix Notation for Stress, Strain, Stiffness, and Compliance Tensors

Tensor-to-matrix index conversion		Tensor-to-matrix element conversion	
Tensor indices ij or kl	Matrix indices m or n	Notation	Condition
11	1	$\sigma_m = \sigma_{ij}$ $e_m = e_{ij}$	$m = 1, 2, 3$
22	2	$\sigma_m = \sigma_{ij}$ $e_m = 2e_{ij}$	$m = 4, 5, 6$
33	3	$\mathbf{c}_{mn} = \mathbf{c}_{ijkl}$	all m, n
23 or 32	4	$\mathbf{s}_{mn} = \mathbf{s}_{ijkl}$	$m, n = 1, 2, 3$
13 or 31	5	$\mathbf{s}_{mn} = 2\mathbf{s}_{ijkl}$	$m = 1, 2, 3$ and $n = 4, 5, 6$ $m = 4, 5, 6$ and $n = 1, 2, 3$
12 or 21	6	$\mathbf{s}_{mn} = 4\mathbf{s}_{ijkl}$	$m, n = 4, 5, 6$

Values of the engineering moduli for crystalline materials given in the data tables are estimated from elastic moduli using the Voigt and Reuss methods (noncubic materials) or the Haskin and Shtrickman method[63] (cubic materials) to give shear and bulk moduli. Young's modulus and Poisson's ratio are then calculated assuming isotropy using the following relationships:

$$E = \frac{9 \cdot G \cdot B}{G + 3 \cdot B} \qquad \nu = \frac{3 \cdot B - 2 \cdot G}{6 \cdot B + 2 \cdot G} \tag{39c}$$

Hardness and Strength. Hardness is an empirical and relative measure of a material's resistance to wear (mechanical abrasion). Despite the qualitative nature of the result, hardness testing is quantitative, repeatable, and easy to measure. The first measure of hardness was the Mohs scale which compares the hardness of materials to one of 10 minerals. Usually, the Knoop indent test is used to measure hardness of optical materials. The test determines the resistance of a surface to penetration by a diamond indenter with a fixed load (usually 200 to 250 grams). The Knoop hardness number (in kg/mm^2) is the indenter mass (proportional to load) divided by the area of the indent. Figure 9 compares the Mohs and Knoop scales.[9]

Materials with Knoop values less than $100\,kg/mm^2$ are very soft, difficult to polish, and susceptible to handling damage. Knoop hardness values greater than 750 are quite hard. Typical glasses have hardness values of 350 to $600\,kg/mm^2$. Hardness qualitatively correlates to Young's modulus and to strength. Hardness of crystals is dependent on the orientation of the crystal axes with respect to the tested surface. Coatings can significantly alter hardness.

Strength is a measure of a material's resistance to fracture (or onset of plastic deformation). Strength is highly dependent on material flaws and therefore on the method of manufacture, as well as the method of measurement. For optical materials, strength is most conveniently measured in flexure; tensile strengths are typically 50 to 90 percent of those measured in flexure. Because of high variability in strength values, quoted strength values should only be used as a guide for comparision of materials. Strength of crystals

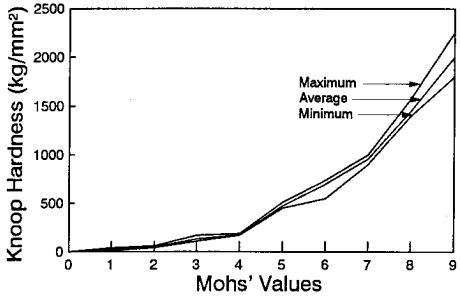

FIGURE 9 A comparison of Mohs and Knoop hardness scales.[9] The Mohs scale is qualitative, comparing the hardness of a material to one of 10 minerals: talc (Moh ≡ 1), gypsum (≡ 2), calcite (≡ 3), fluorite (≡ 4), apatite (≡ 5), orthoclase (≡ 6), quartz (≡ 7), topaz (≡ 8), sapphire (≡ 9), and diamond (Moh ≡ 10). The Knoop scale is determined by area of a mark caused by an indenter; the Knoop value is the indenter mass divided by the indented area. The mass of the indenter (load) is usually specified; 200 or 500 grams are typical. (*Reprinted by permission of Ashlee Publishing Company.*)

TABLE 6 Fracture Toughness of Some Materials

Material	Fracture toughness, $MPa \cdot m^{1/2}$	Material	Fracture toughness, $MPa \cdot m^{1/2}$
Al_2O_3	3	$MgAl_2O_4$	1.5
ALON	1.4	MgF_2	1.0
AlN	3	Si	0.95
C, diamond	2.0	fused SiO_2	0.8
CaF_2	0.5	Y_2O_3	0.7
$CaLa_2S_4$	0.68	ZnS	0.5 0.8 (CVD)
GaP	0.9	ZnSe	0.33
Ge	0.66	$ZrO_2{:}Y_2O_3$	2.0

also is dependent on the orientation of the crystal axes with respect to the applied stress. Applications requiring high strength to avoid failure should use large safety margins (typically a factor of four) over average strength whenever possible.

Fracture toughness is another measure of strength, specifically, a material's ability to resist crack propagation. Fracture toughness measures the applied stress required to enlarge a flaw (crack) of given size and has units of $MPa \cdot m^{1/2}$. Values for representative materials are given in Table 6.

Characteristic Temperatures. Characteristic temperatures of crystalline materials are those of melting (or vaporization or decomposition) and phase transitions. Of particular importance are the phase-transition temperatures. These temperatures mark the boundaries of a particular structure. A phase transition can mean a marked change in properties. One important phase-transition point is the Curie temperature of ferroelectric materials. Below the Curie temperature, the material is ferroelectric; above this temperature it is paraelectric. The Curie temperature phase transition is particularly significant because the change in structure is accompanied by drastic changes in some properties such as the static dielectric constant which approaches infinity as temperature nears the Curie temperature. This transition is associated with the lowest transverse optical frequency (the *soft mode*) approaching zero [hence the static dielectric constant approaches infinity from the Lyddane-Sachs-Teller relationship, Eq. (11)].

The term *glass* applies to a material that retains an amorphous state upon solidification. More accurately, glass is an undercooled, inorganic liquid with a very high viscosity at room temperature and is characterized by a gradual softening with temperature and a hysteresis between glass and crystalline properties. The gradual change in viscosity with temperature is characterized by several temperatures, especially the glass transition temperature and the softening-point temperature. The glass transition temperature defines a second-order phase transition analogous to melting. At this temperature, the temperature dependence of various properties changes (in particular, the linear thermal expansion coefficient) as the material transitions from a liquid to glassy state. Glasses can crystallize if held above the transition temperature for sufficient time. The annealing point is defined as the temperature resulting in a glass viscosity of 10^{13} poise and at which typical glasses can be annealed within an hour or so. In many glasses, the annealing point and the glass transition temperature are close. In an optical system, glass elements need to be kept 150 to 200°C below the glass transition temperature to avoid significant surface distortion. At the *softening temperature,* viscosity is $10^{7.6}$ poise and glass will rapidly deform under its own weight; glasses are typically molded at this temperature. Glasses do not have a true melting point; they become progressively softer (more viscous) with increased temperature. Other amorphous materials may not have a well-defined glass transition; instead they

may have a conventional melting point. Glasses that crystallize at elevated temperature also have a well-defined mellting point.

Glass-ceramics have been developed which are materials with both glasslike and crystalline phases. In particular, low-thermal-expansion ceramics comprise a crystalline phase with a negative thermal expansion and a vitreous phase with a positive thermal expansion. Combined, the two phases result in very high dimensional stability. Typically, the ceramics are made like other glasses, but after stresses are removed from a blank, a special heat-treatment step forms the nuclei for the growth of the crystalline component of the ceramic. Although not strictly ceramics, similar attributes can be found in some two-phase glasses.

Heat Capacity and Debye Temperature. Heat capacity, or specific heat, a scalar quantity, is the change in thermal energy with a change in temperature. Units are typically J/(gm · K). Debye developed a theory of heat capacity assuming that the energy was stored in acoustical photons. This theory, which assumes a particular density of states, results in a Debye molar heat capacity (units = J/(mole · K)) of the form

$$C_V(T) = 9mN_A k_B \left(\frac{T}{\theta_D}\right)^3 \int_0^{\theta_D/T} \frac{x^4 e^x}{(e^x - 1)^2}\, dx \tag{40a}$$

where C_V is the molar heat capacity in J/(mole · K) per unit volume, θ_D is the Debye temperature, m the number of atoms per formula unit, N_A is Avogadro's number, and k_B is Boltzmann's constant. At low temperatures ($T \to 0$ K), heat capacity closely follows the T^3 law of Debye theory

$$C_V(T) = \frac{12\pi^4}{5} mN_A k_B \left(\frac{T}{\theta_D}\right)^3 = 1943.76 \text{ J/(mole} \cdot \text{K)} \cdot \text{m} \left(\frac{T}{\theta_D}\right)^3 \qquad (T \ll \theta_D) \tag{40b}$$

and the high-temperature (classical) limit is

$$C_V(T) = 3mN_A k_B = 24.943 \text{ J/(mole} \cdot \text{K)} \cdot \text{m} \qquad (T \gg \theta_D) \tag{40c}$$

If heat capacity data are fit piecewise to the Debye equation, a temperature-dependent θ_D can be found. Frequently, a Debye temperature is determined from room-temperature elastic constants, and is therefore different from the low-temperature value. The Debye temperature given in the tables is, when possible, derived from low-temperature heat capacity data.

The Debye equations can be used to estimate heat capacity C_V over the entire temperature range, typically to within 5 percent of the true value using a single Debye temperature value. Usually, however, C_P, the constant pressure heat capacity, rather than C_V, is desired. At low temperatures, thermal expansion is small, and $C_P \approx C_V$. At elevated temperature, the relationship between C_V and C_P is given by the thermodynamic relationship

$$C_P(T) = C_V(T) + 9\alpha^2 TVB \tag{41}$$

where T is temperature (K), V is the molar volume (m^3/mole), α is the thermal expansion coefficient, and B is the bulk modulus (Pa = Nt/m^2).

Molar heat capacity can be converted to usual units by dividing by the molecular weight (see the physical property tables for crystals) in g/mole. Since molar heat capacity

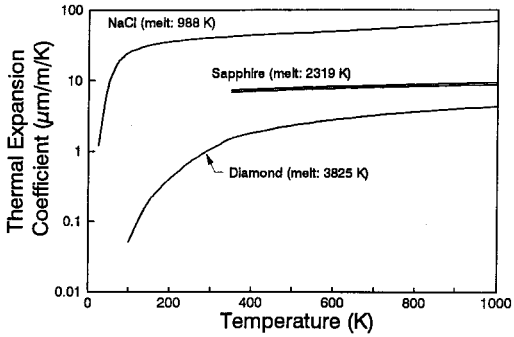

FIGURE 10 Thermal expansion of several materials. Expansion arises from the anharmonicity of the interatomic potential. At low temperature, expansion is very low and the expansion coefficient is low. As temperature increases, the expansion coefficient rises, first quickly, then less rapidly.

approaches the value of 24.943 J/(mole · K), the heat capacity per unit weight is inversely proportional to molecular weight at high temperature (i.e., above the Debye temperature).

Thermal Expansion. The linear thermal expansion coefficient α is the fractional change in length with a change in temperature as defined by

$$\alpha(T) = \frac{1}{L}\frac{dL}{dT} \tag{42a}$$

and units are 1/K. The units of length are arbitrary. Thermal expansion is a second-rank tensor; nonisometric crystals have a different thermal expansion coefficient for each principal direction. At low temperature, thermal expansion is low, and the coefficient of thermal expansion approaches zero as $T \to 0$. The expansion coefficient generally rises with increasing temperature; Fig. 10 shows temperature dependence of the expansion coefficient for several materials. Several compilations of data exist.[64,65]

The volume expansion coefficient α_V is the fractional change in volume with an increase in temperature. For a cubic or isotropic material with a single linear thermal expansion coefficient,

$$\alpha_V(T) = \frac{1}{V}\frac{dV}{dT} = 3\alpha \tag{42b}$$

which can be used to estimate the temperature change of density.

The Grüneisen relationship relates the thermal expansion coefficient to molar heat capacity

$$\alpha(T) = \frac{\gamma C_V(T)}{3B_0V_0} \tag{42c}$$

where B_0 is the bulk modulus at $T = 0$ K, V_0 is the volume at $T = 0$ K, and γ is the Grüneisen parameter. This relationship shows that thermal expansion has the same temperature dependence as the heat capacity. Typical values of γ lie between 1 and 2.

Thermal Conductivity. Thermal conductivity κ determines the rate of heat flow through a material with a given thermal gradient. Conductivity is a second-rank tensor with up to

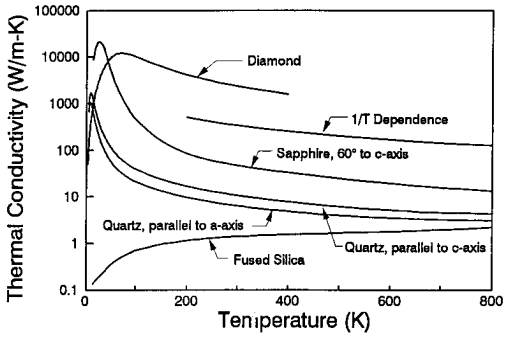

FIGURE 11 Thermal conductivity of several materials. The thermal conductivity of materials initially rises rapidly as the heat capacity increases. Peak thermal conductivity of crystals is high due to the long phonon mean free path of the periodic structure which falls with increasing temperature as the phonon free path length decreases ($\approx 1/T$). The phonon mean free path of amorphous materials is small and nearly independent of temperature, hence thermal conductivity rises monotonically and approaches the crystalline value at high temperature.

three principal values. This property is especially important in relieving thermal stress and optical distortions caused by rapid heating or cooling. Units are $W/(m \cdot K)$.

Kinetic theory gives the following expression for thermal conductivity κ

$$\kappa = \tfrac{1}{3} C_V v \ell \tag{43}$$

where v is the phonon (sound) velocity and ℓ is the phonon mean free path. At very low temperature ($T < \theta_D/20$), temperature dependence of thermal conductivity is governed by C_V, which rises as T^3 [see Eq. (40*b*)]. At high temperature ($T > \theta_D/10$), the phonon mean free path is limited by several mechanisms. In crystals, scattering by other phonons usually governs ℓ. In the high-temperature limit, the phonon density rises proportional to T and thermal conductivity is inversely proportional to T. Figure 11 illustrates the temperature dependence of thermal conductivity of several crystalline materials.

Thermal conductivity in amorphous substances is quite different compared to crystals. The phonon mean free path in glasses is significantly less than in crystals, limited by structural disorder. The mean free path of amorphous materials is typically the size of the fundamental structural units (e.g., 10 Å) and has little temperature dependence; hence the temperature dependence of thermal conductivity is primarily governed by the temperature dependence of heat capacity. At room temperature, the thermal conductivity of oxide glasses is a factor of 10 below typical oxide crystals. Figure 11 compares the thermal conductivity of fused silica to crystalline silica (quartz).

Thermal conductivity of crystals is highly dependent on purity and order. Mixed crystals, second-phase inclusion, nonstoichiometry, voids, and defects can all lower the thermal conductivity of a material. Values given in the data table are for the highest-quality material. Thermal conductivity data are found in compilations[65] and reviews.[66]

Correlation of Properties. All material properties are correlated to a relatively few factors, e.g., constituent atoms, the bonding between the atoms, and the structural symmetry. The binding forces, or chemical bonds, play a major role in properties. Tightly bonded materials have high moduli, high hardness and strength, and high Debye

temperature (hence high room-temperature thermal conductivity). Strong bonds also mean lower thermal expansion, lower refractive index, higher-frequency optical vibrational modes (hence less infrared transparency), and higher energy band gaps (hence more ultraviolet transparency). Increased mass of the constituent atoms lowers the frequency of both electronic and ionic resonances. Similarly, high structural symmetry can increase hardness and eliminate (to first order) ionic vibrations (cf., diamond, silicon, and germanium).

Combinations of Properties. A given material property is influenced by many factors. For example, the length of a specimen is affected by stress (producing strain), by electric fields (piezo-electric effect), and by temperature (thermal expansion). The total strain is then a combination of these linear effects and can be written as

$$\Delta e_{ij} = \left(\frac{\partial e_{ij}}{\partial \sigma_{kl}}\right)_{E,T} \Delta\sigma_{kl} + \left(\frac{\partial e_{ij}}{\partial E_k}\right)_{\sigma,T} \Delta E_k + \left(\frac{\partial e_{ij}}{\partial T}\right)_{\sigma,E} \Delta T$$
$$\Delta e_{ij} = s_{ijkl}\,\Delta\sigma_{kl} + d_{ijk}\,\Delta E_k + \alpha_{ij}\,\Delta T \tag{44}$$

Often, these effects are interrelated, and frequently dependent on measurement conditions. Some properties of some materials are very sensitive to measurement conditions (the subscripts in the preceding equation denote the variable held constant for each term). For example, if the measurement conditions for the elastic contribution were adiabatic, stress will cause temperature to fall, which, in turn, decreases strain (assuming positive thermal expansion coefficient). Thus the elastic contribution to strain is measured under isothermal (and constant **E** field) conditions so as not to include the temperature effects already included in the thermal expansion term.

The conditions of measurement are given a variety of names that may cause confusion. For example, the mechanical state of ''clamped,'' constant volume, and constant strain all refer to the same measurement condition which is paired with the corresponding condition of ''free,'' ''unclamped,'' constant pressure, or constant stress. In many cases, the condition of measurement is not reported and probably unimportant (i.e., different conditions give essentially the same result). Another common measurement condition is constant **E** field (''electrically free'') or constant **D** field (''electrically clamped'').

Some materials, particularly ferroelectrics, have large property variation with temperature and pressure, hence measurement conditions may greatly alter the data. The piezoelectric effect contributes significantly to the clamped dielectric constant of ferroelectrics. The difference between the isothermal clamped and free dielectric constants is

$$\epsilon_0 \cdot (\epsilon_i^e - \epsilon_i^\sigma) = -d_{ij} d_{ik} c_{jk}^{\mathbf{E}} \tag{45}$$

where d_{ij} is the piezo-electric coefficient and $c_{jk}^{\mathbf{E}}$ is the (electrically free) elastic stiffness. If the material structure is centrosymmetric, all components of d_{ij} vanish, and the two dielectric constants are the same.

33.5 PROPERTIES TABLES

The following tables summarize the basic properties for representative crystals and glasses. In general, the presented materials are (1) of general interest, (2) well-characterized (within the limitations imposed by general paucity of data and conflicting property values), and (3) represent a wide range of representative types and properties. Few

materials can be regarded as well-characterized. Crystalline materials are represented by alkali halides, oxides, chalcogenides, and a variety of crystals with nonlinear, ferroelectric, piezoelectric, and photorefractive materials.

The physical property tables define the composition, density, and structure (of crystalline materials). Table 7 gives data for over 90 crystalline materials. Table 8 gives similar data for 30 representative "optical" glasses intended for visible and near-infrared use (typically to 2.5 μm). Table 9 gives physical property data for 24 specialty glasses and substrate materials. The specialty glasses include fused silica and germania, calcium aluminate, fluoride, germanium-, and chalcogenide-based glasses, many of which are intended for use at longer wavelengths. The three substrate materials, Pyrex, Zerodur, and ULE, are included because of their widespread use for mirror blanks.

Mechanical properties for crystals are given in two forms, room-temperature elastic constants (or moduli) for crystals (Tables 10 through 15), and engineering moduli, flexure strength, and hardness for both crystals (Table 16) and glasses (Table 17). Engineering moduli for crystalline materials should only be applied by polycrystalline forms of these materials. Accurate representation of the elastic properties of single crystals requires the use of elastic constants in tensor form. Strength is highly dependent on manufacture method and many have significant sample-to-sample variability. These characteristics account for the lack of strength data. For these reasons, the provided strength data is intended only as a guide. Glasses and glass-ceramics flexure strengths typically range from 30 to 200 MPa, although glass fibers with strength exceeding 1000 MPa have been reported.

Thermal properties are given in Tables 18 and 19 for crystals and glasses, respectively. Characteristic temperatures (Debye, phase change, and melt for crystals; glass transitions, soften, and melt temperatures for glasses), heat capacity, thermal expansion, and thermal conductivity data are included. Directional thermal properties of crystals are given when available. Only room-temperature properties are reported except for thermal conductivity of crystals, which is also given for temperatures above and below ambient, if available.

Optical properties are summarized in Tables 20 and 21 for crystals and glasses, respectively. These tables give the wavelength boundaries of the optical transparent region (based on a 1-cm^{-1} absorption coefficient), $\bar{n}_\infty$, the electronic contribution to the refractive index, and values of dn/dT at various wavelengths. Tables 22 and 23 give dispersion formulas for crystals and glasses. Tables 24, 25, 26, 27, and 28 give tabular refractive index data for some crystals.

Vibrational characteristics of many optical materials are summarized in Tables 29 through 44 for a number of common optical crystal types. These tables give number and type of zone-center (i.e., the wave vector ≈ 0, where Γ is the usual symbol denoting the center of the Brillouin zone) optical modes predicted by group theory (and observed in practice) as well as the frequency (in wave number) of the infrared-active and Raman modes. Mulliken notation is used. Table 45 summarizes the available lattice vibration dispersion models for many crystals.

Table 46 summarizes Urbach tail parameters [Eq. (15)] for several crystals. Table 47 gives room-temperature ultraviolet and infrared absorption edge parameters for a number of glasses. These parameters are given in a form similar to Eqs. (15*a*) and (17*a*) for exponential absorption edges:

$$\begin{aligned} \beta_{\mathrm{ABS}} &= \beta_0(\mathrm{UV}) \exp\left(\sigma_{\mathrm{UV}} E\right) = \beta_0(\mathrm{UV}) \exp\left[\frac{1.24\sigma_{\mathrm{UV}}}{\lambda}\right] \\ \beta_{\mathrm{ABS}} &= \beta_0(\mathrm{IR}) \exp\left(-\sigma_{\mathrm{IR}} \nu\right) \end{aligned} \tag{46}$$

where **E** is energy in eV, λ is wavelength in micrometers, and ν is wave number in cm^{-1}. Table 48 summarizes available room-temperature infrared absorption edge parameters for a number of crystalline and amorphous materials in the format of Eq. (17*a*).

TABLE 7 Composition, Structure, and Density of Crystals

Material	Crystal system & space group	Unit cell dimension (Å)	Molecular weight (amu)	Formulae/ unit cell	Density (g/cm^3)
Ag_3AsS_3	Hexagonal	a = 10.80	494.72	6	5.615
(proustite)	R3c (C_{3v}^6) #161	c = 8.69			
AgBr	Cubic	5.7745	187.77	4	6.477
(bromyrite)	Fm3m (O_h^5) #225				
AgCl	Cubic	5.547	143.32	4	5.578
(cerargyrite)	Fm3m (O_h^5) #225				
$AgGaS_2$	Tetragonal	a = 5.757	241.72	4	4.701
	$I\bar{4}2d$ (D_{2d}^{12}) #122	c = 10.304			
$AgGaSe_2$	Tetragonal	a = 5.973	335.51	4	5.741
	$I\bar{4}2d$ (D_{2d}^{12}) #122	c = 10.88			
β-AgI	Hexagonal	a = 4.5924	234.77	2	5.684
(iodyrite)	$P6_3mc$ (C_{6v}^4) #186	c = 7.5104			
AlAs	Cubic	5.6611	101.90	4	3.731
	$F\bar{4}3m$ (T_d^2) #216				
AlN	Hexagonal	a = 3.1127	40.988	2	3.257
	$P6_3mc$ (C_{6v}^4) #186	c = 4.9816			
Al_2O_3	Hexagonal	a = 4.759	101.96	6	3.987
(sapphire, alumina)	$R\bar{3}c$ (D_{3d}^6) #167	c = 12.989			
$Al_{23}O_{27}N_5$, ALON	Cubic	7.948	1122.59	1	3.713
	Fd3m (O_h^7) #227				
$Ba_3[B_3O_6]_2$, BBO	Hexagonal	a = 12.547	668.84	6	3.838
	R3 (C_3^4) #146	c = 12.736			
BaF_2	Cubic	6.2001	175.32	4	4.886
	Fm3m (O_h^5) #225				
$BaTiO_3$	Tetragonal	a = 39920	233.21	1	6.021
	$P4_2/mnm$ (D_{4h}^{14}) #136	c = 4.0361			
BeO	Hexagonal	a = 2.693	25.012	2	3.009
(bromellite)	$P6_3mc$ (C_{6v}^4) #186	c = 4.395			
$Bi_{12}GeO_{20}$, BGO	Cubic	10.143	2900.43	2	9.231
	I23 (T^3) #197				
$Bi_{12}SiO_{20}$, BSO	Cubic	10.1043	2855.84	2	9.194
(sellenite)	I23 (T^3) #197				
BN	Cubic	3.6157	24.818	4	3.489
	$F\bar{4}3m$ (T_d^2) #216				
BP	Cubic	4.538	41.785	4	2.970
	$F\bar{4}3m$ (T_d^2) #216				
C	Cubic	3.56696	12.011	8	3.516
(diamond)	Fd3m (O_h^7) #227				
$CaCO_3$	Hexagonal	a = 4.9898	100.09	6	2.711
(calcite)	$R\bar{3}c$ (D_{3d}^5) #167	c = 17.060			
CaF_2	Cubic	5.46295	78.07	4	3.181
(fluorite)	Fm3m (O_h^5) #225				
$CaLa_2S_4$	Cubic	8.685	446.15	4	4.524
	$I\bar{4}3d$ (T_d^6) #220				
$CaMoO_4$	Tetragonal	a = 5.23	200.02	4	4.246
(powellite)	$I4_1/a$ (C_{4h}^6) #88	c = 11.44			
$CaWO_4$	Tetragonal	a = 5.243	287.93	4	6.116
(scheelite)	$I4_1/a$ (C_{4h}^6) #88	c = 11.376			
$CdGeAs_2$	Tegragonal	a = 5.9432	334.86	4	5.614
	$I\bar{4}2d$ (D_{2d}^{12}) #122	c = 11.216			
CdS	Hexagonal	a = 4.1367	144.48	2	4.821
(greenockite)	$P6_3mc$ (C_{6v}^4) #186	c = 6.7161			
CdSe	Hexagonal	a = 4.2972	191.37	2	5.672
	$P6_3mc$ (C_{6v}^4) #186	c = 7.0064			

TABLE 7 Composition, Structure, and Density of Crystals (*Continued*)

Material	Crystal system & space group	Unit cell dimension (Å)	Molecular weight (amu)	Formulae/ unit cell	Density (g/cm^3)
CdTe	Cubic $F\bar{4}3m$ (T_d^2) #216	6.4830	240.01	4	5.851
CsBr	Cubic $Pm3m$ (O_h^5) #221	4.286	212.81	1	4.488
CsCl	Cubic $Pm3m$ (O_h^5) #221	4.121	168.36	1	3.995
CsI	Cubic $Pm3m$ (O_h^5) #221	4.566	259.81	1	4.532
CuCl (nantokite)	Cubic $F\bar{4}3m$ (T_d^2) #216	5.416	98.999	4	4.139
$CuGaS_2$	Tetragonal $I\bar{4}2d$ (D_{2d}^{12}) #122	a = 5.351 c = 10.480	197.40	4	4.369
GaAs	Cubic $F\bar{4}3m$ (T_d^2) #216	5.65325	144.64	4	5.317
GaN	Hexagonal $P6_3mc$ (C_{6v}^4) #186	a = 3.186 c = 5.178	83.73	2	6.109
GaP	Cubic $F\bar{4}3m$ (T_d^2) #216	5.4495	100.70	4	4.133
Ge	Cubic $Fd3m$ (O_h^7) #227	5.65741	72.61	8	5.327
InAs	Cubic $F\bar{4}3m$ (T_d^2) #216	6.0584	189.74	4	5.668
InP	Cubic $F\bar{4}3m$ (T_d^2) #216	5.8688	145.79	4	4.791
KBr	Cubic $Fm3m$ (O_h^5) #225	6.600	119.00	4	2.749
KCl	Cubic $Fm3m$ (O_h^5) #225	6.293	74.55	4	1.987
KF	Cubic $Fm3m$ (O_h^5) #225	5.347	58.10	4	2.524
KH_2PO_4, KDP	Tetragonal $I\bar{4}2d$ (D_{2d}^{12}) #122	a = 7.452 c = 6.959	136.09	4	2.339
KI	Cubic $Fm3m$ (O_h^5) #225	7.065	166.00	4	3.127
$KNbO_3$	Orthorhombic $Bmm2$ (C_{2v}^{14}) #38	a = 5.6896 b = 3.9692 c = 5.7256	180.00	2	4.621
$KTaO_3$	Cubic $Pm3m$ (O_h^5) #221	3.9885	268.04	1	7.015
$KTiOPO_4$, KTP	Orthorhombic $Pna2_1$ (C_{2v}^9) #33	a = 12.8172 b = 6.4029 c = 10.5885	197.95	8	3.025
LaF_3	Hexagonal $P\bar{3}c1$ (D_{3v}^4) #165	a = 7.183 c = 7.352	195.90	6	5.941
LiB_3O_5, LBO	Orthorhombic $Pna2_1$ (C_{2v}^9) #33	a = 8.4473 b = 7.3788 c = 5.1395	238.74	4	2.475
LiF	Cubic $Fm3m$ (O_h^5) #225	4.0173	25.939	4	2.657
α-$LiIO_3$	Hexagonal $P6_3$ (C_6^6) #173	a = 5.4815 c = 5.1709	181.84	2	4.488
$LiNbO_3$	Hexagonal $R3c$ (C_{3v}^6) #161	a = 5.1483 c = 13.8631	147.85	6	4.629

TABLE 7 Composition, Structure, and Density of Crystals (*Continued*)

Material	Crystal system & space group	Unit cell dimension (Å)	Molecular weight (amu)	Formulae/ unit cell	Density (g/cm^3)
$LiYF_4$, YLF	Tetragonal $I4_1/a$ (C_{4h}^6) #88	a = 5.175 c = 10.74	171.84	4	3.968
$MgAl_2O_4$ (spinel)	Cubic Fd3m (O_h^7) #227	8.084	142.27	8	3.577
MgF_2 (sellaite)	Tetragonal $P4_2/mnm$ (D_{4h}^{14}) #136	a = 4.623 c = 3.053	62.302	2	3.171
MgO (periclase)	Cubic Fm3m (O_h^5) #225	4.2117	40.304	4	3.583
NaBr	Cubic Fm3m (O_h^5) #225	5.9732	102.89	4	3.207
NaCl (halite, rock salt)	Cubic Fm3m (O_h^5) #225	5.63978	58.44	4	2.164
NaF (valliaumite)	Cubic Fm3m (O_h^5) #225	4.6342	41.99	4	2.802
NaI	Cubic Fm3m (O_h^5) #225	6.475	149.89	4	3.668
$[NH_4]_2CO$ (urea, carbamide)	Tetragonal $I\bar{4}2_1m$ (D_{2d}^3) #113	a = 5.661 c = 4.712	60.056	2	1.321
$NH_4H_2PO_4$, ADP	Tetragonal $I\bar{4}2d$(D_{2d}^{12}) #122	a = 7.4997 c = 7.5494	115.03	4	1.799
PbF_2	Cubic Fm3m (O_h^5) #225	5.951	245.20	4	7.728
$PbMoO_4$ (wulfenite)	Tetragonal $I4_1/a$ (C_{4h}^6) #88	a = 5.4312 c = 12.1065	367.14	4	6.829
PbS (galena)	Cubic Fm3m (O_h^5) #225	5.935	239.26	4	7.602
PbSe (clausthalite)	Cubic Fm3m (O_h^5) #225	6.122	286.16	4	8.284
PbTe (altaite)	Cubic Fm3m (O_h^5) #225	6.443	334.80	4	8.314
$PbTiO_3$	Tetragonal $P4_2/mnm$ (D_{4h}^{14}) #136	a = 3.8966 c = 4.1440	303.08	1	7.999
Se	Hexagonal $P3_121$ (D_3^4) #152	a = 4.35448 c = 4.94962	78.96	3	4.840
Si	Cubic Fd3m (O_h^7) #227	5.43085	28.0855	8	2.329
β-SiC (3C)	Cubic $F\bar{4}3m$ (T_d^2) #216	4.3596	40.097	4	3.214
α-SiC (2H)	Hexagonal $P6_3mc$ (C_{6v}^4) #186	a = 3.0763 c = 5.0480	40.097	2	3.219
SiO_2 (α-quartz)	Hexagonal $P3_221$ (D_3^6) #154	a = 4.9136 c = 5.4051	60.084	3	2.648
SrF_2	Cubic Fm3m (O_h^5) #225	5.7996	125.62	4	4.277
$SrMoO_4$	Tetragonal $I4_1/a$ (C_{4h}^6) #88	a = 5.380 c = 11.97	247.56	4	7.746
$SrTiO_3$	Cubic Pm3m (O_h^5) #221	3.9049	183.50	1	5.117
Te	Hexagonal $P3_121$ (D_3^4) #152	a = 4.44693 c = 5.91492	127.60	3	6.275
TeO_2 (paratellurite)	Tetragonal $P4_12_12$ (D_4^4) #92	a = 4.810 c = 7.613	159.60	4	6.019
TiO_2 (rutile)	Tetragonal $P4_2/mnm$ (D_{4h}^{14}) #136	a = 4.5937 c = 2.9618	79.879	2	4.245

TABLE 7 Composition, Structure, and Density of Crystals (*Continued*)

Material	Crystal system & space group	Unit cell dimension (Å)	Molecular weight (amu)	Formulae/ unit cell	Density (g/cm^3)
Tl_3AsSe_3, TAS	Hexagonal R3m (C_{3v}^5) #160	a = 9.870 c = 7.094	924.95	3	7.70
TlBr	Cubic Pm3m (O_h^5) #221	3.9846	284.29	1	7.462
Tl[Br, I], KRS-5	Cubic Pm3m (O_h^5) #221	4.108	307.79	1	7.372
TlCl	Cubic Pm3m (O_h^5) #221	3.8452	239.84	1	7.005
Tl[0.7Cl, 0.3Br], KRS-6	Cubic Pm3m (O_h^5) #221		253.17	1	
$Y_3Al_5O_{12}$, YAG	Cubic Ia3d (O_h^{10}) #230	12.008	593.62	8	4.554
Y_2O_3 (yttria)	Cubic Ia3 (T_h^7) #206	10.603	225.81	16	5.033
$ZnGeP_2$	Tetragonal $I\bar{4}2d$ (D_{2d}^{12}) #122	a = 5.466 c = 10.722	199.95	4	4.146
ZnO (zincite)	Hexagonal $P6_3mc$ (C_{6v}^4) #186	a = 3.242 c = 5.176	81.39	2	5.737
β-ZnS (zincblende)	Cubic $F\bar{4}3m$ (T_d^2) #216	5.4094	97.456	4	4.090
α-ZnS (wurtzite)	Hexagonal $P6_3mc$ (C_{6v}^4) #186	a = 3.8218 c = 6.2587	97.456	2	4.088
ZnSe	Cubic $F\bar{4}3m$ (T_d^2) #216	5.6685	144.34	4	5.264
ZnTe	Cubic $F\bar{4}3m$ (T_d^2) #216	6.1034	192.99	4	5.638
ZrO_2:0.12Y_2O_3 (cubic zirconia)	Cubic Fm3m (O_h^5) #225	5.148	121.98	4	5.939

TABLE 8 Physical Properties of Optical Glasses

Glass type	Selected glass code	Density (g/cm^3)	Example composition (for the general type)
Deep crown	479587 TiK1	2.39	Alkali alumo-borosilicate glass
Fluor crown	487704 FK5	2.45	(Boro)phosphide glass w/high fluoride content
Titanium flint	511510 TiF1	2.47	Titanium alkali alumoborosilicate glass
Borosilicate	517642 BK7	2.51	70%SiO_2, 10%B_2O_3, 8%Na_2O, 8%K_2O, 3%BaO, 1%CaO
Phosphate crown	518651 PK2	2.51	70%P_2O_5, 12%K_2O, 10%Al_2O_3, 5%CaO, 3%B_2O_3
Crown	522595 K5	2.59	74%SiO_2, 11%K_2O, 9%Na_2O, 6%CaO
Crown flint	523515 KF9	2.71	67%SiO_2, 16%Na_2O, 12%PbO, 3%ZnO, 2%Al_2O_3
Light barium crown	526600 BaLK1	2.70	Borosilicate glass
Antimony flint	527511 KzF6	2.54	Antimony borosilicate glass
Zinc crown	533580 ZK1	2.71	71%SiO_2, 17%Na_2O, 12%ZnO
Extra light flint	548458 LLF1	2.94	63%SiO_2, 24%PbO, 8%K_2O, 5%Na_2O
ULTRAN 30	548743	4.02	
Dense phosphate crown	552635 PSK3	2.91	60%P_2O_5, 28%BaO, 5%Al_2O_3, 3%B_2O_3
Barium crown	573575 BaK1	3.19	60%SiO_2, 19%BaO, 10%K_2O, 5%ZnO, 3%Na_2O, 3%B_2O_3
Light barium flint	580537 BaLF4	3.17	51%SiO_2, 20%BaO, 14%ZnO, 6%Na_2O, 5%K_2O, 4%PbO
Light flint	581409 LF5	3.22	53%SiO_2, 34%PbO, 8%K_2O, 5%Na_2O
Special long crown	586610 LgSK2	4.15	Alkali earth aluminum fluoroborate glass
Fluor flint*	593355 FF5	2.64	

TABLE 8 Physical Properties of Optical Glasses (*Continued*)

Glass type	Selected glass code	Density (g/cm^3)	Example composition (for the general type)
Dense barium crown	613586 SK4	3.57	39%SiO_2, 41%BaO, 15%B_2O_3, 5%Al_2O_3
Special short flint	613443 KzFSN4	3.20	Aluminum lead borate glass
Extra-dense barium crown	618551 SSK4	3.63	35%SiO_2, 42%BaO, 10%B_2O_3, 8%ZnO, 5%Al_2O_3
Flint	620364 F2	3.61	47%SiO_2, 44%PbO, 7%K_2O, 2%Na_2O
Dense barium flint	650392 BaSF10	3.91	43%SiO_2, 33%PbO, 11%BaO, 7%K_2O, 5%ZnO, 1%Na_2O
Barium flint*	670472 BaF10	3.61	46%SiO_2, 22%PbO, 16%BaO, 8%ZnO, 8%K_2O
Lanthanum crown	720504 LaK10	3.81	Silicoborate glass w. rare earth oxides
Tantalum crown*	741526 TaC2	4.19	$B_2O_3/La_2O_3/ThO_2$/RO
Niobium flint*	743492 NbF1	4.17	
Lanthanum flint	744447 LaF2	4.34	Borosilicate glass w. rare earth oxides
Dense flint	805254 SF6	5.18	33%SiO_2, 62%PbO, 5%K_2O
Dense tantalum flint*	835430 TaFD5	4.92	$B_2O_3/La_2O_3/ThO_2/Ta_2O_3$

* Hoya glasses; others are Schott glasses.

TABLE 9 Physical Properties of Specialty Glasses and Substrate Materials

Glass type	Density (g/cm^3)	Typical composition
Fused silica (SiO_2) (e.g., Corning 7940)	2.202	100%SiO_2
Fused germania (GeO_2)	3.604	100%GeO_2
BS-39B (Barr & Stroud)	3.1	50%CaO, 34%Al_2O_3, 9%MgO
CORTRAN 9753 (Corning)	2.798	29%SiO_2, 29%CaO, 42%Al_2O_3
CORTRAN 9754 (Corning)	3.581	33%GeO_2, 20%CaO, 37%Al_2O_3, 5%BaO, 5%ZnO
IRG 2 (Schott)	5.00	Germanium glass
IRG 9 (Schott)	3.63	Fluorophosphate glass
IRG 11 (Schott)	3.12	Calcium aluminate glass
IRG 100 (Schott)	4.67	Chalcogenide glass
HTF-1 (Ohara) [443930]	3.94	Fluoride glass
ZBL	4.78	62%ZrF_4, 33%BaF_2, 5%LaF_3,
ZBLA	4.61	58%ZrF_4, 33%BaF_2, 5%LaF_3, 4%AlF_3
ZBLAN	4.52	56%ZrF_4, 14%BaF_2, 6%LaF_3, 4%AlF_3, 20%NaF
ZBT	4.8	60%ZrF_4, 33%BaF_2, 7%ThF_4
HBL	5.78	62%HfF_4, 33%BaF_2, 5%LaF_3
HBLA	5.88	58%HfF_4, 33%BaF_2, 5%LaF_3, 4%AlF_3
HBT	6.2	60%HfF_4, 33%BaF_2, 7%ThF_4
Arsenic trisulfide (As_2S_3)	3.198	100%As_2S_3
Arsenic triselenide (As_2Se_3)	4.69	100%As_2Se_3
AMTRI-1/TI-20	4.41	55%Se, 33%Ge, 12%As
AMTIR-3/TI-1173	4.70	60%Se, 28%Ge, 12%Sb
Pyrex (e.g., Corning 7740)	2.23	81%SiO_2, 13%B_2O_3, 4%Na_2O, 2%Al_2O_3 [two-phase glass]
Zerodur (Schott)	2.53	56%SiO_2, 25%Al_2O_3, 8%P_2O_5, 4%Li_2O, 2%TiO_2 2%ZrO_2, ZnO/MgO/Na_2O/As_2O_3 [glass ceramic]
ULE (Corning 7971)	2.205	92.5%SiO_2, 7.5%TiO_2 [glass ceramic]

TABLE 10 Room-temperature Elastic Constants of Cubic Crystals

Material	Stiffness (GPa)			Compliance (TPa^{-1})			Refs.
	$\mathbf{c}_{11}$	$\mathbf{c}_{12}$	$\mathbf{c}_{44}$	$\mathbf{s}_{11}$	$\mathbf{s}_{12}$	$\mathbf{s}_{44}$	
AgBr	56.3	32.8	7.25	31.1	−11.5	138	57, 67
AgCl	59.6	36.1	6.22	31.1	−11.7	161	57, 68
AlAs	116.3	57.6	54.1	12.8	−4.24	18.5	69
ALON	393	108	119	2.89	−0.62	8.40	70
BaF_2	90.7	41.0	25.3	15.2	−4.7	39.6	57
$Bi_{12}GeO_{20}$ (BGO)	125.0	32.4	24.9	8.96	−1.84	40.4	71
$Bi_{12}SiO_{20}$ (BSO)	129.8	29.7	24.7	8.42	−1.57	40.2	72
BN	783	146	418	1.36	−0.21	2.39	73
BP	315	100	160	3.75	−0.90	6.25	74
C (diamond)	1040	170	550	1.01	−0.14	1.83	57
CaF_2	165	46	33.9	6.94	−1.53	29.5	57
$CaLa_2S_4$	98	47	50	15	−5	20	75
CdTe	53.8	37.4	20.18	43.24	−17.73	49.55	76
CsBr	30.7	8.4	7.49	36.9	−7.9	134	57
CsCl	36.6	9.0	8.07	30.2	−6.0	124	57
CsI	24.5	6.6	6.31	46.1	−9.7	158	57
CuCl	45.4	36.3	13.6	76.1	−33.8	73.5	77
GaAs	118	53.5	59.4	11.75	−3.66	16.8	57
GaP	142	63	71.6	9.60	−2.93	14.0	57
Ge	129	48	67.1	9.73	−2.64	14.9	57
InAs	83.4	45.4	39.5	19.46	−6.86	25.30	78
InP	102	58	46.0	16.4	−5.9	21.7	57
KBr	34.5	5.5	5.10	30.3	−4.2	196	57
KCl	40.5	6.9	6.27	25.9	−3.8	159	57
KF	65.0	15.0	12.5	16.8	−3.2	79.8	57
KI	27.4	4.3	3.70	38.2	−5.2	270	57
$KTaO_3$	431	103	109	2.7	−0.63	9.2	57
LiF	112	46	63.5	11.6	−3.35	15.8	57
$MgAl_2O_4$	282.9	155.4	154.8	5.79	−2.05	6.49	79
MgO	297.8	95.1	155.8	3.97	−0.96	6.42	79
NaBr	40.0	10.6	9.96	28.1	−5.8	100	57
NaCl	49.1	12.8	12.8	22.9	−4.8	78.3	57
NaF	97.0	24.2	28.1	11.5	−2.3	35.6	57
NaI	30.2	9.0	7.36	38.3	−8.8	136	57
PbF_2	96.37	46.63	21.04	15.3	−4.9	47.6	80
PbS	126	16.2	17.1	8.16	−0.93	58.5	81
PbSe	117.8	13.9	15.53	8.71	−0.92	64.4	82
PbTe	105.3	7.0	13.22	9.58	−0.60	75.6	83
Si	165	64	79.2	7.74	−2.16	12.6	57
β-SiC	350	142	256	3.18	−0.85	3.91	84
SrF_2	124	45	31.7	9.89	−2.59	31.6	57
$SrTiO_3$	315.6	102.7	121.5	3.77	−0.93	8.23	85
TlBr	37.6	14.8	7.54	34.2	−9.6	133	57
Tl[0.5Br, 0.5I], (KRS-5)	34.1	13.6	5.79	38.0	−10.8	173	57
TCl	40.3	15.5	7.69	31.6	−8.8	130	57
Tl[0.7Cl, 0.3Br], (KRS-6)	39.7	14.9	7.23	31.9	−8.8	139	57
$Y_3Al_5O_{12}$ (YAG)	328.1	106.4	113.7	3.62	−0.89	8.80	86
Y_2O_3	233	101	67	5.82	−1.76	14.93	70
ZnS	101	64.4	44.3	19.7	−7.6	22.6	57
ZnSe	85	50.2	40.7	21.1	−7.8	24.6	57
ZnTe	71.5	40.8	31.1	23.9	−8.5	32.5	57
ZrO_2:Y_2O_3	405.1	105.3	61.8	2.77	−0.57	16.18	87

TABLE 11 Room-temperature Elastic Constants of Tetragonal Crystals (Point Groups 4mm, $\bar{4}$2m, 422, and 4/mmm)

		Subscript of stiffness (GPa) or compliance (TPa^{-1})						
Material	**c** or **s**	11	12	13	33	44	66	Refs.
$AgGaS_2$	**c**	87.9	58.4	59.2	75.8	24.1	30.8	88
	s	26.5	−7.7	−14.5	35.9	41.5	32.5	
$AgGaSe_2$	**c**							
	s							
$BaTiO_3$	$\mathbf{c}^E$	275	179	152	165	54.4	113	57
	$\mathbf{s}^E$	8.05	−2.35	−5.24	15.7	18.4	8.84	
	$\mathbf{c}^E$	211	107	114	160	56.2	127	89
	$\mathbf{s}^E$	8.01	−1.57	−4.60	12.8	17.8	7.91	
$CdGeAs_2$	**c**	94.5	59.6	59.7	83.4	42.1	40.8	90
	s	21.6	−7.04	−10.4	26.9	23.8	24.5	
$CuGaS_2$	**c**							
	s							
KH_2PO_4	**c**	70.9	−5.5	14.3	56.7	12.7	6.24	57
(KDP)	**s**	15.1	2.1	−4.3	19.8	78.7	160	
MgF_2	**c**	137	87	61.5	199	56.4	95.5	57
	s	12.6	−7.2	−1.7	6.1	17.7	10.5	
$[NH_4]_2CO$	**c**	21.7	8.9	24	53.2	6.26	0.45	91
(Urea)	**s**	95	16	−50	64	160	2220	
$NH_4H_2PO_4$	**c**	67.3	5.0?	19.8	33.7	8.57	6.02	57
(ADP)	**s**	18.3	2.2	−12.0	43.7	117	166	
$PbTiO_3$	**c**							57
	s	7.2	−2.1		32.5	12.2	7.9	
TeO_2	**c**	56.12	51.55	23.03	105.71	26.68	66.14	92, 93
	s	114.5	−104.3	−2.3	10.5	37.5	15.1	
TiO_2	**c**	270	176	147	480	124	193	57
	s	6.71	−3.92	−0.85	2.60	8.04	5.20	
$ZnGeP_2$	**c**							
	s							

TABLE 12 Room-temperature Elastic Constants of Tetragonal Crystals (Point Groups 4, $\bar{4}$, and 4/m)

		Subscript of stiffness (GPa) or compliance (TPa^{-1})							
Material	**c** or **s**	11	12	13	16	33	44	66	Refs.
$CaMoO_4$	**c**	144	64.8	44.8	−14.2	126	36.9	46.1	94
	s	9.92	−4.3	−2.0	4.4	9.4	27.1	24.4	
$CaWO_4$	**c**	146	62.6	39.2	−19.1	127	33.5	38.7	95
	s	10.1	−5.1	−1.7	7.7	8.8	29.8	33.5	
$PbMoO_4$	**c**	109	68.0	53.0	−14.0	92.0	26.7	33.7	96
	s	21.0	−12.4	−4.9	13.3	16.6	37.5	40.6	
$SrMoO_4$	**c**	119	62.0	48.0	−12.0	104	34.9	42.0	97
	s	13.6	−6.3	−3.4	5.7	12.7	28.7	27.1	
$YLiF_4$	**c**	121	60.9	52.6	−7.7	156	40.9	17.7	98
	s	12.8	−6.0	−2.3	8.16	7.96	24.4	63.6	

TABLE 13 Room-temperature Elastic Constants of Hexagonal Crystals (Point Groups 6, $\bar{6}$, 6/m, 622, 6mm, $\bar{6}2$m, and 6/mmm)

		Subscript of stiffness (GPa) or compliance (TPa^{-1})					
Material	**c** or **s**	11	12	13	33	44	Refs.
β-AgI	$\mathbf{c}^E$	29.3	21.3	19.6	35.4	3.73	99
	$\mathbf{s}^E$	79	−46	−19	49	268	
AlN	**c**	345	125	120	395	118	100
	s	3.53	−1.01	−0.77	3.00	8.47	
BeO	**c**	470	168	119	494	153	57
	s	2.52	−0.80	−0.41	2.22	6.53	
CdS	**c**	87.0	54.6	47.5	94.1	14.9	57
	s	20.8	−10.1	−5.4	16.0	66.8	
CdSe	**c**	74.1	45.2	38.9	84.3	13.4	57
	s	23.2	−11.2	−5.5	16.9	74.7	
GaN	**c**	296	130	158	267	241	101
	s	5.10	−0.92	−2.48	6.68	4.15	
$LiIO_3$	$\mathbf{c}^E$	81.24	31.84	9.25	52.9	17.83	102
	$\mathbf{s}^E$	14.7	−5.6	−1.6	19.5	56.1	
α-SiC	**c**	502	95	56	565	169	57
	s	2.08	−0.37	−0.17	1.80	5.92	
ZnO	**c**	209	120	104	218	44.1	57
	s	7.82	−3.45	−2.10	6.64	22.4	
ZnS	**c**	122	58	42	138	28.7	57
	s	11.0	−4.5	−2.0	8.6	34.8	

TABLE 14 Room-temperature Elastic Constants of Hexagonal (Trigonal) Crystals (Point Groups 32, 3m, and $\bar{3}$m)

		Subscript of stiffness (GPa) or compliance (TPa^{-1})						
Material	**c** or **s**	11	12	13	14	33	44	Refs.
Ag_3AsS_3	**c**	57.0	31.8			36.4	9.0	103
	s							
Al_2O_3	**c**	495	160	115	−23	497	146	57
	s	2.38	−0.70	−0.38	0.49	2.19	7.03	
β-$Ba_3B_6O_{12}$	**c**	123.8	60.3	49.4	12.3	53.3	7.8	104
(BBO)	**s**	25.63	−14.85	−9.97	−63.97	37.21	331.3	
$CaCO_3$	**c**	144	53.9	51.1	−20.5	84	33.5	57
(Calcite)	**s**	11.4	−4.0	−4.5	9.5	17.4	41.4	
LaF_3	**c**	180	88	59	<0.5	222	34	105
	s	7.6	−3.3	−1.1		5.1	29.4	
$LiNbO_3$	**c**	202	55	71	8.3	242	60.1	57
	s	5.81	−1.15	−1.36	−0.96	4.94	16.9	
Se	**c**	19.8	6.6	20.2	|6.9|	83.6	18.3	106
	s	92.6	−32.5	−14.5	|47.2|	19.0	90.2	
α-SiO_2	**c**	86.6	6.7	12.6	−17.8	106.1	57.8	57
	s	12.8	−1.74	−1.32	4.48	9.75	20.0	
Te	**c**	32.57	8.45	25.7	|12.38|	71.7	30.94	106
	s	57.3	−13.1	−15.9	|28.2|	25.3	54.9	
Tl_3AsSe_3	**c**							
	s							

TABLE 15 Room-temperature Elastic Constants of Orthorhombic Crystals

		Subscript of stiffness (GPa) or compliance (TPa^{-1})									
Material	**c** or **s**	11	12	13	22	23	33	44	55	66	Refs.
$KNbO_3$	$\mathbf{c}^E$	224	102	182	273	130	245	75	28.5	45	107
	$\mathbf{s}^E$	11.3	−0.3	−8.2	4.9	−2.4	11.5	13.3	35.1	10.5	
$KTiOPO_4$ (KTP)	**c**	159			154		175				108
	s										
LiB_3O_5 (LBO)	**c**										
	s										

TABLE 16 Mechanical Properties of Crystals

	Moduli (GPa)			Poisson's ratio	Flexure strength (MPa)	Knoop hardness (kg/mm^2)
Material	Elastic	Shear	Bulk			
Ag_3AsS_3	[28]	[10]	[37]	[0.38]		
AgBr	24.7	8.8	40.5	0.39_9		7.0
AgCl	22.9	8.1	44.0	0.41	26	9.5
$AgGaS_2$	52	19	67	0.37		320
$AgGaSe_2$			[60]			230
β-AgI	12	4.4	24	0.4		
AlAs	108	42.4	77.2	0.27		490
AlN	294	117	202	0.26	225	1230
Al_2O_3	400	162	250	0.23	1200	2250
ALON	317	128	203	0.24	310	1850
$Ba_3B_6O_{12}$, BBO	30	11	60.6	0.41		
BaF_2	65.8	25.1	57.6	0.31	27	78
$BaTiO_3$	145	53	174	0.36		580
BeO	395	162	240	0.23	275	1250
$Bi_{12}GeO_{20}$, BGO	82	32	63.3	0.28		
$Bi_{12}SiO_{20}$, BSO	84	33	63.1	0.28		
BN	833	375	358	0.11		>4600
BP	324	136	172	0.19		4700
C, diamond	1100	500	460	0.10	2940	9000
$CaCO_3$, calcite	83	32	73.2	0.31		100
CaF_2	110	42.5	85.7	0.29	90	170
$CaLa_2S_4$	96	[38.4]	[64]	0.25	81	570
$CaMoO_4$	103	40	80	0.29		250
$CaWO_4$	96	37	78	0.29		300
$CdGeAs_2$	74	28	70	0.32		470
CdS	42	15	59	0.38	28	122
CdSe	42	15.3	53	0.37	21	65
CdTe	8.4	14.2	42.9	0.35	26	50
CsBr	22	8.8	15.8	0.27	8.4	18
CsCl	25	10.0	18.2	0.27		
CsI	18	7.3	12.6	0.26	5.6	
CuCl	24.8	8.9	39.3	0.30_5		
$CuGaS_2$			[94]			430
GaAs	116	46.6	75.0	0.24	55	710
GaN	294	118	195	0.25	70	750
GaP	140	56.5	89.3	0.24	100	875

TABLE 16 Mechanical Properties of Crystals (*Continued*)

Material	Moduli (GPa)			Poisson's ratio	Flexure strength (MPa)	Knoop hardness (kg/mm^2)
	Elastic	Shear	Bulk			
Ge	132	54.8	75.0	0.20_6	100	850
InAs	74	28	61	0.30		390
InP	89	34	72.7	0.30		520
KBr	18	7.2	15.2	0.30	11	6.5
KCl	22	8.5	18.4	0.29	10	8
KF	41	16	31.8	0.28		
KH_2PO_4, KDP	[38]	[15]	[28]	[0.26]		
KI	14	5.5	11.9	0.30		5
$KNbO_3$	[250]	[71]	[95]	[0.22]		500
$KTaO_3$	316	124	230	0.27		
$KTiOPO_4$, KTP						
LaF_3	120	46	100	0.32	33	450
$Li_2B_6O_{10}$, LBO						600
LiF	110	45	65.0	0.22_5	27	115
$LiIO_3$	55	22.4	33.5	0.23		
$LiNbO_3$	170	68	112	0.25		~5
$LiYF_4$, YLF	85	32	81	0.32	35	300
$MgAlO_4$	276	109	198	0.26_8	170	1650
MgF_2	137	53.9	99.1	0.26_9	100	500
MgO	310	131	163	0.18	130	675
NaBr	29	11.6	19.9	0.26		
NaCl	37	14.5	25.3	0.26	9.6	16.5
NaF	76	30.7	48.5	0.24		
NaI	22	8.4	16.1	0.28		
$[NH_4]_2CO$, urea	~9	~3	17	0.41		
$NH_4H_2PO_4$, ADP	29	11	27.9	0.32_5		
PbF_2	59.8	22.4	60.5	0.33_5		200
$PbMoO_4$	66	24	72	0.35		
PbS	70.2	27.5	52.8	0.28		
PbSe	64.8	25.4	48.5	0.28		
PbTe	56.9	22.6	39.8	0.26		
$PbTiO_3$						
Se	24	9	17	0.27		
Si	162	66.2	97.7	0.22_4	130	1150
β-SiC	447	191	224	0.17	250	2880
α-SiC	455	197	221	0.16		3500
SiO_2, α-quartz	95	44	38	0.08		740
SrF_2	89	34.6	71.3	0.29		150
$SrMoO_4$	87	33	73	0.30		
$SrTiO_3$	283	115	174	0.23		600
Te	35	14	24	0.25	11	18
TeO_2	45	17	46	0.33		
TiO_2	293	115	215	0.27		880
Tl_3AsSe_3, TAS						
TlBr	24	8.9	22.4	0.32		12
Tl[Br, I], KRS-5	19.6	7.3	20.4	0.34	26	40
TlCl	25	9.3	23.8	0.33		13
Tl[0.7Cl, 0.3Br], KRS-6	24	9.0	32.2	0.33	21	30
$Y_3Al_5O_{12}$, YAG	280	113	180	0.24		1350
Y_2O_3	173	67	145	0.30	150	700

TABLE 16 Mechanical Properties of Crystals (*Continued*)

Material	Moduli (GPa)			Poisson's ratio	Flexure strength (MPa)	Knoop hardness (kg/mm^2)
	Elastic	Shear	Bulk			
$ZnGeP_2$			[86]			980
ZnO	127	47	144	0.35		
β-ZnS	82.5	31.2	76.6	0.32	60	175
α-ZnS	87	33	74	0.30	69	
ZnSe	75.4	29.1	61.8	0.30	55	115
ZnTe	61.1	23.5	51.0	0.30	24	82
ZrO_2:12%Y_2O_3	233	88.6	205	0.31	(200)	1150

TABLE 17 Mechanical Properties of Optical and Specialty Glasses and Substrate Materials

Selected glass code or designation	Moduli (GPa)			Poisson's ratio	Flexure strength (MPa)	Knoop hardness (kg/mm^2)
	Elastic	Shear	Bulk			
479587 TiK1	40	16	27	0.254		330
487704 FK5	62	26	35	0.205		450
511510 TiF1	58	23	37	0.239		440
517642 BK7	81	34	46	0.208		520
518651 PK2	84	35	48	0.209		520
522595 K5	71	29	43	0.227		450
523515 KF9	67	28	37	0.202		440
526600 BaLK1	68	28	43	0.234		430
527511 KzF6	52	21	30	0.212		380
533580 ZK1	68	27	44	0.240		430
548458 LLF1	60	25	34	0.210		390
548743 Ultran-30	76	29	62	0.297		380
552635 PSK3	84	34	51	0.226		510
573575 BaK1	74	30	50	0.253		460
580537 BaLF4	76	31	49	0.244		460
581409 LF5	59	24	36	0.226		410
586610 LgSK2	76	29	60	0.290		340
593355 FF5	[65]	[26]	[41]	[0.238]		500
613586 SK4	82	32	59	0.268		500
613443 KzFSN4	60	24	45	0.276		380
618551 SSK4	79	31	56	0.265		460
620364 F2	58	24	35	0.225		370
650392 BaSF10	67	27	46	0.256		400
670472 BaF10	95	37	71	0.277	104	610
720504 LaK10	111	43	87	0.288		580
741526 TaC2	117	45	97	0.299		715
743492 NbF1	108	41	94	0.308		675
744447 LaF2	93	36	73	0.289		480
805254 SF6	56	22	37	0.248		310
835430 TaFD5	126	48	104	0.299		790
Fused silica	72.6	31	36	0.164	110	635
Fused germania	43.1	18	23	0.192		
BS-39B	104	40	83	0.29	90	760
CORTRAN 9753	98.6	39	75	0.28		600
CORTRAN 9754	84.1	33	67	0.290	44	560

TABLE 17 Mechanical Properties of Optical and Specialty Glasses and Substrate Materials (*Continued*)

Selected glass code or designation	Moduli (GPa)			Poisson's ratio	Flexure strength (MPa)	Knoop hardness (kg/mm^2)
	Elastic	Shear	Bulk			
IRG 2	95.9	37	73	0.282		481
IRG 9	77.0	30	61	0.288		346
IRG 11	107.5	42	83	0.284		610
IRG 100	21	8	15	0.261		150
HTF-1	64.2	25	49	0.28		320
ZBL	60	23	53	0.31		228
ZBLA	60.2	24	40	0.25	11	235
ZBLAN	60	23	53	0.31		225
ZBT	60	23	45	0.279	62	250
HBL	55	21	46	0.3		228
HBLA	56	22	47	0.3		240
HBT	55	21	46	0.3	62	250
Arsenic trisulfide	15.8	6	13	0.295	16.5	180
Arsenic triselenide	18.3	7	14	0.288		120
AMTIR-1/TI-20	21.9	9	16	0.266	18.6	170
AMTIR-3/TI-1173	21.7	9	15	0.265	17.2	150
Pyrex	62.8	26	35	0.200		
Zerodur	91	37	58	0.24		630
ULE	67.3	29	34	0.17	50	460

TABLE 18 Thermal Properties of Crystals

Material	CC*	Temperature (K)		Heat capacity ($J/g \cdot K$)	Thermal expansion ($10^{-6}/K$)	Thermal conductivity ($W/m \cdot K$)		
		Debye	Melt†			@ 250 K	@ 300 K	@ 500 K
Ag_3AsS_3	H		763 m					
AgBr	C	145	705 m	0.2790	33.8	1.11	0.93	0.57
AgCl	C	162	728 m	0.3544	32.4	1.25	1.19	
$AgGaS_2$	T	255	1269 m		28.5 ‖ a −18.7 ‖ c			
$AgGaSe_2$	T	156	1129 m		35.5 ‖ a −15.0 ‖ c			
β-AgI	H	116	423 p	0.242			0.4	
AlAs	C	416	2013 m	0.452	3.5		(80)	
AlN	H	950	3273 m	0.796	5.27 ‖ a 4.15 ‖ c	500	320	150
Al_2O_3	H	1030	2319 m	0.777	6.65 ‖ a 7.15 ‖ c	58	46	24.2
ALON	C		2323 m	0.830	5.66		12.6	7.0
$Ba_3B_6O_{12}$, BBO	H		900 p		0.5 ‖ a 33.3 ‖ c		0.08 ‖ a 0.80 ‖ c	
BaF_2	C	283	1553 m	0.4474	18.4	7.5	12?	
$BaTiO_3$	T	—	278 p 406 p	0.439	16.8 ‖ a −9.07 ‖ c	—	6	—
BeO	H	1280	2373 p 2725 m	1.028	5.64 ‖ a 7.47 ‖ c	420	350	200

TABLE 18 Thermal Properties of Crystals (*Continued*)

Material	CC*	Temperature (K)		Heat capacity (J/g · K)	Thermal expansion (10^{-6}/K)	Thermal conductivity (W/m · K)		
		Debye	Melt†			@ 250 K	@ 300 K	@ 500 K
$Bi_{12}GeO_{20}$ (BGO)	C				16.8			
$Bi_{12}SiO_{20}$ (BSO)	C							
BN	C	1900	1100 p	0.513	3.5		760	
BP	C	985	1400 d	0.71	3.65	460	360	
C, diamond	C	2240	1770 p	0.5169	1.25	2800	2200	1300
$CaCO_3$, calcite	H		323 p	0.8820	−3.7 ‖ a	5.1 ‖ a	4.5 ‖ a	(3.4) ‖ a
			3825 m		25.1 ‖ c	6.2 ‖ c	5.4 ‖ c	(4.2) ‖ c
CaF_2	C	510	1424 p	0.9113	18.9	13	9.7	5.5
$CaLa_2S_4$	C		2083 m	(0.36)	14.6		1.7	1.5
$CaMoO_4$	T		1730 m	0.573	7.6 ‖ a		4.0 ‖ a	
					11.8 ‖ c		3.8 ‖ c	
$CaWO_4$	T		1855 m	0.396	6.35 ‖ a		16	9.5
					12.38 ‖ c			
$CdGeAs_2$	T	253	900 p		8.4 ‖ a			
			943 m		0.25 ‖ c			
CdS	H	215	1560 m	0.3814	4.6 ‖ a		27	13
					2.5 ‖ c			
CdSe	H	181	1580 m	0.272	4.9 ‖ a		(9)	
					2.9 ‖ c			
CdTe	C	160	1320 m	0.210	5.0	8.2	6.3	
CsBr	C	145	908 m	0.2432	47.2		0.85	
CsCl	C	175	918 m	0.3116	45.0			
CsI	C	124	898 m	0.2032	48.6		1.05	
CuCl	C	179	700 m	0.490	14.6	1.0	0.8	0.5
$CuGaS_2$	T	356	1553 m	0.452	11.2 ‖ a			
					6.9 ‖ c			
GaAs	C	344	1511 m	0.345	5.0	(65)	54	27
GaN	H		1160 d		3.17 ‖ a			
					5.59 ‖ c		130 ‖ c	
GaP	C	460	1740 m	0.435	5.3	120	100	(45)
Ge	C	380	1211 m	0.3230	5.7	74.9	59.9	33.8
InAs	C	251	1216 m	0.2518	4.4	(50)	27.3	15
InP	C	302	1345 m	0.3117	4.5	90	68	32
KBr	C	174	1007 m	0.4400	38.5	5.5	4.8	2.4
KCl	C	235	1043 m	0.6936	36.5	8.5	6.7	3.8
KF	C	336	1131 m	0.8659	31.4		8.3	
KH_2PO_4, KDP	T	—	123 p	0.88	22.0 ‖ a	2.0	2.1	
			450 p		39.2 ‖ c			
			526 m					
KI	C	132	954 m	0.3192	40.3		2.1	
$KNbO_3$	O	—	223 p		(37)			
			476 p					
$KTaO_3$	C	311				0.2	0.17	
$KTiOPO_4$, KTP	O		1209 c	0.728	11 ‖ a		2 ‖ a	
			1423 d		9 ‖ b		3 ‖ b	
					0.6 ‖ c		3 ‖ c	
LaF_3	H	392	1700 m	0.508	15.8 ‖ a	5.4	5.1	
					11.0 ‖ c			
LiB_3O_5, LBO	O		1107 p					
LiF	C	735	1115 m	1.6200	34.4	19	14	7.5

TABLE 18 Thermal Properties of Crystals (*Continued*)

Material	CC*	Temperature (K)		Heat capacity (J/g · K)	Thermal expansion (10^{-6}/K)	Thermal conductivity (W/m · K)		
		Debye	Melt†			@ 250 K	@ 300 K	@ 500 K
$LiIO_3$	H		520 p		28 ‖ a			
			693 m		48 ‖ c			
$LiNbO_3$	H	560	1470 c	0.63	14.8 ‖ a		5.6	
			1523 m		4.1 ‖ c			
$LiYF_4$, YLF	T		1092 m	0.79	13.3 ‖ a		6.3	
					8.3 ‖ c			
$MgAlO_4$	C	850	2408 m	0.8191	6.97	30	25	
MgF_2	T	535	1536 m	1.0236	9.4 ‖ a			
					13.6 ‖ c		30 ‖ a	
							21 ‖ c	
MgO	C	950	3073 m	0.9235	10.6	73	59	32
NaBr	C	225	1028 m	0.5046	41.8		5.6	
NaCl	C	321	1074 m	0.8699	41.1	8	6.5	4
NaF	C	492	1266 m	1.1239	33.5	22		168
NaI	C	164	934 m	0.3502	44.7			4.7
$[NH_4]_2CO$, urea	T		408 m	1.551				
$NH_4H_2PO_4$, ADP	T	—	148 p	1.26	27.2 ‖ a		1.26 ‖ a	
			463 m		10.7 ‖ c		0.71 ‖ c	
PbF_2	C	225	422 p	0.3029	29.0		(28)	
			1094 m					
$PbMoO_4$	T		1338 m	0.326	8.7 ‖ a			
					20.3 ‖ c			
PbS	C	227	1390 m	0.209	19.0		2.5	
PbSe	C	138	1338 m	0.175	19.4	2	1.7	1
PbTe	C	125	1190 m	0.151	19.8	2.5	2.3	1.8
$PbTiO_3$	T		763 p				4	2.8
Se	H	151	490 m	0.3212	69.0 ‖ a	1.5 ‖ a	1.3 ‖ a	—
					−0.3 ‖ c	5.1 ‖ c	4.5 ‖ c	—
Si	C	645	1680 m	0.7139	2.62	191	140	73.6
β-SiC (3C)	C	(1000)	3103 d	0.670	2.77		490	
α-SiC (6H)	H		3000 v	0.690			450 ‖ a	
SiO_2, α-quartz	H	271	845 p	0.7400	12.38 ‖ a	7.5 ‖ a	6.2 ‖ a	3.9 ‖ a
					6.88 ‖ c	12.7 ‖ c	10.4 ‖ c	6.0 ‖ c
SrF_2	C	378	1710 m	0.6200	18.1	11	8.3	
$SrMoO_4$	T		1763 m	0.619			4.0 ‖ a	
							4.2 ‖ c	
$SrTiO_3$	C	—	110 p	0.536	8.3	12.5	11.2	
			2358 m					
Te	H	152	621 p	0.202	27.5 ‖ a	2.5 ‖ a	2.1 ‖ a	1.5 ‖ a
			723 m		−1.6 ‖ c	4.9 ‖ c	3.9 ‖ c	2.5 ‖ c
TeO_2	T		1006 m	[0.41]	15.0 ‖ a			
					4.9 ‖ c			
TiO_2	T	760	2128 m	0.6910	6.86 ‖ a	8.3 ‖ a	7.4 ‖ a	(5.5) ‖ a
					8.97 ‖ c	11.8 ‖ c	10.4 ‖ c	(8.0) ‖ c
Tl_3AsSe_3, TAS	H		583 m	0.19	28 ‖ a		0.35	
					18 ‖ c			
TlBr	C	116	740 m	0.1778	51		0.53	
Tl[Br, I], KRS-5	C	(110)	687 m	(0.16)	58		0.32	
TlCl	C	126	703 m	0.2198	52.7		0.74	
Tl[Cl, Br], KRS-6	C	(120)	697 m	0.201	51		0.50	

TABLE 18 Thermal Properties of Crystals (*Continued*)

Material	CC*	Temperature (K)		Heat capacity (J/g · K)	Thermal expansion (10^{-6}/K)	Thermal conductivity (W/m · K)		
		Debye	Melt†			@ 250 K	@ 300 K	@ 500 K
$Y_3Al_5O_{12}$, YAG	C	754	2193 p	0.625	7.7		13.4	
Y_2O_3	C	465	2640 p	0.4567	6.56		13.5	
$ZnGeP_2$	T	428	1225 p		7.8 ‖ a		18	
			1300 m		5.0 ‖ c			
						16.7		9.2
						(30)		7.6
ZnO	H	416	2248 m	0.495	6.5 ‖ a		30	15
					3.7 ‖ c			
β-ZnS	C	340	1293 p	0.4732	6.8		16.7	10
α-ZnS	H	351	2100 m	0.4723	6.54 ‖ a			
					4.59 ‖ c			
ZnSe	C	270	1790 m	0.339	7.1		13	8
ZnTe	C	225	1510 m	0.218	8.4		10	
ZrO_2:12%Y_2O_3	C	563	3110 m	0.46	10.2		1.8	1.9

* CC = crystal class; C = cubic; H = hexagonal; O = orthorhombic; T = tetragonal.

† *Temperature codes*: m = melt temperature; c = Curie temperature; d = decomposition temperature; p = phase change (to different structure) temperature; v = vaporization (sublimation) temperature.

TABLE 19 Thermal Properties of Optical and Specialty Glasses and Substrate Materials

Selected glass code	Temperature (K)			Heat capacity (J/g · K)	Thermal expansion (10^{-6}/K)	Thermal conductivity (W/m · K)
	Glass	Soften	Melt*			
479587 TiK1	613			0.842	10.3	0.773
487704 FK5	737	945		0.808	9.2	0.925
511510 TiF1	716	[892]		[0.81]	9.1	[0.953]
517642 BK7	836	989		0.858	7.1	1.114
518651 PK2	841	994		[0.80]	6.9	1.149
522595 K5	816	993		0.783	8.2	0.950
523515 KF9	718	934		[0.75]	6.8	[1.01]
526600 BaLK1	782	954		0.766	9.1	1.043
527511 KzF6	717			[0.82]	5.5	[0.946]
533580 ZK1	835	1005		[0.77]	7.5	[0.894]
548458 LLF1	721	901		[0.71]	8.1	[0.960]
548743 Ultran-30	786	873		0.58	11.9	0.667
552635 PSK3	875	1009		[0.72]	8.6	[1.004]
573575 BaK1	875	1019		0.687	7.6	0.795
580537 BaLF4	842	1004		0.670	6.4	0.827
581409 LF5	692	858		0.657	9.1	0.866
586610 LgSK2	788			[0.51]	12.1	0.866
593355 FF5	788	843		[0.80]	8.6	[0.937]
613586 SK4	916	1040		0.582	6.4	0.875
613443 KzFSN4	765	867		[0.64]	5.0	[0.769]
618551 SSK4	912	1064		[0.57]	6.1	[0.806]
620364 F2	705	866		0.557	8.2	0.780
650392 BaSF10	757	908		[0.54]	8.6	[0.714]
670472 BaF10	853	908		0.569	7.2	0.967
720504 LaK10	893	976		[0.53]	5.7	[0.814]
741526 TaC2	928	958		[0.48]	5.2	[0.861]

TABLE 19 Thermal Properties of Optical and Specialty Glasses and Substrate Materials (*Continued*)

Selected glass code	Temperature (K)			Heat capacity (J/g · K)	Thermal expansion (10^{-6}/K)	Thermal conductivity (W/m · K)
	Glass	Soften	Melt*			
743492 NbF1	863	898		[0.48]	5.3	[0.845]
744447 LaF2	917	1013		[0.47]	8.1	[0.695]
805254 SF6	696	811		0.389	8.1	0.673
835430 TaFD5	943	973		[0.41]	6.4	
Fused silica	1273		1983	0.746	0.51	1.38
Fused germania	800		1388		6.3	
BS-39B		[970]		0.865	8.0	1.23
CORTRAN 9753	1015	1254		0.795	6.0	2.3
CORTRAN 9754	1008	1147		0.54	6.2	0.81
IRG 2	975			0.495	8.8	0.91
IRG 9	696			0.695	16.1	0.88
IRG 11	1075			0.749	8.2	1.13
IRG 100	550	624			15.0	0.3
HTF-1	658				16.1	
ZBL	580		820	0.538	18.8	
ZBLA	588		820	0.534	18.7	
ZBLAN	543		745	0.520	17.5	0.4
ZBT	568	723		0.511	4.3	
HBL	605		832	0.413	18.3	
HBLA	580		835	0.414	17.3	
HBT	593		853	0.428	6.0	
Arsenic trisulfide	436	573		0.473	26.1	0.17
Arsenic triselenide		345		0.349	24.6	0.205
AMTIR-1/TI-20	635	678		0.293	12.0	0.25
MATIR-3/TI-1173	550	570		0.276	14.0	0.22
Zerodur				0.821	0.5 (20–300°C)	1.64
Pyrex	560	821		1.05	3.25	1.13
ULE	1000	1490		0.776	±0.03 (5–35°C)	1.31

* Or liquidus temperature.

TABLE 20 Summary Optical Properties of Crystals

Material	Transparency (μm)		Refractive index	Thermo-optic coefficients (10^{-6}/K)						
	UV	IR	n_∞	λ (μm)	dn/dT	λ (μm)	dn/dT	λ (μm)	dn/dT	Refs.
Ag_3AsS_3	0.63(o)	12.5(o)	2.736(o)							
	0.61(e)	13.5(e)	2.519(e)							
AgBr	0.49	35	2.166			3.39	−61	10.6	−50	109
AgCl	0.42	23	2.002	0.633	−61					110
						3.39	−58	10.6	−35	109
$AgGaS_2$	0.50(o)	12.0(o)	2.408(o)	0.6	258(o)	1.0	176(o)	10.0	153(o)	111
	0.52(e)	12.5(e)	2.355(e)		255(e)		179(e)		155(e)	
$AgGaSe_2$	0.75	17.5	2.617(o)							
			2.586(3)							
β-AgI			[2.1(o)]							
			[2.1(e)]							
AlAs			2.857							
AlN			2.17(o)							
			2.22(e)							
Al_2O_3	0.19(o)	5.0(o)	1.7555(o)	0.458	11.7(o)	0.589	13.6(o)	0.633	12.6	112, 113,
		5.2(e)	1.7478(e)		12.8(e)		14.7(e)			114
ALON	0.23	4.8	1.771	0.633	11.7					115
BBO	0.205	3.0	1.540(o)	0.4047	−16.6(o)	0.5790	−16.4(o)	1.014	−16.8(o)	104
			1.655(e)		−9.8(e)		−9.4(e)		−8.8(e)	
BaF_2	0.14	12.2	1.4663	0.633	−16.0	3.39	−15.9	10.6	−14.5	113
$BaTiO_3$			2.277(o)							
			2.250(e)							
BeO	0.21	3.5	1.709(o)	0.458	8.2(o)	0.633	8.2(o)			116
			1.724(e)		13.4(e)		13.4(e)			
BGO	0.50	3.1	2.37	0.51	−34.5	0.65	−34.9			117
BSO	0.52		[2.15]							
BN	[0.2]		2.12							
BP	[0.5]		2.78							
Diamond	0.24	2.7	2.380	0.546	10.1			30	9.6	118, 119
$CaCO_3$	0.24(o)	2.2(o)	2.942(o)	0.365	3.6(o)	0.458	3.2(o)	0.633	2.1(o)	4
	0.21(e)	3.3(e)	2.850(e)		14.4(e)		13.1(e)		11.9(e)	
CaF_2	0.135	9.4	1.4278	0.254	−7.5	0.663	−10.4	3.39	−8.1	120
$CaLa_2S_4$	0.65	14.3	2.6							
$CaMoO_4$			1.945(o)	0.588	−9.6(o)					121
			1.951(e)		−10.0(e)					
$CaWO_4$	(0.2)	5.3	1.884(o)	0.546	−7.1(o)					122
			1.898(e)		−10.2(e)					

$CdGeAs_2$	2.5	15	3.522(o) 3.608(e)							
CdS	0.52(o) 0.51(e)	14.8(o) 14.8(e)	1.7085(o) 1.7234(e)	10.6	58.6(o) 62.4(e)					123
CdSe	0.75	20	2.448(o) 2.467(e)							
CdTe	0.85	29.9	2.6829	1.15	147	3.39	98.2	10.6	98.0	124
CsBr	0.230	43.5	1.669	0.254	−82.0	0.633	−84.7	30.0	−75.8	125
CsCl	0.41	18.5	1.620	0.365	−78.7	0.633	−77.4	20.0	−70.0	125
CsI	0.245	62	1.743	0.365	−87.5	0.633	−99.3	30.0	−88.0	126
CuCl	0.45	(15)	1.974							
$CuGaS_2$			2.493(o) 2.487(e)	0.55	130(o) 173(e)	1.0	59(o) 60(e)	10.0	56(o) 57(e)	127 128
GaAs	0.90	17.3	3.32	1.15	250	3.39	200	10.6	200	129
GaN			2.35(o) 2.31(e)	1.15	61					
GaP	0.54	10.5	3.015	0.546	200	0.633	160			130
Ge	1.8	15	4.001	2.5	462	5.0	416	20.0	401	131
$HfO_2:Y_2O_3$	0.35	6.5	2.074	0.365	14.1	0.436	11.0	1.01	5.8	132
InAs	3.9	20	3.44	4.0	500	6.0	400	10.0	300	129
InP	0.93	20	3.09	5.0	83	10.6	82	20.0	77	109
KBr	0.200	30.2	1.537	0.458	−39.3	1.15	−41.9	10.6	−41.1	113
KCl	0.18	23.3	1.475	0.458	−34.9	1.15	−36.2	10.6	−34.8	113
KF	0.14	15.8	1.357	0.254	−19.9	1.15	−23.4	10.6	−17.0	113
KH_2PO_4	0.176	1.42	1.502(o) 1.460(e)	0.624	−39.6(o) −38.2(e)					133
KI	0.250	38.5	1.629	0.458	−41.5	1.15	−44.7	30	−30.8	113
$KNbO_3$	0.4	5.0	2.199(x) 2.233(y) 2.102(z)	0.436	67(x) −26(y) 125(z)	1.064	23(x) −34(y) 63(z)	3.00	21(x) −23(y) 55(z)	134
$KTaO_3$			2.14							
$KTiOPO_4$	0.35	4.5	1.733(x) 1.740(y) 1.822(z)		11(x) 13(y) 16(z)					135
LaF_3	0.15	10	1.593(o) 1.586(e)							
LiB_3O_5	0.17	2.5	1.571(x) 1.594(y) 1.612(z)	0.532	−0.9 −13.5 −7.4	1.064	−1.9 −13.0 −8.3			136
LiF	0.120	6.60	1.388	0.458	−16.0	1.15	−16.9	3.39	−14.5	113
$LiIO_3$	0.38	5.5	1.846(o) 1.711(e)	0.4	−74.5(o) −63.5(e)	1.0	−84.9(o) −69.2(e)			54

TABLE 20 Summary Optical Properties of Crystals (*Continued*)

Material	Transparency (μm)		Refractive index	Thermo-optic coefficients (10^{-6}/K)						
	UV	IR	n_∞	λ (μm)	dn/dT	λ (μm)	dn/dT	λ (μm)	dn/dT	Refs.
$LiNbO_3$	0.5	5.0	2.214(o) 2.140(e)	0.66	4.4(o) 37.9(e)	3.39	0.3(o) 28.9(e)			137
$LiYF_4$	0.18	6.7	1.447(o) 1.469(e)	0.436	−0.54(o) −2.44(e)	0.546	−0.67(o) −2.30(e)	0.578	−0.91(o) −2.86(e)	138
$MgAl_2O_4$	0.2	5.3	1.701	0.589	9.0					112
MgF_2	0.13(o) 0.13(e)	7.7(o) 7.7(e)	1.3734(o) 1.3851(e)	0.633	1.12(o) 0.58(e)	1.15	0.88(o) 0.32(e)	3.39	1.19(o) 0.6(e)	113
MgO	0.35	6.8	1.720	0.365	19.5	0.546	16.5	0.768	13.6	139, 140
NaBr	0.20	24	1.615	0.365	−30.4	1.15	−40.2	10.6	−37.9	125
NaCl	0.174	18.2	1.555	0.458	−34.2	0.633	−35.4	3.39	−36.3	113
NaF	0.135	11.2	1.320	0.458	−11.9	1.15	−13.2	3.39	−12.5	113
NaI	0.26	24	1.73	0.458	−38.4	1.15	−49.6	10.6	−48.6	125
$[NH_4]_2CO$	0.21	1.4	1.481(o) 1.594(e)							
$NH_4H_2PO_4$	0.185	1.45	1.516(o) 1.470(e)	0.624	−47.1(o) −4.3(e)					133
PbF_2	0.29	12.5	1.731							
$PbMoO_4$	0.5	5.4	2.132(o) 2.127(e)	0.588	−75(o) −41(e)					121
PbS	0.29		4.1	3.39	−2100	5.0	−1900	10.6	−1700	141
PbSe	4.6		4.7	3.39	−2300	5.0	−1400	10.6	−860	141
PbTe	4.0	20	5.67	3.39	−2100	5.0	−1500	10.6	−1200	141
$PbTiO_3$			2.52(o) 2.52(e)							
Se	(1)	(30)	2.65(o) 3.46(e)							
Si	1.1	6.5	3.415	2.5	166	5.0	159	10.6	157	131

β-SiC	0.5	4	2.563							
α-SiC	0.5	4	2.560(o) 2.596(e)							
α-SiO_2	0.155	4.0	1.5352(o) 1.5440(e)	0.254	−2.9(o) −4.0(e)	0.365	−5.4(o) −6.2(e)	0.546	−6.2(o) −7.0(e)	140
SrF_2	0.13	11.0	1.4316	0.633	−16.0	1.15	−16.2	10.6	−14.5	113
$SrMoO_4$			1.867(o) 1.869(e)							
$SrTiO_3$	0.5	5.1	2.283							
Te	3.5	32	4.778(o) 6.222(e)							
TeO_2	0.34	4.5	2.18(o) 2.32(e)	0.436	30(o) 25(e)	0.644	9(o) 8(e)			142
TiO_2	0.42	4.0	2.432(o) 2.683(e)	0.405	4(o) −9(e)					143
Tl_3AsSe_3	1.3	16	3.35(o) 3.16(e)	2–10	−45(o) 36(e)					144
TlBr	0.44	38	2.271							
KRS-5	0.58	42	2.38	0.633	−250	10.6	−233	30	−195	145
TlCl	0.38	25	2.136							
KRS-6	0.42	27	2.196							
$Y_3Al_5O_{12}$	0.21	5.2	1.815	0.458	11.9	0.633	9.4	1.06	9.1	146
Y_2O_3	0.29	7.1	1.892	0.663	8.3					115
$ZnGeP_2$	0.8	12.5	3.121(o) 3.158(e)	0.64	359(o) 376(e)	1.0	212(o) 230(e)	10	165(o) 170(e)	128, 147
ZnO	0.38(o) 0.37(e)		1.922(o) 1.936(e)							
β-ZnS	0.4	12.5	2.258	0.633	63.5	1.15	49.8	10.6	46.3	124
α-ZnS			2.271(o) 2.275(e)							
ZnSe	0.51	19.0	2.435	0.633	91.1	1.15	59.7	10.6	52.0	124
ZnTe	0.6	25	2.70							
$ZrO_2:Y_2O_3$	0.38	6.0	2.0892	0.365	16.0	0.458	10.0	0.633	7.9	148

TABLE 21 Summary Optical Properties of Optical and Specialty Glasses

Material	Transparency (μm)		Refractive index	Abbe number	Thermo-optic coeff. (10^{-6}/K)*				Refs.
	UV	IR	n_d	ν_d	λ (μm)	dn/dT	λ (μm)	dn/dT	
TiK1	0.35		1.47869	58.70	0.4358	−1.8	1.060	−2.6	149
FK5	0.29	(2.5)	1.48749	70.41	0.4358	−1.1	1.060	−1.8	149
TiF1	0.35		1.51118	51.01	0.4358	−0.1†	1.014	−1.5†	149, 150
BK7	0.31	2.67	1.51680	64.17	0.4358	3.4	1.060	2.3	149
PK2	0.31	(2.5)	1.51821	65.05	0.4358	3.7	1.060	2.3	149
K5	0.31	2.7	1.52249	59.48	0.4358	2.4	1.060	1.1	149
KF9	0.33	(2.5)	1.52341	51.49	0.4358	5.1	1.060	3.3	149
BaLK1	0.32	(2.6)	1.52642	60.03	0.4358	1.1	1.060	0.1	149
KzF6	0.32		1.52682	51.13	0.4358	5.8†	1.014	4.2†	149, 150
ZK1	0.31		1.53315	57.98	0.4358	4.4†	1.014	2.8†	149, 150
LLF1	0.32		1.54814	45.75	0.4358	4.4	1.060	2.1	149
Ultran 30	0.23	3.95	1.54830	74.25	0.4358	−5.5	1.060	−6.2	149
PSK3	0.30	(2.5)	1.55232	63.46	0.4358	3.5	1.060	2.3	149
BaK1	0.31	2.7	1.57250	57.55	0.4358	3.3	1.060	1.9	149
BaLF4	0.335	(2.6)	1.57957	53.71	0.4358	6.3	1.060	4.3	149
LF5	0.32	(2.5)	1.58144	40.85	0.4358	4.4	1.060	1.6	149
LgSK2	0.35		1.58599	61.04	0.4358	−2.5	1.060	−4.0	149
FF5	0.36		1.59270	35.45	0.6328	0.7			151
SK4	0.325	2.68	1.61272	58.63	0.4358	3.5	1.060	2.1	149
KzFSN4	0.325	2.38	1.61340	44.30	0.4358	6.2	1.060	4.4	149
SSK4	0.325	2.9	1.61765	55.14	0.4358	4.0	1.060	2.2	149
F2	0.33	2.73	1.62004	36.37	0.4358	5.9	1.060	2.8	149
BaSF10	0.34	(2.6)	1.65016	39.15	0.4358	5.5	1.060	2.1	149
BaF10	0.35	2.7	1.67003	47.20	0.6328	4.7			151
LaK10	0.34	(2.5)	1.72000	50.41	0.4358	5.8	1.060	3.8	149
TaC2	0.325		1.74100	52.29	0.6328	6.8			151
NbF1	0.325		1.74330	59.23	0.6328	7.9			151
LaF2	0.355	(2.5)	1.74400	44.72	0.4358	2.2	1.060	0.2	149
SF6	0.37	2.74	1.80518	25.43	0.4358	16.2	1.060	6.9	149
TaFD5	0.34		1.83500	42.98	0.6328	4.6			151
SiO_2	0.16	3.8	1.45857	67.7	0.5893	10			152
GeO_2	0.30	4.9	$n_D = 1.60832$	41.2					153
BS-39B	0.38	4.9	$n_D = 1.6764$	44.5	0.5893	7.4			154
Corning 9753	0.38	4.3	$n_D = 1.60475$	54.98					155
Corning 9754	0.36	4.8	$n_D = 1.6601$	46.5					155
Schott IRG 2	0.44	5.1	1.8918	30.03					149
Schott IRG9	0.38	4.1	1.4861	81.02					149
Schott IRG 11	0.44	4.75	1.6809	44.21					149
Schott IRG 100	0.93	13	$n_1 = 2.7235$	—	2,5	103	10.6	56	149
Ohara HTF-1	0.21	6.9	1.44296	92.46					150
ZBL	0.25	7.0	$n_D = 1.523$						156, 157
ZBLA	0.29	7.0	$n_D = 1.521$	62					156, 157, 158
ZBLAN	0.25	6.9	$n_D = 1.480$	64	0.6328	−14.5			158, 159
ZBT	0.32	6.8	$n_D = 1.53$						160, 161
HBL	0.25	7.3	$n_D = 1.498$						158
HBLA	0.29	7.3	$n_D = 1.504$						158, 162
HBT	0.22	7.7	$n_D = 1.53$						160
As_2S_3	0.62	11.0	$n_1 = 2.47773$	—	0.6	85	1.0	17	163, 164
As_2Se_3	0.87	17.2	$n_{12} = 2.7728$	—	0.83	55	1.15	33	165, 166
AMTIR-1/TI-20	0.75	(14.5)	$n_1 = 2.6055$	—	1.0	101	10.0	72	166, 167
AMTIR-3/TI-1173	0.93	16.5	$n_3 = 2.6366$	—	3.0	98	12.0	93	166, 167

* Thermo-optic coefficient in air: $(dn/dT)_{rel}$.
† Data from comparable Ohara glass.

TABLE 22 Room-temperature Dispersion Formulas for Crystals

Material	Dispersion formula (wavelength, λ, in μm)	Range (μm)	Ref.
Ag_3AsS_3	$n_o^2 = 7.483 + \frac{0.474}{\lambda^2 - 0.09} - 0.0019\lambda^2$	0.63–4.6(o) 0.59–4.6(e)	168
	$n_e^2 = 6.346 + \frac{0.342}{\lambda^2 - 0.09} - 0.0011\lambda^2$		
AgBr	$\frac{n^2 - 1}{n^2 + 2} = 0.452505 + \frac{0.09939\lambda^2}{\lambda^2 - 0.070537} - 0.00150\lambda^2$	0.49–0.67	169
AgCl	$n^2 - 1 = \frac{2.062508\lambda^2}{\lambda^2 - (0.1039054)^2} + \frac{0.9461465\lambda^2}{\lambda^2 - (0.2438691)^2} + \frac{4.300785\lambda^2}{\lambda^2 - (70.85723)^2}$	0.54–21.0	110
$AgGaS_2$	$n_o^2 = 3.6280 + \frac{2.1686\lambda^2}{\lambda^2 - 0.1003} + \frac{2.1753\lambda^2}{\lambda^2 - 950}$	0.49–12	170
	$n_e^2 = 4.0172 + \frac{1.5274\lambda^2}{\lambda^2 - 0.1310} + \frac{2.1699\lambda^2}{\lambda^2 - 950}$		
$AgGaSe_2$	$n_o^2 = 4.6453 + \frac{2.2057\lambda^2}{\lambda^2 - 0.1879} + \frac{1.8377\lambda^2}{\lambda^2 - 1600}$	0.73–13.5	170
	$n_e^2 = 5.2912 + \frac{1.3970\lambda^2}{\lambda^2 - 0.2845} + \frac{1.9282\lambda^2}{\lambda^2 - 1600}$		
β-AgI	$n_o = 2.184; \quad n_e = 2.200@0.659\ \mu m$	—	171
	$n_o = 2.104; \quad n_e = 2.115@1.318\ \mu m$		
AlAs	$n^2 = 2.0792 + \frac{6.0840\lambda^2}{\lambda^2 - (0.2822)^2} + \frac{1.900\lambda^2}{\lambda^2 - (27.62)^2}$	0.56–2.2	172
AlN	$n_o^2 = 3.1399 + \frac{1.3786\lambda^2}{\lambda^2 - (0.1715)^2} + \frac{3.861\lambda^2}{\lambda^2 - (15.03)^2}$	0.22–5.0	173
	$n_e^2 = 3.0729 + \frac{1.6173\lambda^2}{\lambda^2 - (0.1746)^2} + \frac{4.139\lambda^2}{\lambda^2 - (15.03)^2}$		
Al_2O_3	$n_o^2 - 1 = \frac{1.4313493\lambda^2}{\lambda^2 - (0.0726631)^2} + \frac{0.65054713\lambda^2}{\lambda^2 - (0.1193242)^2} + \frac{5.3414021\lambda^2}{\lambda^2 - (18.028251)^2}$	0.2–5.5	174
	$n_e^2 - 1 = \frac{1.5039759\lambda^2}{\lambda^2 - (0.0740288)^2} + \frac{0.55069141\lambda^2}{\lambda^2 - (0.1216529)^2} + \frac{6.5927379\lambda^2}{\lambda^2 - (20.072248)^2}$		
ALON	$n^2 - 1 = \frac{2.1375\lambda^2}{\lambda^2 - 0.10256^2} + \frac{4.582\lambda^2}{\lambda^2 - 18.868^2}$	0.4–2.3	175
BBO	$n_o^2 = 2.7405 + \frac{0.0184}{\lambda^2 - 0.0179} - 0.0155\lambda^2$	0.22–1.06	104
	$n_e^2 = 2.3730 + \frac{0.0128}{\lambda^2 - 0.0156} - 0.0044\lambda^2$		
BaF_2	$n^2 - 1 = \frac{0.643356\lambda^2}{\lambda^2 - (0.057789)^2} + \frac{0.506762\lambda^2}{\lambda^2 - (0.10968)^2} + \frac{3.8261\lambda^2}{\lambda^2 - (46.3864)^2}$	0.27–10.3	176
$BaTiO_3$	$n_o^2 - 1 = \frac{4.187\lambda^2}{\lambda^2 - (0.223)^2}$	0.4–0.7	177
	$n_e^2 - 1 = \frac{4.064\lambda^2}{\lambda^2 - (0.211)^2}$		
BeO	$n_o^2 - 1 = \frac{1.92274\lambda^2}{\lambda^2 - (0.07908)^2} + \frac{1.24209\lambda^2}{\lambda^2 - (9.7131)^2}$	0.44–7.0	178
	$n_e^2 - 1 = \frac{1.96939\lambda^2}{\lambda^2 - (0.08590)^2} + \frac{1.67389\lambda^2}{\lambda^2 - (10.4797)^2}$		

TABLE 22 Room-temperature Dispersion Formulas for Crystals (*Continued*)

Material	Dispersion formula (wavelength, λ, in μm)	Range (μm)	Ref.
$Bi_{12}SiO_{20}$, BSO	$n^2 = 2.72777 + \dfrac{3.01705\lambda^2}{\lambda^2 - (0.2661)^2}$	0.48–0.7	72 179
$Bi_{12}GeO_{20}$, BGO	$n^2 - 1 = \dfrac{4.601\lambda^2}{\lambda^2 - (0.242)^2}$	0.4–0.7	117 180
BN	$n \approx 2.117$	0.589	181
BP	$n^2 - 1 = \dfrac{6.841\lambda^2}{\lambda^2 - (0.267)^2}$	0.45–0.63	74
C, diamond	$n^2 - 1 = \dfrac{4.3356\lambda^2}{\lambda^2 - (0.1060)^2} + \dfrac{0.3306\lambda^2}{\lambda^2 - (0.1750)^2}$	0.225–∞	182
$CaCO_3$, calcite	$n_o - 1 = \dfrac{0.8559\lambda^2}{\lambda^2 - (0.0588)^2} + \dfrac{0.8391\lambda^2}{\lambda^2 - (0.141)^2} + \dfrac{0.0009\lambda^2}{\lambda^2 - (0.197)^2} + \dfrac{0.6845\lambda^2}{\lambda^2 - (7.005)^2}$	0.2–2.2	4
	$n_e - 1 = \dfrac{1.0856\lambda^2}{\lambda^2 - (0.07897)^2} + \dfrac{0.0988\lambda^2}{\lambda^2 - (0.142)^2} + \dfrac{0.317\lambda^2}{\lambda^2 - (11.468)^2}$	0.2–3.3	4
CaF_2	$n^2 - 1 = \dfrac{0.5675888\lambda^2}{\lambda^2 - (0.050263605)^2} + \dfrac{0.4710914\lambda^2}{\lambda^2 - (0.1003909)^2} + \dfrac{3.8484723\lambda^2}{\lambda^2 - (34.649040)^2}$	0.23–9.7	120
$CaLa_2S_4$	$n \approx 2.6$	—	75
$CaMoO_4$	$n_o^2 - 1 = \dfrac{2.7840\lambda^2}{\lambda^2 - (0.1483)^2} + \dfrac{1.2425\lambda^2}{\lambda^2 - (11.576)^2}$	0.45–3.8	183
	$n_e^2 - 1 = \dfrac{2.8045\lambda^2}{\lambda^2 - (0.1542)^2} + \dfrac{1.0055\lambda^2}{\lambda^2 - (10.522)^2}$		
$CaWO_4$	$n_o^2 - 1 = \dfrac{2.5493\lambda^2}{\lambda^2 - (0.1347)^2} + \dfrac{0.9200\lambda^2}{\lambda^2 - (10.815)^2}$	0.45–4.0	183
	$n_e^2 - 1 = \dfrac{2.6041\lambda^2}{\lambda^2 - (0.1379)^2} + \dfrac{4.1237\lambda^2}{\lambda^2 - (21.371)^2}$		
$CdGeAs_2$	$n_o^2 = 10.1064 + \dfrac{2.2988\lambda^2}{\lambda^2 - 1.0872} + \dfrac{1.6247\lambda^2}{\lambda^2 - 1370}$	2.4–11.5	170
	$n_e^2 = 11.8018 + \dfrac{1.2152\lambda^2}{\lambda^2 - 2.6971} + \dfrac{1.6922\lambda^2}{\lambda^2 - 1370}$		
CdS	$n_o^2 - 1 = \dfrac{3.96582820\lambda^2}{\lambda^2 - (0.23622804)^2} + \dfrac{0.18113874\lambda^2}{\lambda^2 - (0.48285199)^2}$	0.51–1.4	42
	$n_e^2 - 1 = \dfrac{3.97478769\lambda^2}{\lambda^2 - (0.22426984)^2} + \dfrac{0.26680809\lambda^2}{\lambda^2 - (0.46693785)^2} + \dfrac{0.00074077\lambda^2}{\lambda^2 - (0.50915139)^2}$		
CdSe	$n_o^2 = 4.2243 + \dfrac{1.7680\lambda^2}{\lambda^2 - 0.2270} + \dfrac{3.1200\lambda^2}{\lambda^2 - 3380}$	1–22	170
	$n_e^2 = 4.2009 + \dfrac{1.8875\lambda^2}{\lambda^2 - 0.2171} + \dfrac{3.6461\lambda^2}{\lambda^2 - 3629}$		
CdTe	$n^2 - 1 = \dfrac{6.1977889\lambda^2}{\lambda^2 - (0.317069)^2} + \dfrac{3.2243821\lambda^2}{\lambda^2 - (72.0663)^2}$	6–22	184
CsBr	$n^2 - 1 = \dfrac{0.9533786\lambda^2}{\lambda^2 - (0.0905643)^2} + \dfrac{0.8303809\lambda^2}{\lambda^2 - (0.1671517)^2} + \dfrac{2.847172\lambda^2}{\lambda^2 - (119.0155)^2}$	0.36–39	185
CsCl	$n^2 = 1.33013 + \dfrac{0.98369\lambda^2}{\lambda^2 - (0.119)^2} + \dfrac{0.00009\lambda^2}{\lambda^2 - (0.137)^2} + \dfrac{0.00018\lambda^2}{\lambda^2 - (0.145)^2} + \dfrac{0.30914\lambda^2}{\lambda^2 - (0.162)^2} + \dfrac{4.320\lambda^2}{\lambda^2 - (100.50)^2}$	0.18–40	125
CsI	$n^2 - 1 = \dfrac{0.34617251\lambda^2}{\lambda^2 - (0.0229567)^2} + \dfrac{1.0080886\lambda^2}{\lambda^2 - (0.1466)^2} + \dfrac{0.28551800\lambda^2}{\lambda^2 - (0.1810)^2} + \dfrac{0.39743178\lambda^2}{\lambda^2 - (0.2120)^2} + \dfrac{3.3605359\lambda^2}{\lambda^2 - (161.0)^2}$	0.29–50	126

TABLE 22 Room-temperature Dispersion Formulas for Crystals (*Continued*)

Material	Dispersion formula (wavelength, λ, in μm)	Range (μm)	Ref.
CuCl	$n^2 = 3.580 + \frac{0.03162\lambda^2}{\lambda^2 - 0.1642} + \frac{0.09288}{\lambda^2}$	0.43–2.5	186
$CuGaS_2$	$n_o^2 = 3.9064 + \frac{2.3065\lambda^2}{\lambda^2 - 0.1149} + \frac{1.5479\lambda^2}{\lambda^2 - 738.43}$	0.55–11.5	127 128
	$n_e^2 = 4.3165 + \frac{1.8692\lambda^2}{\lambda^2 - 0.1364} + \frac{1.7575\lambda^2}{\lambda^2 - 738.43}$		
GaAs	$n^2 = 3.5 + \frac{7.4969\lambda^2}{\lambda^2 - (0.4082)^2} + \frac{1.9347\lambda^2}{\lambda^2 - (37.17)^2}$	1.4–11	187
GaN	$n_o^2 = 3.60 + \frac{1.75\lambda^2}{\lambda^2 - (0.256)^2} + \frac{4.1\lambda^2}{\lambda^2 - (17.86)^2}$	<10	188
	$n_e^2 = 5.35 + \frac{5.08\lambda^2}{\lambda^2 - (18.76)^2}$		
GaP	$n^2 - 1 = \frac{1.390\lambda^2}{\lambda^2 - (0.172)^2} + \frac{4.131\lambda^2}{\lambda^2 - (0.234)^2} + \frac{2.570\lambda^2}{\lambda^2 - (0.345)^2} + \frac{2.056\lambda^2}{\lambda^2 - (27.52)^2}$	0.8–10	189
Ge	$n^2 = 9.28156 + \frac{6.72880\lambda^2}{\lambda^2 - 0.44105} + \frac{0.21307\lambda^2}{\lambda^2 - 3870.1}$	2–12	190
HfO_2: 9.8% Y_2O_3	$n^2 - 1 = \frac{1.9558\lambda^2}{\lambda^2 - (0.15494)^2} + \frac{1.345\lambda^2}{\lambda^2 - (0.0634)^2} + \frac{10.41\lambda^2}{\lambda^2 - (27.12)^2}$	0.365–5	132
InAs	$n^2 = 11.1 + \frac{0.71\lambda^2}{\lambda^2 - (2.551)^2} + \frac{2.75\lambda^2}{\lambda^2 - (45.66)^2}$	3.7–31.3	191
InP	$n^2 = 7.255 + \frac{2.316\lambda^2}{\lambda^2 - (0.6263)^2} + \frac{2.765\lambda^2}{\lambda^2 - (32.935)^2}$	0.95–10	192
KBr	$n^2 = 1.39408 + \frac{0.79221\lambda^2}{\lambda^2 - (0.146)^2} + \frac{0.01981\lambda^2}{\lambda^2 - (0.173)^2} + \frac{0.15587\lambda^2}{\lambda^2 - (0.187)^2}$ $+ \frac{0.17673\lambda^2}{\lambda^2 - (60.61)^2} + \frac{2.06217\lambda^2}{\lambda^2 - (87.72)^2}$	0.2–40	125
KCl	$n^2 = 1.26486 + \frac{0.30523\lambda^2}{\lambda^2 - (0.100)^2} + \frac{0.41620\lambda^2}{\lambda^2 - (0.131)^2} + \frac{0.18870\lambda^2}{\lambda^2 - (0.162)^2} + \frac{2.6200\lambda^2}{\lambda^2 - (70.42)^2}$	0.18–35	125
KF	$n^2 = 1.55083 + \frac{0.29162\lambda^2}{\lambda^2 - (0.126)^2} + \frac{3.60001\lambda^2}{\lambda^2 - (51.55)^2}$	0.15–22.0	125
KH_2PO_4 KDP	$n_o^2 - 1 = \frac{1.256618\lambda^2}{\lambda^2 - 0.0084478168} + \frac{33.89909\lambda^2}{\lambda^2 - 1113.904}$	0.4–1.06	193
	$n_e^2 - 1 = \frac{1.131091\lambda^2}{\lambda^2 - 0.008145980} + \frac{5.75675\lambda^2}{\lambda^2 - 811.7537}$		
KI	$n^2 = 1.47285 + \frac{0.16512\lambda^2}{\lambda^2 - (0.129)^2} + \frac{0.41222\lambda^2}{\lambda^2 - (0.175)^2} + \frac{0.44163\lambda^2}{\lambda^2 - (0.187)^2}$ $+ \frac{0.16076\lambda^2}{\lambda^2 - (0.219)^2} + \frac{0.33571\lambda^2}{\lambda^2 - (69.44)^2} + \frac{1.92474\lambda^2}{\lambda^2 - (98.04)^2}$	0.25–50	125
$KNbO_3$	$n_x^2 - 1 = \frac{2.49710\lambda^2}{\lambda^2 - (0.12909)^2} + \frac{1.33660\lambda^2}{\lambda^2 - (0.25816)^2} - 0.025174\lambda^2$	0.40–3.4	134
	$n_y^2 - 1 = \frac{2.54337\lambda^2}{\lambda^2 - (0.13701)^2} + \frac{1.44122\lambda^2}{\lambda^2 - (0.27275)^2} - 0.028450\lambda^2$		
	$n_z^2 - 1 = \frac{2.37108\lambda^2}{\lambda^2 - (0.11972)^2} + \frac{1.04825\lambda^2}{\lambda^2 - (0.25523)^2} - 0.019433\lambda^2$		

TABLE 22 Room-temperature Dispersion Formulas for Crystals (*Continued*)

Material	Dispersion formula (wavelength, λ, in μm)	Range (μm)	Ref.
$KTaO_3$	$n^2 - 1 = \frac{3.591\lambda^2}{\lambda^2 - (0.193)^2}$	0.4–1.06	194
$KTiOPO_4$ KTP	$n_x^2 = 2.16747 + \frac{0.83733\lambda^2}{\lambda^2 - 0.04611} - 0.01713\lambda^2$	0.4–1.06	195
	$n_y^2 = 2.19229 + \frac{0.83547\lambda^2}{\lambda^2 - 0.04970} - 0.01621\lambda^2$		
	$n_z^2 = 2.25411 + \frac{1.06543\lambda^2}{\lambda^2 - 0.05486} - 0.02140\lambda^2$		
LaF_3	$n_o^2 - 1 = \frac{1.5376\lambda^2}{\lambda^2 - (0.0881)^2}$	0.35–0.70	196
	$n_e^2 - 1 = \frac{1.5149\lambda^2}{\lambda^2 - (0.0878)^2}$		
LiB_3O_5 LBO	$n_x^2 = 2.45768 + \frac{0.0098877}{\lambda^2 - 0.026095} - 0.013847\lambda^2$	0.29–1.06	197
	$n_y^2 = 2.52500 + \frac{0.017123}{\lambda^2 - 0.0060517} - 0.0087838\lambda^2$		
	$n_z^2 = 2.58488 + \frac{0.012737}{\lambda^2 - 0.016293} - 0.016293\lambda^2$		
LiF	$n^2 - 1 = \frac{0.92549\lambda^2}{\lambda^2 - (0.07376)^2} + \frac{6.96747\lambda^2}{\lambda^2 - (32.79)^2}$	0.1–10	125
$LiIO_3$	$n_0^2 = 2.03132 + \frac{1.37623\lambda^2}{\lambda^2 - 0.0350823} + \frac{1.06745\lambda^2}{\lambda^2 - 169.0}$	0.5–5	56
	$n_e^2 = 1.83086 + \frac{1.08807\lambda^2}{\lambda^2 - 0.0313810} + \frac{0.554582\lambda^2}{\lambda^2 - 158.76}$		
$LiNbO_3$	$n_o^2 = 2.39198 + \frac{2.51118\lambda^2}{\lambda^2 - (0.217)^2} + \frac{7.1333\lambda^2}{\lambda^2 - (16.502)^2}$	0.4–3.1	198
	$n_e^2 = 2.32468 + \frac{2.25650\lambda^2}{\lambda^2 - (0.210)^2} + \frac{14.503\lambda^2}{\lambda^2 - (25.915)^2}$		
$LiYF_4$	$n_o^2 = 1.38757 + \frac{0.70757\lambda^2}{\lambda^2 - 0.00931} + \frac{0.18849\lambda^2}{\lambda^2 - 50.99741}$	0.23–2.6	138
	$n_e^2 = 1.31021 + \frac{0.84903\lambda^2}{\lambda^2 - 0.00876} + \frac{0.53607\lambda^2}{\lambda^2 - 134.9566}$		
$MgAl_2O_4$	$n^2 - 1 = \frac{1.8938\lambda^2}{\lambda^2 - (0.09942)^2} + \frac{3.0755\lambda^2}{\lambda^2 - (15.826)^2}$	0.35–5.5	199
MgF_2	$n_o^2 - 1 = \frac{0.48755108\lambda^2}{\lambda^2 - (0.04338408)^2} + \frac{0.39875031\lambda^2}{\lambda^2 - (0.09461442)^2} + \frac{2.3120353\lambda^2}{\lambda^2 - (23.793604)^2}$	0.20–7.04	200
	$n_e^2 - 1 = \frac{0.41344023\lambda^2}{\lambda^2 - (0.03684262)^2} + \frac{0.50497499\lambda^2}{\lambda^2 - (0.09076162)^2} + \frac{2.4904862\lambda^2}{\lambda^2 - (12.771995)^2}$		
MgO	$n^2 - 1 = \frac{1.111033\lambda^2}{\lambda^2 - (0.0712465)^2} + \frac{0.8460085\lambda^2}{\lambda^2 - (0.1375204)^2} + \frac{7.808527\lambda^2}{\lambda^2 - (26.89302)^2}$	0.36–5.4	139
NaBr	$n^2 = 1.06728 + \frac{1.10463\lambda^2}{\lambda^2 - (0.125)^2} + \frac{0.18816\lambda^2}{\lambda^2 - (0.145)^2} + \frac{0.00243\lambda^2}{\lambda^2 - (0.176)^2} + \frac{0.24454\lambda^2}{\lambda^2 - (0.188)^2} + \frac{3.7960\lambda^2}{\lambda^2 - (74.63)^2}$	0.21–34	125

TABLE 22 Room-temperature Dispersion Formulas for Crystals (*Continued*)

Material	Dispersion formula (wavelength, λ, in μm)	Range (μm)	Ref.
NaCl	$n^2 = 1.00055 + \frac{0.19800\lambda^2}{\lambda^2-(0.050)^2} + \frac{0.48398\lambda^2}{\lambda^2-(0.100)^2} + \frac{0.38696\lambda^2}{\lambda^2-(0.128)^2} + \frac{0.25998\lambda^2}{\lambda^2-(0.158)^2}$	0.2–30	125
	$+ \frac{0.08796\lambda^2}{\lambda^2-(40.50)^2} + \frac{3.17064\lambda^2}{\lambda^2-(60.98)^2} + \frac{0.30038\lambda^2}{\lambda^2-(120.34)^2}$		
NaF	$n^2 = 1.41572 + \frac{0.32785\lambda^2}{\lambda^2-(0.117)^2} + \frac{3.18248\lambda^2}{\lambda^2-(40.57)^2}$	0.15–17	125
NaI	$n^2 = 1.478 + \frac{1.532\lambda^2}{\lambda^2-(0.170)^2} + \frac{4.27\lambda^2}{\lambda^2-(86.21)^2}$	0.25–40	125
$[NH_4]_2CO$ Urea	$n_o^2 = 2.1823 + \frac{0.0125}{\lambda^2-0.0300}$	0.3–1.06	201
	$n_e^2 = 2.51527 + \frac{0.0240}{\lambda^2-0.0300} + \frac{0.020(\lambda-1.52)}{(\lambda-1.52)^2+0.8771}$		
$NH_4H_2PO_4$ ADP	$n_o^2 - 1 = \frac{1.298990\lambda^2}{\lambda^2-0.0089232927} + \frac{43.17364\lambda^2}{\lambda^2-1188.531}$	0.4–1.06	193
	$n_e^2 - 1 = \frac{1.162166\lambda^2}{\lambda^2-0.0085932421} + \frac{12.01997\lambda^2}{\lambda^2-831.8239}$		
PbF_2	$n^2 - 1 = \frac{0.66959342\lambda^2}{\lambda^2-(0.00034911)^2} + \frac{1.3086319\lambda^2}{\lambda^2-(0.17144455)^2} + \frac{0.01670641\lambda^2}{\lambda^2-(0.28125513)^2} + \frac{2007.8865\lambda^2}{\lambda^2-(796.67469)^2}$	0.3–11.9	202
$PbMoO_4$	$n_o^2 - 1 = \frac{3.54642\lambda^2}{\lambda^2-(0.18518)^2} + \frac{0.58270\lambda^2}{\lambda^2-(0.33764)^2}$	0.44–1.08	203
	$n_e^2 - 1 = \frac{3.52555\lambda^2}{\lambda^2-(0.17950)^2} + \frac{0.20660\lambda^2}{\lambda^2-(0.32537)^2}$		
PbS	$n^2 - 1 = \frac{15.9\lambda^2}{\lambda^2-(0.77)^2} + \frac{133.2\lambda^2}{\lambda^2-(141)^2}$	3.5–10	141
PbSe	$n^2 - 1 = \frac{21.1\lambda^2}{\lambda^2-(1.37)^2}$	5.0–10	141
PbTe	$n^2 - 1 = \frac{30.046\lambda^2}{\lambda^2-(1.563)^2}$	4.0–12.5	204
$PbTiO_3$	$n_o^2 - 1 = \frac{5.363\lambda^2}{\lambda^2-(0.224)^2}$	0.45–1.15	205
	$n_e^2 - 1 = \frac{5.366\lambda^2}{\lambda^2-(0.217)^2}$		
Se	$n_o = 2.790; \quad n_e = 3.608@1.06\ \mu m$	—	206
	$n_0 = 2.64; \quad n_e = 3.41@10.6\ \mu m$		
Si	$n^2 - 1 = \frac{10.6684293\lambda^2}{\lambda^2-(0.301516485)^2} + \frac{0.003043475\lambda^2}{\lambda^2-(1.13475115)^2} + \frac{1.54133408\lambda^2}{\lambda^2-(1104.0)^2}$	1.36–11	42
β-SiC	$n^2 - 1 = \frac{5.5705\lambda^2}{\lambda^2-(0.1635)^2}$	0.47–0.69	207
α-SiC	$n_o^2 - 1 = \frac{5.5515\lambda^2}{\lambda^2-(0.16250)^2}$	0.49–1.06	208
	$n_e^2 - 1 = \frac{5.7382\lambda^2}{\lambda^2-(0.16897)^2}$		

TABLE 22 Room-temperature Dispersion Formulas for Crystals (*Continued*)

Material	Dispersion formula (wavelength, λ, in μm)	Range (μm)	Ref.
α-SiO_2 quartz	$n_o^2 - 1 = \frac{0.663044\lambda^2}{\lambda^2 - (0.060)^2} + \frac{0.517852\lambda^2}{\lambda^2 - (0.106)^2} + \frac{0.175912\lambda^2}{\lambda^2 - (0.119)^2} + \frac{0.565380\lambda^2}{\lambda^2 - (8.844)^2} + \frac{1.675299\lambda^2}{\lambda^2 - (20.742)^2}$	0.18–0.71	140
	$n_e^2 - 1 = \frac{0.665721\lambda^2}{\lambda^2 - (0.060)^2} + \frac{0.503511\lambda^2}{\lambda^2 - (0.106)^2} + \frac{0.214792\lambda^2}{\lambda^2 - (0.119)^2} + \frac{0.539173\lambda^2}{\lambda^2 - (8.792)^2} + \frac{1.807613\lambda^2}{\lambda^2 - (197.70)^2}$		
SrF_2	$n^2 - 1 = \frac{0.67805894\lambda^2}{\lambda^2 - (0.05628989)^2} + \frac{0.37140533\lambda^2}{\lambda^2 - (0.10801027)^2} + \frac{3.8484723\lambda^2}{\lambda^2 - (34.649040)^2}$	0.21–11.5	113
$SrMoO_4$	$n_o^2 - 1 = \frac{2.4839\lambda^2}{\lambda^2 - (0.1451)^2} + \frac{0.1015\lambda^2}{\lambda^2 - (4.603)^2}$	0.45–2.4	183
	$n_e^2 - 1 = \frac{2.4923\lambda^2}{\lambda^2 - (0.1488)^2} + \frac{0.1050\lambda^2}{\lambda^2 - (4.544)^2}$		
$SrTiO_3$	$n^2 - 1 = \frac{3.042143\lambda^2}{\lambda^2 - (0.1475902)^2} + \frac{1.170065\lambda^2}{\lambda^2 - (0.2953086)^2} + \frac{30.83326\lambda^2}{\lambda^2 - (33.18606)^2}$	0.43–3.8	80
Te	$n_o^2 = 18.5346 + \frac{4.3289\lambda^2}{\lambda^2 - 3.9810} + \frac{3.7800\lambda^2}{\lambda^2 - 11813}$	4–14	170
	$n_e^2 = 29.5222 + \frac{9.3068\lambda^2}{\lambda^2 - 2.5766} + \frac{9.2350\lambda^2}{\lambda^2 - 13521}$		
TeO_2	$N_o^2 - 1 = \frac{2.584\lambda^2}{\lambda^2 - (0.1342)^2} + \frac{1.157\lambda^2}{\lambda^2 - (0.2638)^2}$	0.4–1.0	142
	$n_e^2 - 1 = \frac{2.823\lambda^2}{\lambda^2 - (0.1342)^2} + \frac{1.542\lambda^2}{\lambda^2 - (0.2631)^2}$		
TiO_2	$n_o^2 = 5.913 + \frac{0.2441}{\lambda^2 - 0.0803}$	0.43–1.5	143
	$n_e^2 = 7.197 + \frac{0.3322}{\lambda^2 - 0.0843}$		
Tl_3AsSe_3 TAS	$n_o^2 - 1 = \frac{10.210\lambda^2}{\lambda^2 - (0.444)^2} + \frac{0.522\lambda^2}{\lambda^2 - (25.0)^2}$	2–12	144
	$n_e^2 - 1 = \frac{8.993\lambda^2}{\lambda^2 - (0.444)^2} + \frac{0.308\lambda^2}{\lambda^2 - (25.0)^2}$		
TlBr	$\frac{n^2 - 1}{n^2 + 2} = 0.48484 + \frac{0.10279\lambda^2}{\lambda^2 - 0.090000} - 0.0047896\lambda^2$	0.54–0.65	169
Tl[Br, I] KRS-5	$n^2 - 1 = \frac{1.8293958\lambda^2}{\lambda^2 - (0.150)^2} + \frac{1.6675593\lambda^2}{\lambda^2 - (0.250)^2} + \frac{1.1210424\lambda^2}{\lambda^2 - (0.350)^2} + \frac{0.04513366\lambda^2}{\lambda^2 - (0.450)^2} + \frac{12.380234\lambda^2}{\lambda^2 - (164.59)^2}$	0.58–39.4	145
TlCl	$\frac{n^2 - 1}{n^2 + 2} = 0.47856 + \frac{0.07858\lambda^2}{\lambda^2 - 0.08277} - 0.00881\lambda^2$	0.43–0.66	169
Tl[Cl, Br] KRS-6	$n^2 - 1 = \frac{3.821\lambda^2}{\lambda^2 - (0.02234)^2} - 0.000877\lambda^2$	0.6–24	209
$Y_3Al_5O_{12}$ YAG	$n^2 - 1 = \frac{2.293\lambda^2}{\lambda^2 - (0.1095)^2} + \frac{3.705\lambda^2}{\lambda^2 - (17.825)^2}$	0.4–4.0	183
Y_2O_3	$n^2 - 1 = \frac{2.578\lambda^2}{\lambda^2 - (0.1387)^2} + \frac{3.935\lambda^2}{\lambda^2 - (22.936)^2}$	0.2–12	210
$ZnGeP_2$	$n_o^2 = 4.4733 + \frac{5.2658\lambda^2}{\lambda^2 - 0.1338} + \frac{1.4909\lambda^2}{\lambda^2 - 662.55}$	0.4–12	128
	$n_e^2 = 4.6332 + \frac{5.3422\lambda^2}{\lambda^2 - 0.1426} + \frac{1.4580\lambda^2}{\lambda^2 - 662.55}$		

TABLE 22 Room-temperature Dispersion Formulas for Crystals (*Continued*)

Material	Dispersion formula (wavelength, λ, in μm)	Range (μm)	Ref.
ZnO	$n_o^2 = 2.81418 + \dfrac{0.87968\lambda^2}{\lambda^2 - (0.3042)^2} - 0.00711\lambda^2$	0.45–4.0	183
	$n_e^2 = 2.80333 + \dfrac{0.94470\lambda^2}{\lambda^2 - (0.3004)^2} - 0.00714\lambda^2$		
β-ZnS	$n^2 - 1 = \dfrac{0.33904026\lambda^2}{\lambda^2 - (0.31423026)^2} + \dfrac{3.7606868\lambda^2}{\lambda^2 - (0.1759417)^2} + \dfrac{2.7312353\lambda^2}{\lambda^2 - (33.886560)^2}$	0.55–10.5	113
α-ZnS	$n_o^2 - 1 = 3.4175 + \dfrac{1.7396\lambda^2}{\lambda^2 - (0.2677)^2}$	0.36–1.4	211
	$n_e^2 - 1 = 3.4264 + \dfrac{1.7491\lambda^2}{\lambda^2 - (0.2674)^2}$		
ZnSe	$n^2 - 1 = \dfrac{4.2980149\lambda^2}{\lambda^2 - 0.1920630^2} + \dfrac{0.62776557\lambda^2}{\lambda^2 - 0.37878260^2} + \dfrac{2.8955633\lambda^2}{\lambda^2 - 46.994595^2}$	0.55–18	113
ZnTe	$n^2 = 9.92 + \dfrac{0.42530}{\lambda^2 - (0.37766)^2} + \dfrac{2.63580}{\lambda^2/(56.5)^2 - 1}$	0.55–30	212
ZrO_2:12%Y_2O_3	$n^2 - 1 = \dfrac{1.347091\lambda^2}{\lambda^2 - (0.062543)^2} + \dfrac{2.117788\lambda^2}{\lambda^2 - (0.166739)^2} + \dfrac{9.452943\lambda^2}{\lambda^2 - (24.320570)^2}$	0.36–5.1	148

TABLE 23 Room-temperature Dispersion Formula for Glasses

Material	Dispersion formula (wavelength, λ, in μm)	Range (μm)	Ref.
TiK1	$n^2 = 2.1573978 - 8.4004189 \cdot 10^{-3}\lambda^2 + 1.0457582 \cdot 10^{-2}\lambda^{-2} + 2.1822593 \cdot 10^{-4}\lambda^{-4} - 5.5063640 \cdot 10^{-6}\lambda^{-6} + 5.4469060 \cdot 10^{-7}\lambda^{-8}$	0.37–1.01	149
FK5	$n^2 = 2.1887621 - 9.5572007 \cdot 10^{-3}\lambda^2 + 8.9915232 \cdot 10^{-3}\lambda^{-2} + 1.4560516 \cdot 10^{-4}\lambda^{-4} - 5.2843067 \cdot 10^{-6}\lambda^{-6} + 3.4588010 \cdot 10^{-7}\lambda^{-8}$	0.37–1.01†	149
	$n^2 - 1 = \dfrac{1.036330719\lambda^2}{\lambda^2 - (0.0776227030)^2} + \dfrac{0.152107703\lambda^2}{\lambda^2 - (0.138959626)^2} + \dfrac{0.913166269\lambda^2}{\lambda^2 - (9.93162512)^2}$	0.37–2.33	42
TiF1	$n^2 = 2.2473124 - 8.9044058 \cdot 10^{-3}\lambda^2 + 1.2493525 \cdot 10^{-2}\lambda^{-2} + 4.2650638 \cdot 10^{-4}\lambda^{-4} - 2.1564809 \cdot 10^{-6}\lambda^{-6} + 2.6364065 \cdot 10^{-6}\lambda^{-8}$	0.37–1.01	149
BK7	$n^2 = 2.2718929 - 1.0108077 \cdot 10^{-2}\lambda^2 + 1.0592509 \cdot 10^{-2}\lambda^{-2} + 2.0816965 \cdot 10^{-4}\lambda^{-4} - 7.6472538 \cdot 10^{-6}\lambda^{-6} + 4.9240991 \cdot 10^{-7}\lambda^{-8}$	0.37–1.01†	149
PK2	$n^2 = 2.2770533 - 1.0532010 \cdot 10^{-2}\lambda^2 + 1.0188354 \cdot 10^{-2}\lambda^{-2} + 2.9001564 \cdot 10^{-4}\lambda^{-4} - 1.9602856 \cdot 10^{-5}\lambda^{-6} + 1.0967718 \cdot 10^{-6}\lambda^{-8}$	0.37–1.01	149
K5	$n^2 = 2.2850299 - 8.6010725 \cdot 10^{-3}\lambda^2 + 1.1806783 \cdot 10^{-2}\lambda^{-2} + 2.0765657 \cdot 10^{-4}\lambda^{-4} - 2.1314913 \cdot 10^{-6}\lambda^{-6} + 3.2131234 \cdot 10^{-7}\lambda^{-8}$	0.37–1.01†	149
KF9	$n^2 = 2.2824396 - 8.5960144 \cdot 10^{-3}\lambda^2 + 1.3442645 \cdot 10^{-2}\lambda^{-2} + 2.7803535 \cdot 10^{-4}\lambda^{-4} - 4.9998960 \cdot 10^{-7}\lambda^{-6} + 7.7105911 \cdot 10^{-7}\lambda^{-8}$	0.37–1.01†	149
BaLK1	$n^2 = 2.2966923 - 8.2975549 \cdot 10^{-3}\lambda^2 + 1.1907234 \cdot 10^{-2}\lambda^{-2} + 1.9908305 \cdot 10^{-4}\lambda^{-4} - 2.0306838 \cdot 10^{-6}\lambda^{-6} + 3.1429703 \cdot 10^{-7}\lambda^{-8}$	0.37–1.01	149
KzF6	$n^2 = 2.2934044 - 1.0346122 \cdot 10^{-2}\lambda^2 + 1.3319863 \cdot 10^{-2}\lambda^{-2} + 3.4833226 \cdot 10^{-4}\lambda^{-4} - 9.9354090 \cdot 10^{-6}\lambda^{-6} + 1.1227905 \cdot 10^{-6}\lambda^{-8}$	0.37–1.01	149
ZK1	$n^2 = 2.3157951 - 8.7493905 \cdot 10^{-3}\lambda^2 + 1.2329645 \cdot 10^{-2}\lambda^{-2} + 2.6311112 \cdot 10^{-4}\lambda^{-4} - 8.2854201 \cdot 10^{-6}\lambda^{-6} + 7.3735801 \cdot 10^{-7}\lambda^{-8}$	0.37–1.01	149

TABLE 23 Room-temperature Dispersion Formula for Glasses (*Continued*)

Material	Dispersion formula (wavelength, λ, in μm)	Range (μm)	Ref.
LLF1	$n^2 = 2.3505162 - 8.5306451 \cdot 10^{-3}\lambda^2 + 1.5750853 \cdot 10^{-2}\lambda^{-2} + 4.2811388 \cdot 10^{-4}\lambda^{-4} - 6.9875718 \cdot 10^{-6}\lambda^{-6} + 1.7175517 \cdot 10^{-6}\lambda^{-8}$	0.37–1.01†	149
Ultran 30	$n^2 = 2.3677942 - 6.0818906 \cdot 10^{-3}\lambda^2 + 1.0509568 \cdot 10^{-2}\lambda^{-2} + 1.3105575 \cdot 10^{-4}\lambda^{-4} - 4.9854380 \cdot 10^{-7}\lambda^{-6} + 1.0473652 \cdot 10^{-7}\lambda^{-8}$	0.37–1.01†	149
	$n^2 - 1 = \dfrac{1.36689\lambda^2}{\lambda^2 - (0.089286)^2} + \dfrac{0.34711\lambda^2}{\lambda^2 - (7.9103)^2}$	0.37–2.3	149*
PSK3	$n^2 = 2.3768193 - 1.0146514 \cdot 10^{-2}\lambda^2 + 1.2167148 \cdot 10^{-2}\lambda^{-2} + 1.1916606 \cdot 10^{-4}\lambda^{-4} + 6.4250627 \cdot 10^{-6}\lambda^{-6} - 1.7478706 \cdot 10^{-7}\lambda^{-8}$	0.37–1.01	149
BaK1	$n^2 = 2.4333007 - 8.4931353 \cdot 10^{-3}\lambda^2 + 1.3893512 \cdot 10^{-2}\lambda^{-2} + 2.6798268 \cdot 10^{-4}\lambda^{-4} - 6.1946101 \cdot 10^{-6}\lambda^{-6} + 6.2209005 \cdot 10^{-7}\lambda^{-8}$	0.37–1.01†	149
BaLF4	$n^2 = 2.4528366 - 9.2047678 \cdot 10^{-3}\lambda^2 + 1.4552794 \cdot 10^{-2}\lambda^{-2} + 4.3046688 \cdot 10^{-4}\lambda^{-4} - 2.0489836 \cdot 10^{-5}\lambda^{-6} + 1.5924415 \cdot 10^{-6}\lambda^{-8}$	0.37–1.01†	149
	$n^2 - 1 = \dfrac{1.25385390\lambda^2}{\lambda^2 - (0.0856548405)^2} + \dfrac{0.198113511\lambda^2}{\lambda^2 - (0.173243878)^2} + \dfrac{1.01615191\lambda^2}{\lambda^2 - (10.8069635)^2}$	0.37–2.33	42
LF5	$n^2 = 2.4441760 - 8.3059695 \cdot 10^{-3}\lambda^2 + 1.9000697 \cdot 10^{-2}\lambda^{-2} + 5.4129697 \cdot 10^{-4}\lambda^{-4} - 4.1973155 \cdot 10^{-6}\lambda^{-6} + 2.3742897 \cdot 10^{-6}\lambda^{-8}$	0.37–1.01†	149
LgSK2	$n^2 = 2.4750760 - 5.4304528 \cdot 10^{-3}\lambda^2 + 1.3893210 \cdot 10^{-2}\lambda^{-2} + 2.2990560 \cdot 10^{-4}\lambda^{-4} - 1.6868474 \cdot 10^{-6}\lambda^{-6} + 4.3959703 \cdot 10^{-7}\lambda^{-8}$	0.37–1.01	149
FF5	$n^2 = 2.4743324 - 1.0955338 \cdot 10^{-2}\lambda^2 + 1.9293801 \cdot 10^{-2}\lambda^{-2} + 1.4497732 \cdot 10^{-3}\lambda^{-4} - 1.1038744 \cdot 10^{-4}\lambda^{-6} + 1.1136008 \cdot 10^{-5}\lambda^{-8}$	0.37–1.01	151
SK4	$n^2 = 2.5585228 - 9.8824951 \cdot 10^{-3}\lambda^2 + 1.5151820 \cdot 10^{-2}\lambda^{-2} + 2.1134478 \cdot 10^{-4}\lambda^{-4} - 3.4130130 \cdot 10^{-6}\lambda^{-6} + 1.2673355 \cdot 10^{-7}\lambda^{-8}$	0.37–1.01†	149
KzFSN4	$n^2 = 2.5293446 - 1.3234586 \cdot 10^{-2}\lambda^2 + 1.8586165 \cdot 10^{-2}\lambda^{-2} + 5.4759655 \cdot 10^{-4}\lambda^{-4} - 1.1717987 \cdot 10^{-5}\lambda^{-6} + 2.0042905 \cdot 10^{-6}\lambda^{-8}$	0.37–1.01†	149
	$n^2 - 1 = \dfrac{1.38374965\lambda^2}{\lambda^2 - (0.0948292206)^2} + \dfrac{0.164626811\lambda^2}{\lambda^2 - (0.201806158)^2} + \dfrac{0.85913757\lambda^2}{\lambda^2 - (8.28807544)^2}$	0.37–2.33	42
SSK4	$n^2 = 2.5707849 - 9.2577764 \cdot 10^{-3}\lambda^2 + 1.6170751 \cdot 10^{-2}\lambda^{-2} + 2.7742702 \cdot 10^{-4}\lambda^{-4} + 1.2686469 \cdot 10^{-7}\lambda^{-6} + 4.5044790 \cdot 10^{-7}\lambda^{-8}$	0.37–1.01	149
F2	$n^2 = 2.5554063 - 8.8746150 \cdot 10^{-3}\lambda^2 + 2.2494787 \cdot 10^{-2}\lambda^{-2} + 8.6924972 \cdot 10^{-4}\lambda^{-4} - 2.4011704 \cdot 10^{-5}\lambda^{-6} + 4.5365169 \cdot 10^{-6}\lambda^{-8}$	0.37–1.01†	149
BaSF10	$n^2 = 2.6531250 - 8.1388553 \cdot 10^{-3}\lambda^2 + 2.2995643 \cdot 10^{-2}\lambda^{-2} + 7.3535957 \cdot 10^{-4}\lambda^{-4} - 1.3407390 \cdot 10^{-5}\lambda^{-6} + 3.6962325 \cdot 10^{-6}\lambda^{-8}$	0.37–1.01†	149
BaF10	$n^2 = 2.7324621 - 1.2490460 \cdot 10^{-2}\lambda^2 + 1.8562334 \cdot 10^{-2}\lambda^{-2} + 9.9990536 \cdot 10^{-4}\lambda^{-4} - 6.8388552 \cdot 10^{-5}\lambda^{-6} + 4.9257931 \cdot 10^{-6}\lambda^{-8}$	0.37–1.01	151
LaK10	$n^2 = 2.8984614 - 1.4857039 \cdot 10^{-2}\lambda^2 + 2.0985037 \cdot 10^{-2}\lambda^{-2} + 5.4506921 \cdot 10^{-4}\lambda^{-4} - 1.7297314 \cdot 10^{-5}\lambda^{-6} + 1.7993601 \cdot 10^{-6}\lambda^{-8}$	0.37–1.01	149
TaC2	$n^2 = 2.9717137 - 1.4952593 \cdot 10^{-2}\lambda^2 + 2.0162868 \cdot 10^{-2}\lambda^{-2} + 9.4072283 \cdot 10^{-4}\lambda^{-4} - 8.8614104 \cdot 10^{-5}\lambda^{-6} + 5.3191242 \cdot 10^{-6}\lambda^{-8}$	0.37–1.01	151
NbF1	$n^2 = 2.9753491 - 1.4613470 \cdot 10^{-2}\lambda^2 + 2.1096383 \cdot 10^{-2}\lambda^{-2} + 1.1980380 \cdot 10^{-3}\lambda^{-4} - 1.1887388 \cdot 10^{-4}\lambda^{-6} + 7.3444350 \cdot 10^{-6}\lambda^{-8}$	0.37–1.01	151
LaF2	$n^2 = 2.9673787 - 1.0978767 \cdot 10^{-2}\lambda^2 + 2.5088607 \cdot 10^{-2}\lambda^{-2} + 6.3171596 \cdot 10^{-4}\lambda^{-4} - 7.5645417 \cdot 10^{-6}\lambda^{-6} + 2.3202213 \cdot 10^{-6}\lambda^{-8}$	0.37–1.01†	149
SF6	$n^2 = 3.1195007 - 1.0902580 \cdot 10^{-2}\lambda^2 + 4.1330651 \cdot 10^{-2}\lambda^{-2} + 3.1800214 \cdot 10^{-3}\lambda^{-4} - 2.1953184 \cdot 10^{-4}\lambda^{-6} + 2.6671014 \cdot 10^{-5}\lambda^{-8}$	0.37–1.01†	149

TABLE 23 Room-temperature Dispersion Formula for Glasses (*Continued*)

Material	Dispersion formula (wavelength, λ, in μm)	Range (μm)	Ref.
TaFD5	$n^2 = 3.2729098 - 1.2888257 \cdot 10^{-2}\lambda^2 + 3.3451363 \cdot 10^{-2}\lambda^{-2} + 6.8221381 \cdot 10^{-5}\lambda^{-4} + 1.1215427 \cdot 10^{-4}\lambda^{-6} - 4.0485659 \cdot 10^{-6}\lambda^{-8}$	0.37–1.01	151
Fused silica	$n^2 - 1 = \frac{0.6961663\lambda^2}{\lambda^2 - (0.0684043)^2} + \frac{0.4079426\lambda^2}{\lambda^2 - (0.1162414)^2} + \frac{0.8974794\lambda^2}{\lambda^2 - (9.896161)^2}$	0.21–3.71	152
Fused germania	$n^2 - 1 = \frac{0.80686642\lambda^2}{\lambda^2 - (0.06897261)^2} + \frac{0.71815848\lambda^2}{\lambda^2 - (0.1539661)^2} + \frac{0.85416831\lambda^2}{\lambda^2 - (11.841931)^2}$	0.36–4.3	153
BS-39B	$n^2 - 1 = \frac{1.7441\lambda^2}{\lambda^2 - (0.1155)^2} + \frac{1.6465\lambda^2}{\lambda^2 - (14.981)^2}$	0.43–4.5	154*
CORTRAN 9753	$n = 1.61251@0.4861\ \mu m$ $n = 1.60475@0.5893\ \mu m \qquad n = 1.60151@0.6563\ \mu m$	—	155
CORTRAN 9754	$n^2 - 1 = \frac{1.66570\lambda^2}{\lambda^2 - (0.10832)^2} + \frac{0.04059\lambda^2}{\lambda^2 - (0.23813)^2} + \frac{1.31792\lambda^2}{\lambda^2 - (13.57622)^2}$	0.4–5.5	155
IRG 2	$n^2 - 1 = \frac{2.07670\lambda^2}{\lambda^2 - (0.11492)^2} + \frac{0.35738\lambda^2}{\lambda^2 - (0.23114)^2} + \frac{2.88166\lambda^2}{\lambda^2 - (17.48306)^2}$	0.365–4.6	149*
IRG 9	$n^2 - 1 = \frac{1.1852\lambda^2}{\lambda^2 - (0.084353)^2} + \frac{0.66877\lambda^2}{\lambda^2 - (11.568)^2}$	0.365–4.6	149*
IRG 11	$n^2 - 1 = \frac{1.7531\lambda^2}{\lambda^2 - (0.1185)^2} + \frac{0.4346\lambda^2}{\lambda^2 - (8.356)^2}$	0.48–3.3	149*
IRG 100	$n^2 = 4.5819 + \frac{2.2693\lambda^2}{\lambda^2 - (0.447)^2} - 0.000928\lambda^2$	1–14	149*
HTF-1	$n^2 = 2.0633034 - 3.2906345 \cdot 10^{-3}\lambda^2 + 7.1765160 \cdot 10^{-3}\lambda^{-2} - 1.9110559 \cdot 10^{-4}\lambda^{-4} + 3.8123441 \cdot 10^{-5}\lambda^{-6} - 2.0668501 \cdot 10^{-6}\lambda^{-8}$	0.37–1.01	150
	$n^2 - 1 = \frac{1.06375\lambda^2}{\lambda^2 - (0.078958)^2} + \frac{0.80098\lambda^2}{\lambda^2 - (15.1579)^2}$	0.37–5	150*
ZBL	$n^2 = 2.03 + \frac{0.265\lambda^2}{\lambda^2 - (0.182)^2} + \frac{1.22\lambda^2}{\lambda^2 - (20.7)^2} + \frac{1.97\lambda^2}{\lambda^2 - (37.9)^2}$	1–5	213
ZBLA	$n^2 - 1 = \frac{1.291\lambda^2}{\lambda^2 - (0.0969)^2} + \frac{2.76\lambda^2}{\lambda^2 - (26.0)^2}$	0.64–4.8	158
ZBLAN	$n^2 - 1 = \frac{1.168\lambda^2}{\lambda^2 - (0.0954)^2} + \frac{2.77\lambda^2}{\lambda^2 - (25.0)^2}$	0.50–4.8	158
ZBT			
HBL	$n^2 = 1.96 + \frac{0.299\lambda^2}{\lambda^2 - (0.172)^2} + \frac{0.86\lambda^2}{\lambda^2 - (20.8)^2} + \frac{2.22\lambda^2}{\lambda^2 - (41.5)^2}$	1–5	213
HBLA			
HBT			
Arsenic trisulfide	$n^2 - 1 = \frac{1.8983678\lambda^2}{\lambda^2 - (0.150)^2} + \frac{1.9222979\lambda^2}{\lambda^2 - (0.250)^2} + \frac{0.8765134\lambda^2}{\lambda^2 - (0.350)^2} + \frac{0.1188704\lambda^2}{\lambda^2 - (0.450)^2} + \frac{0.9569903\lambda^2}{\lambda^2 - (27.3861)^2}$	0.56–12	163
Arsenic triselenide	$n^2 - 1 = \frac{6.6906\lambda^2}{\lambda^2 - (0.3468)^2}$	0.83–1.15	165
AMTIR-1/TI-20	$n^2 - 1 = \frac{5.298\lambda^2}{\lambda^2 - (0.29007)^2} + \frac{0.6039\lambda^2}{\lambda^2 - (32.022)^2}$	1–14	167*
AMTIR-3/TI-1173	$n^2 - 1 = \frac{5.8505\lambda^2}{\lambda^2 - (0.29192)^2} + \frac{1.4536\lambda^2}{\lambda^2 - (42.714)^2}$	3-14	167*
	$n^2 - 1 = \frac{5.8357\lambda^2}{\lambda^2 - (0.29952)^2} + \frac{1.064\lambda^2}{\lambda^2 - (38.353)^2}$	0.9–14	214

* Out dispersion equation from referenced data.
† Schott dispersion formula range; data available to 2.3 μm.

TABLE 24 Refractive Index of Calcite ($CaCO_3$)[4]

λ, μm	n_o	n_e	λ, μm	n_o	n_e
0.198		1.57796	0.768	1.64974	1.48259
0.200	1.90284	1.57649	0.795	1.64886	1.48216
0.204	1.88242	1.57081	0.801	1.64869	1.48216
0.208	1.86733	1.56640	0.833	1.64772	1.48176
0.211	1.85692	1.56327	0.867	1.64676	1.48137
0.214	1.84558	1.55976	0.905	1.64578	1.48098
0.219	1.83075	1.55496	0.946	1.64480	1.48060
0.226	1.81309	1.54921	0.991	1.64380	1.48022
0.231	1.80233	1.54541	1.042	1.64276	1.47985
0.242	1.78111	1.53782	1.097	1.64167	1.47948
0.257	1.76038	1.53005	1.159	1.64051	1.47910
0.263	1.75343	1.52736	1.229	1.63926	1.47870
0.267	1.74864	1.52547	1.273	1.63849	
0.274	1.74139	1.52261	1.307	1.63789	1.47831
0.291	1.72774	1.51705	1.320	1.63767	
0.303	1.71959	1.51365	1.369	1.63681	
0.312	1.71425	1.51140	1.396	1.63637	1.47789
0.330	1.70515	1.50746	1.422	1.63590	
0.340	1.70078	1.50562	1.479	1.63490	
0.346	1.69833	1.50450	1.497	1.63457	1.47744
0.361	1.69316	1.50224	1.541	1.63381	
0.394	1.68374	1.49810	1.609	1.63261	
0.410	1.68014	1.49640	1.615		1.47695
0.434	1.67552	1.49430	1.682	1.63127	
0.441	1.67423	1.49373	1.749		1.47638
0.508	1.66527	1.48956	1.761	1.62974	
0.533	1.66277	1.48841	1.849	1.62800	
0.560	1.66046	1.48736	1.909		1.47573
0.589	1.65835	1.48640	1.946	1.62602	
0.643	1.65504	1.48490	2.053	1.62372	
0.656	1.65437	1.48459	2.100		1.47492
0.670	1.65367	1.48426	2.172	1.62099	
0.706	1.65207	1.48353	3.324		1.47392

TABLE 25 Refractive Index of Calcium Molybdate ($CaMoO_4$) and Lead Molybdate ($PbMoO_4$)[203]

Calcium molybdate (19.5°C)			Lead molybdate (19.5°C)		
λ, μm	n_o	n_e	λ, μm	n_o	n_e
0.40466	2.04452	2.06156	0.40466		2.44317
0.43584	2.02553	2.04029	0.43584	2.60487	2.39011
0.46782	2.01091	2.02409	0.46782	2.53415	2.35258
0.47999	2.00629	2.01898	0.47999	2.51398	2.34119
0.50858	1.99697	2.00873	0.50858	2.47589	2.31877
0.54607	1.98730	1.99810	0.54607	2.43929	2.29618
0.57696	1.98089	1.99109	0.57696	2.41651	2.28162
0.57906	1.98049	1.99066	0.57906	2.41515	2.28073
0.58756	1.97893	1.98897	0.58756	2.40977	2.27729
0.64385	1.97033	1.97961	0.64385	2.38119	2.25835
0.66781	1.96737	1.97639	0.66781	2.37170	2.25197
0.70652	1.96321	1.97189	0.70652	2.35878	2.24311
1.0830	1.94317	1.95030	1.0830	2.30177	2.20267

TABLE 26 Refractive Index of Lead Fluoride (PbF_2)[202,203]

λ, μm	*n*
0.30	1.93665
0.35	1.85422
0.40	1.81804
0.45	1.79644
0.50	1.78220
0.55	1.77221
0.60	1.76489
0.65	1.75934
0.70	1.75502
0.75	1.75158
0.80	1.74879
0.85	1.74648
0.90	1.74455
0.95	1.74291
1.00	1.74150
1.50	1.73371
2.00	1.72983
2.50	1.72672
3.00	1.72363
3.50	1.72030
4.00	1.71663
4.50	1.71255
5.00	1.70805
5.50	1.70310
6.00	1.69769
6.50	1.69181
7.00	1.68544
7.50	1.67859
8.00	1.67125
8.50	1.66340
9.00	1.65504
9.50	1.64615
10.00	1.63674
10.50	1.62679
11.00	1.61629
11.50	1.60523
12.00	1.59597

TABLE 27 Refractive Index of New Oxide Materials[215]

	Material and supplier		
Wavelength (μm)	ALON* (Raytheon)	Spinel* (Alpha Optical)	Y_2O_3:La_3O_3† (GTE Laboratories)
0.40466	1.81167	1.73574	1.96939
0.43583	1.80562	1.73054	1.95660
0.54607	1.79218	1.71896	1.92941
0.85211	1.77758	1.70728	1.90277
1.01398	1.77375	1.70300	1.89643
1.52958	1.76543	1.69468	1.88446
1.97009	1.75838	1.68763	1.87585
2.32542	1.75268	1.68194	1.86822

* Accuracy: $\pm 1 \cdot 10^{-5}$.
† Accuracy: $\pm 1 \cdot 10^{-4}$.

TABLE 28 Refractive Index of Strontium Titanate ($SrTiO_3$)[203]

λ, μm	n
0.40	2.66386
0.44	2.56007
0.48	2.49751
0.52	2.45553
0.56	2.40285
0.60	2.40285
0.64	2.38532
0.68	2.37135
0.72	2.35998
0.76	2.35055
0.80	2.34260
0.84	2.33583
0.88	2.32997
0.92	2.32486
0.96	2.32035
1.00	2.31633
1.40	2.29073
1.80	2.27498
2.20	2.26109
2.60	2.24676
3.00	2.23111
3.40	2.21370
3.80	2.19428
4.20	2.17265
4.60	2.14865
5.00	2.12212
5.40	2.09290

TABLE 29 Optical Modes of Crystals with Diamond Structure; Space Group: Fd3m (O_h^7) #227; $\Gamma = F_{2g}(R)$

	Raman mode location (cm^{-1})	
Material	F_{2g}	Reference
C (diamond)	1332.4	216
Si	519.5	217
Ge	300.6	218

TABLE 30 Optical Modes of Crystals with Cesium Chloride Structure; Space Group: Pm3m (O_h^5) #221; $\Gamma = F_{1u}(IR)$

	Mode location (cm^{-1})		
Material	ω_{T0}	ω_{LO}	Refs.
CsBr	75	113	219
CsCl	99	160	219, 220
CsI	62	88	219
TlBr	43	101	221
TlCl	63	158	221
TlI	52		222

TABLE 31 Optical Modes of Crystals with Sodium Chloride Structure; Space Group: Fm3m (O_h^1) #225; $\Gamma = F_{1u}(IR)$

Material	Mode location (cm^{-1})		Refs.
	ω_{T0}	ω_{LO}	
AgBr	79	138	221
AgCl	106	196	221
BaO	132	425	223
BaS	158	230	224
CaO	295	557	223, 225
CaS	256	376	224
CdO	270	380	226
KBr	113	165	221
KCl	142	214	221
KF	190	326	221
KI	101	139	221
LiF	306	659	221, 227
MgO	401	718	221, 227
MgS	237	430	224
NaBr	134	209	221
NaCl	164	264	221
NaF	244	418	221
NaI	117	176	221
NiO	401	580	221
SrO	227	487	223, 225
SrS	194	284	224
PbS	71	212	228
PbSe	39	116	229
PbTe	32	112	230

TABLE 32 Optical Modes of Crystals with Zincblende Structure; Space Group: $F\bar{4}3m$ (T_d^2) #216; $\Gamma = F_2(R, IR)$

Material	Mode location (cm^{-1})		Refs.
	ω_{T0}	ω_{LO}	
AlAs	364	402	231
AlSb	319	340	232
BN	1055	1305	233, 234
BP	799	829	233, 234
CdTe	141	169	235
CuCl	172	210	236
GaAs	269	292	232
GaP	367	403	232, 237
GaSb	230	240	238
InAs	217	239	238, 239
InP	304	345	232
InSb	179	191	239, 240
β-SiC	793	970	218, 241
ZnS	282	352	235, 242
ZnSe	206	252	235
ZnTe	178	208	235, 243

TABLE 33 Optical Modes of Crystals with Fluorite Structure; Space Group: Fm3m (O_h^1) #225; $\Gamma = F_{1u}(IR) + F_{2g}(R)$

		Mode locations (cm^{-1})		
Material	Ref.	$F_{1u}(\omega_{TO})$	$F_{1u}(\omega_{LO})$	F_{2g}
$BaCl_2$	244			185
BaF_2	245, 246, 247	184	319	241
CaF_2	245, 246, 247	258	473	322
CdF_2	247, 248	202	384	317
EuF_2	244	194	347	287
β-PbF_2	244, 248	102	337	256
$SrCl_2$	244, 249, 250	147	243	182
SrF_2	245, 246, 247	217	366	286
ThO_2	251	281	568	
UO_2	251, 252	281	555	445
ZrO_2	253	354	680	605

TABLE 34 Optical Modes of Crystals with Corundum Structure; Space Group: $R\bar{3}c$ (D_{3d}^6) #167; $\Gamma = 2A_{1g}(R) + 2A_{1u}(-) + 3A_{2g}(-) + 2A_{2u}(IR, E \parallel c) + 5E_g(R) + 4E_u(IR, E \perp c)$

	Mode locations (cm^{-1})												
	Infrared modes (LO in parentheses)						Raman modes						
Material	E_u	E_u	E_u	E_u	A_{1u}	A_{1u}	E_g	E_g	E_g	E_g	E_g	A_{1g}	A_{1g}
Al_2O_3	385	422	569	635	400	583	378	432	451	578	751	418	645
(Refs: 253, 254)	(388)	(480)	(625)	(900)	(512)	(871)							
Cr_2O_3	417	444	532	613	538	613	—	351	397	530	609	303	551
(Refs: 255, 256)	(420)	(446)	(602)	(766)	(602)	(759)							
Fe_2O_3	227	286	437	524	299	526	245	293	298	413	612	226	500
(Refs: 256, 257)	(230)	(368)	(494)	(662)	(414)	(662)							

TABLE 35 Optical Modes of Crystals with Wurtzite Structure. Space Group: $P6_3mc$ (C_{6v}^4) #186; $\Gamma = A_1(R, IR\ E \parallel c) + 2B_1(-) + E_1(R, IR\ E \perp c) + 2E_2(R)$

	Mode locations (cm^{-1})				
	Infrared modes (LO)		Raman modes		
Material	E_1	A_1	E_2	E_2	Refs.
β-AgI	106	106	17	112	258
	(124)	(124)			
AlN	672	659		655	234, 259
	(895)	(888)			
BeO	725	684	340	684	260, 261
	(1095)	(1085)			
CdS	235	228	44	252	261, 263
	(305)	(305)			
CdSe	172	166	34	?	264
	(210)	(211)			
GaN	560	533	145	568	188, 265
	(746)	(744)			
α-SiC	797	788	149	788	266
	970	964			
ZnO	407	381	101	437	261, 262
	(583)	(574)			
ZnS	274	274	55	280	261
	(352)	(352)			

TABLE 36 Optical Modes of Crystals with Trigonal Selenium Structure; Space Group: $P3_121$ (D_3^4) #152; $\Gamma = A_1(R) + A_2(IR, E \parallel c) + 2E(IR, E \perp c, R)$

	Mode locations (cm^{-1})				
	Raman	Infrared, $E \perp c$		Infrared, $E \parallel c$	
Material	A_1	E	E	A_2	References
Se	237	144	225	102	267, 268
		(150)	(225)	(106)	
Te	120	92	144	90	269
		(106)	(145)	(96)	

TABLE 37 Optical Modes of Crystals with α-Quartz Structure; Space Group: $P3_221$ (D_3^6) #154; $\Gamma = 4A_1(R) + 4A_2(IR, E \parallel c) + 8E(IR, E \perp c, R)$

	Infrared modes, $E \perp c$							
Material	E	E	E	E	E	E	E	E
SiO_2	128	265	394	451	697	796	1067	1164
(Refs: 270, 271, 272)	(128)	(270)	(403)	(511)	(699)	(809)	(1159)	(1230)
GeO_2	121	166	326	385	492	583	857	961
(Refs: 273)	(121)	(166)	(372)	(456)	(512)	(595)	(919)	(972)

	Infrared modes, $E \parallel c$				Raman modes			
Material	A_2	A_2	A_2	A_2	A_1	A_1	A_1	A_1
SiO_2	364	500	777	1080	207	356	464	1085
(Refs: 270, 271, 272)	(388)	(552)	(789)	(1239)				
GeO_2					212	261	440	880
(Ref: 273)								

TABLE 38 Optical Modes of Crystals with Rutile Structure; Space Group: $P4_2/mnm$ (D_{4h}^{14}) #136; $\Gamma = A_{1g}(R) + A_{2g}(-) + A_{2u}(IR, E \parallel c) + B_{1g}(R) + B_{2g}(R) + 2B_{1u}(-) + E_g(R) + 3E_u(IR, E \perp c)$

	Mode locations (cm^{-1})							
	Infrared modes (LO in parentheses)				Raman modes			
Material	E_u	E_u	E_u	A_{2u}	B_{1g}	E_g	A_{1g}	B_{2g}
CoF_2	190	270	405	345	68	246	366	494
(Refs: 274, 275, 276	(234)	(276)	(529)	(506)				
FeF_2	173	244	405	307	73	257	340	496
(Refs: 275, 277, 278)	(231)	(248)	(530)	(487)				
GeO_2	300	370	635	455	97	680	702	870
(Refs: 273, 279, 280)	(345)	(470)	(815)	(755)				
MgF_2	247	410	450	399	92	295	410	515
(Refs: 277, 278, 281, 282, 283)	(303)	(415)	(617)	(625)				
SnO_2	243	284	605	465	123	475	634	776
(Refs: 284, 285, 286)	(273)	(368)	(757)	(703)				
TiO_2	189	382	508	172	143	447	612	826
(Refs: 22, 26, 277, 287)	(367)	(444)	(831)	(796)				
ZnF_2	173	244	380	294	70	253	350	522
(Refs: 277, 278, 281, 283)	(227)	(264)	(498)	(488)				

TABLE 39 Optical Modes of Crystals with Scheelite Structure; Space Group: $I4_1/a$ (C_{4h}^6) #88; $\Gamma = 3A_g(R) + 4A_u(IR, E \parallel c) + 5B_g(R) + 3B_u(-) + 5E_g(R) + 4E_u(IR, E \perp c)$

		Infrared modes, E ⊥ c				Infrared modes, E ∥ c			
Material	Refs.	E_u	E_u	E_u	E_u	A_u	A_u	A_u	A_u
$CaMoO_4$	288, 289, 290	146	197	322	790	193	247	420	772
		(161)	(258)	(359)	(910)	(202)	(317)	(450)	(898)
$CaWO_4$	288, 289, 290	142	200	313	786	177	237	420	776
		(153)	(248)	(364)	(906)	(181)	(323)	(450)	(896)
$SrMoO_4$	289	125	[181]	[327]	[830]	153	[282]	[404]	[830]
$SrWO_4$	289	[140]	[168]	[320]	[833]	[150]	[278]	[410]	[833]
$PbMoO_4$	289, 290	90	105	301	744	86	258	373	745
		(99)	(160)	(318)	(886)	(132)	(278)	(387)	(865)
$PbWO_4$	289, 290, 291	73	104	288	756	58	251	384	764
		(101)	(137)	(314)	(869)	(109)	(278)	(393)	(866)
$LiYF_4$	292, 293	143	292	326	424	195	252	396	490
		(173)	(303)	(367)	(566)	(224)	(283)		

		Raman modes											
Material	Refs.	A_g	A_g	A_g	B_g	B_g	B_g	B_g	B_g	E_g	E_g	E_g	E_g	E_g
$CaMoO_4$	294	205	333	878	110	219	339	393	844	145	189	263	401	797
$CaWO_4$	294, 295	218	336	912	84	210	336	401	838	117	195	275	409	797
$SrMoO_4$	294	181	327	887	94	157	327	367	842	111	137	231	381	797
$SrWO_4$	294, 295	187	334	925	75		334	370	839	101	131	238	378	797
$PbMoO_4$	296	164	314	868	64	75	317	348	764	61	100	190	356	744
$PbWO_4$	296	178	328	905	54	78	328	358	766	63	78	192	358	753
$LiYF_4$	292, 293	[150]	264	425	177	248	329	382	427	153	199	329	368	446

TABLE 40 Optical Modes of Crystals with Spinel Structure; Space Group: Fd3m (O_h^7) #227; $\Gamma = A_{1g}(R) + E_g(R) + F_{1g}(-) + 3F_{2g}(R) + 2A_{2u}(-) + 2E_u(-) + 4F_{1u}(IR) + 2F_{2u}(-)$

		Mode locations (cm^{-1})								
		Infrared modes				Raman modes				
Material	Refs.	F_{1u}	F_{1u}	F_{1u}	F_{1u}	F_{2g}	F_{2g}	F_{2g}	E_g	A_{1g}
$MgAl_2O_4$	199, 297, 298	305	428	485	670	311	492	611	410	722
		(311)		(497)	(800)					
$CdIn_2S_4$	299, 300	68	171	215	307	93	247	312	185	366
		(69)	(172)	(270)	(311)					
$ZnCr_2O_4$	301	186	372	506	624	186	515	610	457	692
		(194)	(377)	(522)	(711)					
$ZnCr_2S_4$	302, 303, 304	115	249	340	388	116	[290]	361	249	403
		(117)	(250)	(360)	(403)					

TABLE 41 Optical Modes of Crystals with Cubic Perovskite Structure; Space Group: Pm3m (O_h^1) #221; $\Gamma = 3F_{1u}(IR) + F_{2u}(-)$

	Infrared mode locations (cm^{-1})			
Material	F_{1u}*	F_{1u}	F_{1u}	References
$KTaO_3$	85	199	549	305
	(88)	(200)	(550)	
$SrTiO_3$	88	178	544	205, 306, 307
	(173)	(473)	(804)	
$KMgF_3$	168	299	458	308
	(197)	(362)	(551)	
$KMnF_3$	119	193	399	308
	(144)	(270)	(483)	

* "Soft" mode with strong temperature dependence.

TABLE 42 Optical Modes of Crystals with Tetragonal Perovskite Structure; Space Group: $P4_2/mnm$ (D_{4h}^{14}) #136; $\Gamma = 3A_1(IR, E \parallel c, R) + B_1(R) + 4E(IR, E \perp c, R)$

	Mode locations (cm^{-1})								
	Infrared ($E \perp c$)				Raman	Infrared ($E \parallel c$)			
Material	E	E	E	E	B_1	A_1	A_1	A_1	Refs.
$BaTiO_3$	34	181	306	482	305	180	280	507	305, 309, 310
	(180)	(306)	(465)	(706)		(187)	(469)	(729)	
$PbTiO_3$	89	221	250	508	415	127	351	613	311
	(128)		(445)	(717)		(215)	(445)	(794)	

TABLE 43 Optical Modes of Crystals with the Chalcopyrite Structure; Space Group: $I\bar{4}2d$ (D_{2d}^{12}) #122; $\Gamma = A_1(R) + 2A_2(-) + 3B_1(R) + 3B_2(IR, E \parallel c, R) + +6E(IR, E \perp c, R)$

		Mode locations (cm^{-1})						
		Raman modes				Infrared modes ($E \parallel c$)		
Material	Refs.	A_1	B_1	B_1	B_1	B_2	B_2	B_2
$AgGaS_2$	312, 313	295	118	179	334	195	215	366
						(199)	(239)	(400)
$AgGaSe_2$	312, 314	179	12.5				152	246
							(159)	(272)
$CdGeAs_2$	315, 316	[188]	[84]	[167]	[245]	[85]	203	270
						[(85)]	(210)	(278)
$CuGaS_2$	312	312	138	203	243	259	339	371
						(284)	(369)	(402)
$ZnGeP_2$	317, 318	328	120	247	389	[140]	361	411
							(341)	(401)
$ZnSiP_2$	319	344	131				352	511
							(362)	(535)

TABLE 43 Optical Modes of Crystals with the Chalcopyrite Structure; Space Group: $I\bar{4}2d$ (D_{2d}^{12}) #122; $\Gamma = A_1(R) + 2A_2(-) + 3B_1(R) + 3B_2(IR, E \parallel c, R) + +6E(IR, E \perp c, R)$ (*Continued*)

		Infrared mode location ($E \perp c$)					
Material	Refs.	E	E	E	E	E	E
$AgGaS_2$	312, 313	63	93	158	225	323	368
		(64)	(96)	(160)	(230)	(347)	(392)
$AgGaSe_2$	312, 314	78	133		160	208	247
		(78)	(135)	(112)	(163)	(213)	(274)
$CdGeAs_2$	315, 316		95	159	200	255	272
			(98)	(161)	(206)	(258)	(280)
$CuGaS_2$	312	75	95	147	260	335	365
		(76)	(98)	(167)	(278)	(352)	(387)
$ZnGeP_2$	317, 318	94	141	201	328	369	386
		(94)	(141)	(206)	(330)	(375)	(406)
$ZnSiP_2$	319	105	185	270	335	477	511
		(105)	(185)	(270)	(362)	(477)	(535)

TABLE 44 Optical Modes of Other Crystals

Material/space group	Irreducible optical representation and optical modes locations (cm^{-1})
Orpiment, As_2S_3 $P2_1/b$ (C_{2h}^5) #14 (Ref. 320)	$\Gamma = 15A_g(R) + 15B_g(R) + 14A_u(IR, E \parallel b) + 13B_u(IR, E \parallel a, E \parallel c)$ $[7A_1(IR, E \parallel c, R) + 7A_2(R) + 7B_1(IR, E \parallel b, R) + 6B_2(IR, E \parallel a, R)$ for a noninteracting molecular layer structure] $A_g = 136, 154, 204, 311, 355, 382$ $B_u = 140, 159, 198, 278, 311, 354, 383$
Calcite, $CaCO_3$ $R\bar{3}c$ (D_{3d}^6) #167 (Refs. 321, 322)	$\Gamma = A_{1g}(R) + 2A_{1u}(-) + 3A_{2g}(-) + 3A_{2u}(IR, E \parallel c) + 4E_g(R)$ $+ 5E_u(IR, E \perp c)$ $A_{1g} = 1088$ $E_g = 156, 283, 714, 1432$ $A_{2u} = 92(136), 303(387), 872(890)$ $E_u = 102(123), 223(239), 297(381), 712(715), 1407(1549)$
BBO, $Ba_3[B_3O_6]_2$ R3 (C_3^4) #146 (Ref: 323)	$\Gamma =$ $41A(IR, E \parallel c, R) + 41E(IR, E \perp c, R)$
BSO, sellenite, $Bi_{12}SiO_{20}$ I23 (T^3) #197 (Ref: 324)	$\Gamma =$ $A = 8A(R) + 8E(R) + 24F(IR)$ $E = 92, 149, 171, 282, 331, 546, 785$ $F = 68, 88, 132, 252, —, 464, 626$ $44, 51, 59, 89, 99, 106, —, 115, 136, 175, 195, 208, 237, 288, 314, 353, 367,$ $462, 496, 509, 531, 579, 609, 825$
Iron Pyrite, FeS_2 Pa3 (T_h^6) #205 (Refs: 325, 326)	$\Gamma = A_g(R) + E_g(R) + 3F_g(R) + 2A_u(-) + 2E_u(-) + 5F_u(IR)$ $A_g = 379$ $E_g = 343$ $F_g = 435, 350, 377$ $F_u = 293(294), 348(350), 401(411), 412(421), 422(349)$

TABLE 44 Optical Modes of Other Crystals (*Continued*)

Material/space group	Irreducible optical representation and optical modes locations (cm^{-1})
KDP, KH_2PO_4 $I\bar{4}2d$ (D_{2d}^{12}) #122 (Ref: 327)	$\Gamma = 4A_1(R) + 5A_2(-) + 6B_1(R) + 6B_2(IR, E \parallel c, R) + 12E(IR, E \perp c, R)$ $A_1 = 360, 514, 918, 2700$ $B_1 = 156, 479, 570, 1366, 1806, 2390$ $B_2 = 80, 174, —, 386, 510, 1350$ $E = 75, 95, 113, 190, 320, 490, 530, 568, 960, 1145, —, 1325$
KTP $Pna2_1$ (C_{2v}^9) #33 (Ref: 328)	$\Gamma = 47A_1(IR, E \parallel c, R) + 48A_2(R) + 47B_1(IR, E \parallel a, R) + 47B_2(IR, E \parallel b, R)$
Lanthanum fluoride, LaF_3 $P\bar{3}c1$ (D_{3d}^4) #165 (Refs: 329, 330, 331)	$\Gamma = 5A_{1g}(R) + 12E_g(R) + 6A_{2u}(IR, E \parallel c) + 11E_u(IR, E \perp c)$ $A_{1g} = 120, 231, 283, 305, 390$ $E_g = 79, 145, 145, 163, 203, 226, 281, 290, 301, 315, 325, 366$ $A_{2u} = 142(143), 168(176), 194(239), —, 275(296), 323(468)$ $E_u = 100(108), 128(130), 144(145), 168(183), 193(195), 208(222), 245(268), 272(316), 354(364), 356(457)$
Lithium iodate, $LiIO_3$ $P6_3$ (C_6^6) #173 (Refs: 332, 333)	$\Gamma = 4A(IR, E \parallel c, R) + 5B(-) + 4E_1(IR, E \perp c, R) + 5E_2(R)$ $A = 148(148), 238(238), 358(468), 795(817)$ $E_1 = 180(180), 330(340), 370(460), 764(848)$ $E_2 = 98, 200, 332, 347, 765$
Lithium niobate, $LiNbO_3$ R3c (C_{3v}^6) #161 (Refs: 334, 335)	$\Gamma = 4A_1(IR, E \parallel c, R) + 5A_2(-) + 9E(IR, E \perp c, R)$ $A_1 = 255(275), 276(333), 334(436), 633(876)$ $E = 155(198), 238(243), 265(295), 325(371), 371(428), 431(454), 582(668), 668(739), 743(880)$
Potassium niobate, $KNbO_3$ Bmm2 (C_{2v}^{14}) #38 (Ref: 336)	$\Gamma = 4A_1(IR, E \parallel z, R) + 4B_1(IR, E \parallel x, R) + 3B_2(IR, E \parallel y, R) + A_2(R)$ $A_1 = 190(193), 290(296), 299(417), 607(827)$ $B_1 = 187(190), 243(294), 267(413), 534(842)$ $B_2 = 56(189), 195(425), 511(838)$ $A_2 = 283$
Paratellurite, TeO_2 $P4_12_12$ (D_4^4) #92 (Refs: 337, 338)	$\Gamma = 4A_1(R) + 4A_2(IR, E \parallel c) + 5B_1(R) + 4B_2(R) + 8E(IR, E \perp c, R)$ $A_1 = 148, 393, 648$ $A_2 = 82(110), 259(263), 315(375), 575(775)$ $B_1 = 62, 175, 216, 233, 591$ $B_2 = 155, 287, 414, 784$ $E = 121(123), 174(197), 210(237), 297(327), 330(379), 379(415), 643(720), 769(812)$
Yttria, Y_2O_3 Ia3 (T_h^7) #206 (Ref: 339)	$\Gamma = 4E_g(R) + 4A_g(R) + 14F_g(R) + 5E_u(-) + 5A_u(-) + 16F_u(IR)$ $E_g = 333, 830, 948$ $A_g = 1184$ $F_g = (131), 431, 469, 596$ $F_u = 120(121), 172(173), 182(183), 241(242), 303(315), 335(359), 371(412), 415(456), 461(486), 490(535), 555(620)$
Yttrium aluminum garnet (YAG), $Y_3Al_2(AlO_4)_3$ Ia3d (O_h^{10}) #230 (Refs: 340, 341)	$\Gamma = 5A_{1u}(-) + 3A_{1g}(R) + 5A_{2u}(-) + 5A_{2g}(-) + 10E_u(-) + 8E_g(R) + 14F_{1g}(-) + 17F_{1u}(IR) + 14F_{2g}(R) + 16F_{2u}(-)$ $A_{1g} = 373, 561, 783$ $E_g = 162, 310, 340, 403, 531, 537, 714, 758$ $F_{2g} = 144, 218, 243, 259, 296, 408, 436, 544, 690, 719, 857$ $F_{1u} = 122(123), 163(172), 177(180), 219(224), 290(296), 330(340), 373(378), 387(388), 395(403), 428(438), 446(472), 472(511), 516(549), 569(585), 692(712), 723(765), 782(841)$

TABLE 45 Summary of Available Lattice Vibration Model Parameters

Material	Dispersion model reference		Material	Dispersion model reference	
	Classical	Four-parameter		Classical	Four-parameter
AgBr		342	KI	351	
AgCl		342	$KNbO_3$	336	
$AgGaS_2$	312		$KTaO_3$	305	
$AgGaSe_2$	314		$KTiOPO_4$	328	
Al_2O_3	25	26	LaF_3		330
ALON	175		La_2O_3	352	
As_2S_3 (cryst)	320		LiF	227	
As_2S_3 (glass)	343		$LiIO_3$	332, 333	
As_2S_3 (cryst)	320		$LiNbO_3$	353	
As_2Se_3 (glass)	343		$YLiF_4$	292	
BaF_2	245		$MgAl_2O_4$	199	
$BaTiO_3$	305, 344	310	MgF_2	281, 283	278
BeO	260		MgO	227	
BN	233		NaF	354	
$CaCO_3$	322		PbF_2	248	
CaF_2	245		PbSe	355	
$CaMoO_4$	288		$PbWO_4$	291	
$CaWO_4$	288		Se	267, 345	
CdS	235		SiO_2	272, 356	
CdSe	264		SrF_2	245	
CdTe	235, 345		$SrTiO_3$	305	307
CsBr	219		Te	269	
CsCl	219, 220		TeO_2	338, 357	357
CsI	219		TiO_2	244	22
FeS_2	346, 347		TlBr		342
GaAs	348		TlCl		342
GaN	188, 265		$Y_3Al_5O_{12}$	358	341
GaP	237, 349		Y_2O_3	339	
GeO_2	280		ZnS	235	
$HfO_2:Y_2O_3$	132		ZnSe	235	
KBr	350		ZnTe	235	

TABLE 46 Urbach Tail Model Parameters

Material	Urbach model parameters				Temperature range (K)	Absorption range (cm^{-1})	Ref.
	α_0 (cm^{-1})	E_g (eV)	σ_s (−)	E_p (meV)			
AgBr	$[1.5 \cdot 10^4]$	[2.79]	1.0	—	>100		28
AgCl	$[1.6 \cdot 10^6]$	[3.44]	0.8	—	>100	$100–10^4$	28
$AgGaS_2$							
$E \perp c$	$[6.2 \cdot 10^6]$	2.92	1.09	—		$2–10^3$	359
$E \parallel c$	$[1.7 \cdot 10^4]$	2.69	1.14	—		$60–10^3$	359
Al_2O_3							
$E \perp c$	$6.531 \cdot 10^5$	9.1	0.559	—	RT	1–100+	360
ALON	$6.780 \cdot 10^5$	6.5	0.254	—	RT	2–100+	360
BaF_2	$4.17 \cdot 10^8$	10.162	0.58	40	78–573	1–100	361
$Bi_{12}SiO_{20}$	$1.0 \cdot 10^5$	3.54	0.47	25.0	41–293		362
CaF_2	$1.33 \cdot 10^{10}$	11.228	0.61	45	78–573	1–100	361

TABLE 46 Urbach Tail Model Parameters (*Continued*)

Material	Urbach model parameters				Temperature range (K)	Absorption range (cm^{-1})	Ref.
	α_0 (cm^{-1})	E_g (eV)	σ_s (−)	E_p (meV)			
CdS							
E ⊥ c	$[2.7 \cdot 10^9]$	2.584	2.17	—	90–342	10^2–10^4	363
E ∥ c	$[2.7 \cdot 10^9]$	2.608	2.17	—	90–300	10^2–10^4	363
CdSe							
E ⊥ c	$[9 \cdot 10^8]$	[1.887]	2.2	28	110–340	10–10^3	364
E ∥ c	$[5 \cdot 10^8]$	[1.902]	2.2	28	78–300	10–10^3	364
CdTe	$3 \cdot 10^{12}$	1.65	4.39	—			365
CuCl	$1 \cdot 10^6$	3.35	1.35	—	200–400	1–200	366
InP	$8 \cdot 10^7$	1.43	1.35	—	6–298	10–10^4	367
KBr	$6 \cdot 10^9$	6.840	0.774	10.5	70–536	3–10^5	368
KCl	$1.26 \cdot 10^{10}$	7.834	0.745	13.5	10–573		368
KF		[10.0]		[17.1]			368
KI	$6 \cdot 10^9$	5.890	0.830	4.5	65–573	1–10^6	368
LiF	$3.72 \cdot 10^{10}$	13.09			400–600	1–10^3	361
$LiNbO_3$							
E ∥ c	$[6 \cdot 10^7]$	[4.65]	0.75	60	10–667	2–10^4	369
$MgAl_2O_4$	$4.931 \cdot 10^5$	8.0	0.267	—	RT	10–100+	360
NaBr	$6 \cdot 10^9$	6.770	0.765	10.7			368
NaCl	$1.2 \cdot 10^{10}$	8.025	0.741	9.5	10–573	3–500+	368
NaF	$1.0 \cdot 10^{10}$	10.70	0.69	16.5	78–573		368
NaI	$6 \cdot 10^9$	5.666	0.845	8.5			368
SrF_2	$1.35 \cdot 10^9$	10.670	0.60	44	78–573		361
$SrTiO_3$	$1.3 \cdot 10^4$	3.37	1.0	—	4–300	1–1000	370
TeO_2							371
E ∥ c		4.31	0.69	17	80–500	2–1000	
TlCl		3.44	1.1				372
	$4 \cdot 10^4$	3.43	1.04	7			365
YAG	$2.125 \cdot 10^5$	7.012	0.560	37.2	34–292	10–10^3	373
$YAlO_3$							
E ∥ a	$3.30 \cdot 10^6$	8.056	0.553	33.5	10–300	10^2–10^5	374
E ∥ b	$5.27 \cdot 10^5$	8.018	0.479	32.5			
E ∥ c	$1.32 \cdot 10^6$	8.151	0.448	35.8			
Y_2O_3	$8.222 \cdot 10^6$	6.080	0.688	18.6	10–297		375
ZnTe	$1 \cdot 10^{15}$	2.556	2.8	50	77–300	10–300	376

TABLE 47 Ultraviolet and Infrared Room-temperature Absorption Edge Equation Constants

Selected glass code	Ultraviolet absorption edge			Infrared absorption edge		
	λ ($\beta = 1$ cm^{-1})	β_0 (cm^{-1})	σ_{UV} (eV^{-1})	λ ($\beta = 1$ cm^{-1})	β_0 (cm^{-1})	σ_{IR} (cm^{-1})
479587 TiK1	348	$5.34 \cdot 10^{-07}$	4.059			
487704 FK5	287	$1.78 \cdot 10^{-13}$	6.805			
511510 TiF1	352	$4.63 \cdot 10^{-14}$	8.716			
517642 BK7	310	$3.48 \cdot 10^{-14}$	7.753	2.69*	$4.45 \cdot 10^{62}$	0.0388
518651 PK2	311	$2.72 \cdot 10^{-13}$	7.248			
522595 K5	313	$9.47 \cdot 10^{-15}$	8.143			
523515 KF9	325	$8.97 \cdot 10^{-15}$	8.484			
526600 BaLK1	307	$1.48 \cdot 10^{-12}$	6.749			

TABLE 47 Ultraviolet and Infrared Room-temperature Absorption Edge Equation Constants (*Continued*)

Selected glass code	Ultraviolet absorption edge			Infrared absorption edge		
	$\lambda\ (\beta = 1\ \text{cm}^{-1})$	$\beta_0\ (\text{cm}^{-1})$	$\sigma_{UV}\ (\text{eV}^{-1})$	$\lambda\ (\beta = 1\ \text{cm}^{-1})$	$\beta_0\ (\text{cm}^{-1})$	$\sigma_{IR}\ (\text{cm}^{-1})$
527511 KzF6	322	$3.21 \cdot 10^{-08}$	4.485			
533580 ZK1	313	$8.81 \cdot 10^{-15}$	8.165			
548458 LLF1	317	$2.49 \cdot 10^{-18}$	10.354			
548743 Ultran 30	228	$3.72 \cdot 10^{-05}$	1.877	3.98	$2.76 \cdot 10^{21}$	−0.0198
552635 PSK3	304	$1.48 \cdot 10^{-10}$	5.543			
573575 BaK1	305	$2.31 \cdot 10^{-09}$	4.890			
580537 BaLF4	335	$3.80 \cdot 10^{-15}$	8.973			
581409 LF5	321	$1.07 \cdot 10^{-17}$	10.125			
586610 LgSK2	346	$3.55 \cdot 10^{-10}$	6.073			
593355 FF5	359	$1.02 \cdot 10^{-19}$	12.678			
613586 SK4	323	$3.36 \cdot 10^{-11}$	6.274	2.70*	$2.75 \cdot 10^{48}$	0.0301
613443 KzFSN4	326	$3.86 \cdot 10^{-10}$	5.693	2.66*	$1.81 \cdot 10^{33}$	0.0204
618551 SSK4	325	$7.12 \cdot 10^{-13}$	7.327			
620364 F2	330	$4.15 \cdot 10^{-17}$	10.027	2.73	$1.20 \cdot 10^{30}$	0.0189
650392 BaSF10	341	$1.35 \cdot 10^{-13}$	8.146			
670472 BaF10	352	$2.90 \cdot 10^{-13}$	8.201			
720504 LaK10	341	$2.54 \cdot 10^{-10}$	6.083			
741526 TaC2	324	$7.63 \cdot 10^{-06}$	3.081			
743492 NbF1	326	$8.34 \cdot 10^{-08}$	4.281			
744447 LaF2	356	$1.83 \cdot 10^{-13}$	8.420			
805254 SF6	367	$4.42 \cdot 10^{-12}$	7.734	2.73	$7.73 \cdot 10^{28}$	0.0182
835430 TaFD5	340	$1.71 \cdot 10^{-09}$	5.542			

*Infrared edge description limited to absorption coefficients $\geq 2\ \text{cm}^{-1}$ and $\leq 10\ \text{cm}^{-1}$.

TABLE 48 Parameters for the Room-temperature Infrared Absorption Edge [Eq. (17*a*)]

Material	A (cm^{-1})	γ	$\nu_0\ (\text{cm}^{-1})$	Ref.
Al_2O_3, sapphire				
o-ray	55,222	5.03	900	35
	94,778	5.28	914	38
e-ray	33,523	4.73	871	377
ALON	41,255	4.96	969	38
BaF_2	49,641	4.5	344	35
BeO	36,550	5.43	1,090	†
$CaCO_3$, calcite				
o-ray	1,633	2.58	1,549	1
e-ray	456	1.88	890	1
CaF_2	105,680	5.1	482	35
$CaLa_2S_4$	3,910	3.58	314	†
CdTe	5,460	4.25	168	378*
CsI	12,800	3.88	85	379*
GaAs	2,985	3.69	292	380*
KBr	6,077	4.25	166	35, 381
KCl	8,696	4.19	213	35, 381
KI	8,180	3.86	139	382*
LiF	21,317	4.39	673	35, 381

TABLE 48 Parameters for the Room-temperature Infrared Absorption Edge [Eq. (17*a*)] (*Continued*)

Material	A (cm^{-1})	γ	v_0 (cm^{-1})	Ref.
$MgAl_2O_4$, spinel	147,850	5.51	869	38,199*
MgF_2	11,213	4.29	617	35
MgO	41,420	5.29	725	383*
NaCl	24,273	4.79	268	35, 381
NaF	41,000	5.0	425	381
SiO_2, Quartz				
o-ray	107,000	4.81	1,215	1
e-ray	196,000	5.16	1,222	1
SrF_2	22,548	4.4	395	35
KRS-5	5,400	4.0	100	384
TlCl	6	1.58	158	384
Y_2O_3	184,456	5.36	620	38
β-ZnS	227,100	5.31	352	385*
ZnSe	179,100	5.33	250	386*
ZrO_2:Y_2O_3	226,390	4.73	658	387*
Fused SiO_2	54,540	5.10	1,263	†
ZBT	297,000	4.4	500	388
As_2S_3	4,900	2.93	350	389*
As_2Se_3	15,300	3.62	240	390*
AMTIR-3	10,320	3.13	235	391*

* Our fit to the referenced data.
† Estimated from our measurements.

33.6 REFERENCES

1. W. G. Driscoll (ed.), *Handbook of Optics,* McGraw-Hill, New York, 1978.
2. W. L. Wolfe and G. J. Zissis (eds.), *The Infrared Handbook,* Environmental Research Institute of Michigan, 1985.
3. M. J. Weber (ed.), *Handbook of Laser Science and Technology,* CRC Press, Boca Raton, 1986.
4. D. E. Gray (ed.), *American Institute of Physics Handbook,* 3d ed., McGraw-Hill, New York, 1972.
5. E. D. Palik (ed.), *Handbook of Optical Constants of Solids,* Academic Press, Orlando, 1985.
6. E. D. Palik (ed.), *Handbook of Optical Constants of Solids II,* Academic Press, Orlando, 1991.
7. B. O. Seraphin and H. E. Bennett, "Optical Constants," in R. K. Willardson and A. C. Beer (eds.), *Semiconductors and Semimetals, Vol. 3: Optical Properties of III-V Compounds,* Academic Press, New York, 1967.
8. S. Musikant (ed.), *Optical Materials: A Series of Advances,* Marcel Dekker, New York, 1990.
9. F. V. Tooley (ed.), *The Handbook of Glass Manufacture,* Ashlee Publishing Co., New York, 1985.
10. S. Musikant, *Optical Materials: An Introduction to Selection and Application,* Marcel Dekker, New York, 1985.
11. P. Klocek (ed.), *Handbook of Infrared Optical Materials,* Marcel Dekker, Inc., New York, 1991.
12. G. W. Fynn and W. J. A. Powell, *Cutting and Polishing Optical and Electronic Materials,* 2d ed., Adam Hilger, Bristol, 1988.

13. W. Zschommler, *Precision Optical Glassworking,* SPIE, Bellingham, WA, 1986.

14. J. F. Nye, *Physical Properties of Crystals,* Oxford University Press, Oxford, 1985.

15. E. R. Cohen and B. N. Taylor, ''The 1986 CODATA Recommended Values for the Fundamental Physical Constants,'' *J. Phys. Chem. Ref. Data* **17:**1795–1801 (1988).

16. D. Y. Smith, ''Dispersion Theory, Sum Rules, and Their Application to the Analysis of Optical Data,'' in E. D. Palik (ed.), *Handbook of Optical Constants of Solids,* Academic Press, New York, 1985.

17. T. Skettrup, ''Urbach's Rule Derived From Thermal Fluctuations in the Band Gap Energy,'' *Phys. Rev. B* **18:**2622–2631 (1978).

18. F. K. Kneubühl, ''Review of the Theory of the Dielectric Dispersion of Insulators,'' *Infrared Phys.* **29:**925–942 (1989).

19. W. J. Tropf, T. J. Harris, and M. E. Thomas, ''Optical Materials: Visible and Infrared,'' in R. Waynant and W. Ediger (eds), *Electro-optics Handbook,* McGraw-Hill, New York, 1993.

20. R. H. Lyddane, R. G. Sachs, and E. Teller, ''On the Polar Vibrations of Alkali Halides,'' *Phys. Rev.* **59:**673–676 (1941).

21. W. Cochran and R. A. Cowley, ''Dielectric Constants and Lattice Vibrations,'' *J. Phys. Chem. Solids* **23:**447–450 (1962).

22. F. Gervais and B. Piriou, ''Temperature Dependence of Transverse- and Longitudinal-optic Modes in TiO_2 (Rutile),'' *Phys. Rev. B* **10:**1642–1654 (1974).

23. J. W. S. Rayleigh, ''The Theory of Anomalous Dispersion,'' *Phil. Mag.* **48:**151–152 (1889).

24. L. Merten and G. Lamprecht, ''Directional Dependence of Extraordinary Infrared Oscillator Parameters of Uniaxial Crystals,'' *Phys. Stat. Solidi* (*b*) **39:**573–580 (1970). [Also see J. L. Servoin, F. Gervais, A. M. Quittet, and Y. Luspin, ''Infrared and Raman Response in Ferroelectric Perovskite Crystals: Apparent Inconsistencies,'' *Phys. Rev. B.* **21:**2038–2041 (1980).]

25. A. S. Barker, ''Infrared Lattice Vibrations and Dielectric Dispersion in Corundum,'' *Phys. Rev.* **132:**1474–1481 (1963).

26. F. Gervais and B. Piriou, ''Anharmonicity in Several-polar-mode Crystals: Adjusting Phonon Self-energy of LO and TO Modes in Al_2O_3 and TiO_2 to Fit Infrared Reflectivity,'' *J. Phys. C* **7:**2374–2386 (1974).

27. R. H. French, ''Electronic Band Structure of Al_2O_3 with Comparision to ALON and AlN,'' *J. Am. Ceram. Soc.* **73:**477–489 (1990).

28. F. Urbach, ''The Long-Wavelength Edge of Photographic Sensitivity and the Electronic Absorption of Solids,'' *Phys. Rev.* **92:**1324 (1953).

29. H. Sumi and A. Sumi, ''The Urbach–Martienssen Rule Revisited,'' *J. Phys. Soc. Japan* **56:**2211–2220 (1987).

30. D. L. Wood and J. Tauc, ''Weak Absorption Tails in Amorphous Semiconductors,'' *Phys. Rev. B* **5:**3144–3151 (1972).

31. H. Mori and T. Izawa, ''A New Loss Mechanism in Ultralow Loss Optical Fiber Materials,'' *J. Appl. Phys.* **51:**2270–2271 (1980).

32. M. E. Innocenzi, R. T. Swimm, M. Bass, R. H. French, A. B. Villaverde, and M. R. Kokta, ''Room-temperature Optical Absorption in Undoped α-Al_2O_3,'' *J. Appl. Phys.* **67:**7542–7546 (1990).

33. D. T. Gillespie, A. L. Olsen, and L. W. Nichols, ''Transmittance of Optical Materials at High Temperature,'' *Appl. Opt.* **4:**1488–1493 (1965).

34. M. A. Ordal, R. J. Bell, R. W. Alexander, L. L. Long, and M. R. Querry, ''Optical Properties of Fourteen Metals in the Infrared and Far Infrared: Al, Co, Cu, Au, Fe, Pb, Mo, Ni, Pd, Pt, Ag, Ti, V, and W,'' *Appl. Opt.* **24:**4493–4499 (1985).

35. T. F. Deutsch, ''Absorption Coefficient of Infrared Laser Window Materials,'' *J. Phys. Chem. Solids* **34:**2091–2104 (1973). [Also see T. F. Deutsch, ''Laser Window Materials—An Overview,'' *J. Electron. Mater.* **4:**663–719 (1975).]

36. D. L. Mills and A. A. Maradudin, "Theory of Infrared Absorption by Crystals in the High Frequency Wing of their Fundamental Lattice Absorption," *Phys. Rev. B* **8:**1617–1630 (1973). [Also see A. A. Maradudin and D. L. Mills, "Temperature Dependence of the Absorption Coefficient of Alkali Halides in the Multiphonon Regime," *Phys. Rev. Lett.* **31:**718–721 (1973).]

37. H. G. Lipson, B. Bendow, N. E. Massa, and S. S. Mitra, "Multiphonon Infrared Absorption in the Transparent Regime of Alkaline-earth Fluorides," *Phys. Rev. B* **13:**2614–2619 (1976).

38. M. E. Thomas, R. I. Joseph, and W. J. Tropf, "Infrared Transmission Properties of Sapphire, Spinel, Yttria, and ALON as a Function of Frequency and Temperature," *Appl. Opt.* **27:**239–245 (1988).

39. J. A. Harrington, B. L. Bobbs, M. Braunstein, R. K. Kim, R. Stearns, and R. Braunstein, "Ultraviolet-visible Absorption in Highly Transparent Solids by Laser Calorimetry and Wavelength Modulation Spectroscopy," *Appl. Opt.* **17:**1541–1546 (1978).

40. N. C. Frenelius, R. J. Harris, D. B. O'Quinn, M. E. Gangl, D. V. Dempsey, and W. L. Knecht, "Some Optical Properties of Materials Measured at 1.3 μm," *Opt. Eng.* **22:**411–418 (1983).

41. J. A. Harrington, D. A. Gregory, and W. F. Ott, "Infrared Absorption in Chemical Laser Window Materials," *Appl. Opt.* **15:**1953–1959 (1976).

42. B. Tatian, "Fitting Refractive-index Data with the Sellmeier Dispersion Formula," *Appl. Opt.* **23:**4477–4485 (1984).

43. P. G. Nutting, "Disperson Formulas Applicable to Glass," *J. Opt. Soc. Am.* **2–3:**61–65 (1919).

44. H. H. Li, "Refractive Index of ZnS, ZnSe, and ZnTe and Its Wavelength and Temperature Derivatives," *J. Phys. Chem. Ref. Data* **13:**103–150 (1984).

45. F. Zernike, "Refractive Indices of Ammonium Dihydrogen Phosphate and Potassium Dihydrogen Phosphate between 2000 Å and 1.5 μ," *J. Opt. Soc. Am.* **54:**1215–1220 (1964). [Errata: *J. Opt. Soc. Am.* **55:**210E (1965).]

46. M. Herzberger, "Colour Correction in Optical Systems and a New Dispersion Formula," *Opt. Acta* **6:**197–215 (1959).

47. M. Herzberger and C. D. Salzberg, "Refractive Indices of Infrared Optical Materials and Color Correction of Infrared Lenses," *J. Opt. Soc. Am.* **52:**420–427 (1962).

48. A. N. Pikhtin and A. D. Yas'kov, "Dispersion of the Refractive Index of Semiconductors with Diamond and Zinc-blende Structures," *Sov. Phys. Semicond.* **12:**622–626 (1978).

49. J. W. Fleming, "Dispersion in GeO_2-SiO_2 Glasses," *Appl. Opt.* **23:**4486–4493 (1984).

50. D. L. Wood, K. Nassau, and T. Y. Kometani, "Refractive Index of Y_2O_3 Stabilized Zirconia: Variation with Composition and Wavelength," *Appl. Opt.* **29:**2485–2488 (1990).

51. N. P. Barnes and M. S. Piltch, "Temperature-dependent Sellmeier Coefficients and Nonlinear Optics Average Power Limit for Germanium," *J. Opt. Soc. Am.* **69:**178–180 (1979).

52. A. J. Bosman and E. E. Havinga, "Temperature Dependence of Dielectric Constants of Cubic Ionic Compounds," *Phys. Rev.* **129:**1593–1600 (1963).

53. B. Bendow, P. D. Gianino, Y-F. Tsay, and S. S. Mitra, "Pressure and Stress Dependence of the Refractive Index of Transparent Crystals," *Appl. Opt.* **13:**2382–2396 (1974).

54. S. Singh, "Nonlinear Optical Properties," in *Handbook of Laser Science and Technology, Volume III Optical Materials: Part I,* CRC Press, Boca Raton, 1986, pp. 3–228.

55. D. F. Eaton, "Nonlinear Optical Materials," *Science* **253:**281–287 (1991).

56. M. M. Choy and R. L. Byer, "Accurate Second-order Susceptibility Measurements of Visible and Infrared Nonlinear Crystals," *Phys. Rev. B* **14:**1693–1706 (1976).

57. K.-H. Hellwege and A. M. Hellwege (eds.), *Landolt-Börnstein Numerical Data and Functional Relationships in Science and Technology, New Series, Group III: Crystal and Solid State Physics, Volume 11: Elastic, Piezoelectric, Pyroelectric, Piezooptic, Electrooptic Constants and Nonlinear Susceptibilities of Crystals,* Springer-Verlag, Berlin, 1979.

58. M. E. Lines, "Scattering Loss in Optic Fiber Materials. I. A New Parametrization," *J. Appl. Phys.* **55:**4052–4057 (1984); "II. Numerical Estimates," *J. Appl. Phys.* **55:**4058–4063 (1984).

59. J. A. Harrington and M. Sparks, "Inverse-square Wavelength Dependence of Attenuation in Infrared Polycrystalline Fibers," *Opt. Lett.* **8:**223–225 (1983).

60. D. D. Duncan and C. H. Lange, "Imaging Performance of Crystalline and Polycrystalline Oxides," *Proc. SPIE* **1326:**59–70 (1990).

61. J. D. H. Donnay and H. M. Ondik (eds.), *Crystal Data Determination Tables,* 3d ed., U. S. Department of Commerce, 1973.

62. R. W. G. Wyckoff, *Crystal Structures,* John Wiley & Sons, New York, 1963.

63. G. Simmons and H. Wang, *Single Crystal Elastic Constants and Calculated Aggregate Properties: A Handbook,* MIT Press, Cambridge, MA, 1971.

64. R. S. Krishnan, R. Srinivasan, and S. Devanarayanan, *Thermal Expansion of Crystals,* Pergamon Press, Oxford, 1979.

65. Y. S. Touloukian (ed.), *Thermophysical Properties of Matter,* IFI/Plenum, New York, 1970.

66. G. A. Slack, "The Thermal Conductivity of Nonmetallic Crystals," in H. Ehrenreich, F. Seitz, and D. Turnbull (eds.), *Solid State Physics, Vol. 34,* Academic Press, New York, 1979.

67. K. F. Loje and D. E. Schuele, "The Pressure and Temperature Derivative of the Elastic Constants of AgBr and AgCl," *J. Phys. Chem. Solids* **31:**2051–2067 (1970).

68. W. Hidshaw, J. T. Lewis, and C. V. Briscoe, "Elastic Constants of Silver Chloride from 4.2 to 300 K," *Phys. Rev.* **163:**876–881 (1967).

69. S. M. Kikkarin, A. V. Tsarev, V. V. Shashkin, and I. B. Yakovkin, "Elastic Properties of GaAlAs Solid Solutions," *Sov. Phys. Solid State* **30:**1689–1692 (1988). [Also see N. Chetty, A. Muñoz, and R. M. Martin, "First-principles Calculation of the Elastic Constants of AlAs," *Phys. Rev. B* **40:**11934–11936 (1989).]

70. Stiffness and compliance of ALON and yttria are estimated from the engineering moduli.

71. M. Gospodinov, P. Sveshtarov, N. Petkov, T. Milenov, V. Tassev, and A. Nikolov, "Growth of Large Crystals of Bismuth-Germanium Oxide and Their Physical Properties," *Bulgarian J. Phys.* **16:**520–522 (1989).

72. M. Gospodinov, S. Haussühl, P. Sveshtarov, V. Tassev, and N. Petkov, "Physical Properties of Cubic $Bi_{12}SiO_{20}$," *Bulgarian J. Phys.* **15:**140–143 (1988).

73. V. A. Pesin, "Elastic Constants of Dense Modification of Boron Nitride," *Sverkhtverd. Mater.* **6:**5–7 (1980) [in Russian].

74. W. Wettling and J. Windscheif, "Elastic Constants and Refractive Index of Boron Phosphide," *Solid State Commun.* **50:**33–34 (1984).

75. M. E. Hills, "Preparation, Properties, and Development of Calcium Lanthanum Sulfide as an 8- to 12-micrometer Transmitting Ceramic," Naval Weapons Center Report TP 7073, September 1989. [Engineering moduli used to estimate elastic constants.]

76. R. D. Greenough and S. B. Palmer, "The Elastic Constants and Thermal Expansion of Single-crystal CdTe," *J. Phys. D* **6:**587–592 (1973).

77. R. C. Hanson and K. Helliwell, "Anharmonicity in CuCl—Elastic, Dielectric, and Piezoelectric Constants," *Phys. Rev. B* **9:**2649–2654 (1984).

78. Yu. A. Burenkov, S. Yu. Davydov, and S. P. Nikanorov, "The Elastic Properties of Indium Arsenide," *Sov. Phys. Solid State* **17:**1446–1447 (1976).

79. A. Yoneda, "Pressure Derivatives of Elastic Constants of Single Crystal MgO and $MgAl_2O_4$," *J. Phys. Earth* **38:**19–55 (1990).

80. M. O. Manasreh and D. O. Pederson, "Elastic Constants of Cubic Lead Fluoride from 300 to 850 K," *Phys. Rev. B* **30:**3482–3485 (1984).

81. G. I. Peresada, E. G. Ponyatovskii, and Zh. D. Sokolovskaya, "Pressure Dependence of the Elastic Constants of PbS," *Phys. Stat. Sol.* (*a*) **35:**K177–K179 (1976).

82. N. J. Walker, G. A. Saunders, and N. Schäl, "Acoustic Mode Vibrational Anharmonicity of PbSe and other IV–VI Compounds," *J. Phys. Chem. Solids* **48:**91–96 (1987).

83. A. J. Miller, G. A. Saunders, and Y. K. Yoğurtçu, "Pressure Dependence of the Elastic Constants of PbTe, SnTe and $Ge_{0.08}Sn_{0.92}Te$," *J. Phys. C* **14:**1569–1584 (1981).

84. W. R. L. Lambrecht, B. Segall, M. Methfessel, and M. van Schilfgaarde, "Calculated Elastic Constants and Deformation Potentials of Cubic SiC," *Phys. Rev. B* **44:**3685–3694 (1991).

85. J. B. Wachtman, M. L. Wheat, and S. Marzullo, "A Method for Determining the Elastic Constants of a Cubic Crystal from Velocity Measurements in a Single Arbitrary Direction; Application to $SrTiO_3$," *J. Res. Nat. Bur. Stand.* **67A:**193–204 (1963).

86. Y. K. Yoğurtçu, A. J. Miller, and G. A. Saunders, "Elastic Behavior of YAG Under Pressure," *J. Phys. C* **13:**6585–6597 (1980).

87. H. M. Kandil, J. D. Greiner, and J. F. Smith, "Single Crystal Elastic Constants of Yttria-stabilized Zirconia in the Range 20° to 700°C," *J. Am. Ceram. Soc.* **67:**341–346 (1984).

88. M. H. Grimsditch and G. D. Holah, "Brillouin Scattering and Elastic Moduli of Silver Thiogallate ($AgGaS_2$)," *Phys. Rev. B* **12:**4377–4382 (1975).

89. Z. Li, S.-K. Chan, M. H. Grimsditch, and E. S. Zouboulis, "The Elastic and Electromechanical Properties of Tetragonal $BaTiO_3$ Single Crystals," *J. Appl. Phys.* **70:**7327–7332 (1991).

90. T. Hailing, G. A. Saunders, W. A. Lambson, and R. S. Feigelson, "Elastic Behavior of the Chalcopyrite $CdGeAs_2$," *J. Phys. C* **15:**1399–1418 (1982).

91. G. Fischer and J. Zarembowitch, "Elastic Properties of Single-crystal Urea," *C. R. Acad. Sc. Paris* **270B:**852–855 (1970).

92. Y. Ohmachi and N. Uchida, "Temperature Dependence of Elastic, Dielectric, and Piezoelectric Constants in TeO_2 Single Crystals," *J. Appl. Phys.* **41:**2307–2311 (1970).

93. I. M. Silvestrova, Y. V. Pisarevskii, P. A. Senyushenkov, A. I. Krupny, R. Voszka, I. F. Földvári, and J. Janszky, "Temperature Dependence of the Elastic Constants of Paratellurite," *Phys. Stat. Sol.* (*a*) **101:**437–444 (1987).

94. W. J. Alton and A. J. Barlow, "Acoustic-wave Propagation in Tetragonal Crystals and Measurements of the Elastic Constants of Calcium Molybdate," *J. Appl. Phys.* **38:**3817–3820 (1967).

95. J. M. Farley and G. A. Saunders, "Ultrasonic Study of the Elastic Behavior of Calcium Tungstate between 1.5 K and 300 K," *J. Phys. C* **5:**3021–3037 (1972). [Also see J. M. Farley and G. A. Saunders, "The Elastic Constants of $CaWO_4$," *Solid State Commun.* **9:**965–969 (1971).]

96. J. M. Farley, G. A. Saunders, and D. Y. Chung, "Elastic Properties of Scheelite Structure Molybdates and Tungstates," *J. Phys. C* **8:**780–786 (1975).

97. J. M. Farley, G. A. Saunders, and D. Y. Chung, "Elastic Properties of Strontium Molybdate," *J. Phys. C* **6:**2010–2019 (1973).

98. P. Blanchfield and G. A. Saunders, "The Elastic Constants and Acoustic Symmetry of $LiYF_4$," *J. Phys. C* **12:**4673–4689 (1979). [Also see P. Blanchfield, T. Hailing, A. J. Miller, G. A. Saunders, and B. Chapman, "Vibrational Anharmonicity of Oxide and Fluoride Scheelites," *J. Phys. C* **20:**3851–3859 (1983).]

99. T. A. Fjeldly and R. C. Hanson, "Elastic and Piezoelectric Constants of Silver-iodide: Study of a Material Covalent-ionic Phase Transition," *Phys. Rev. B* **10:**3569–3577 (1974).

100. K. Tsubouchi and N. Mikoshiba, "Zero-Temperature-Coefficient SAW Devices on AlN Epitaxial Films," *IEEE Trans. Sonics Ultrason.* **SU-32:**634–644 (1985).

101. V. A. Savastenko and A. U. Sheleg, "Study of the Elastic Properties of Gallium Nitride," *Phys. Stat. Sol.* (*a*) **48:**K135–K139 (1978).

102. S. Haussühl, "The Propagation of Elastic Waves in Hexagonal Lithium Iodate," *Acustica* **23:**165–169 (1970) [In German].

103. I. I. Zubrinov, V. I. Semenov, and D. V. Sheloput, "Elastic and Photoelastic Properties of Proustite," *Sov. Phys. Solid State* **15:**1921–1922 (1974).

104. D. Eimerl, L. Davis, and S. Velsko, "Optical, Mechanical, and Thermal Properties of Barium Borate," *J. Appl. Phys.* **62:**1968–1983 (1987).

105. R. Laiho, M. Lakkisto, and T. Levola, "Brillouin Scattering Investigation of the Elastic Properties of LaF_3, CeF_3, PrF_3, and NdF_3," *Phil. Mag. A* **47:**235–244 (1983).

106. D. Royer and E. Dieulesaint, ''Elastic and Piezoelectric Constants of Trigonal Selenium and Tellurium Crystals,'' *J. Appl. Phys.* **50:**4042–4045 (1979).

107. A. G. Kalinichev, J. D. Bass, C. S. Zha, P. D. Han, and D. A. Payne, ''Elastic Properties of Orthorhombic $KNbO_3$ Single Crystals by Brillouin Scattering,'' *J. Appl. Phys.* **74:**6603–6608 (1993).

108. V. V. Aleksandrov, T. S. Velichkina, V. I. Voronkona, L. V. Koltsova, I. A. Yakovlev, and V. K. Yanovskii, ''Elastic Coefficients of $KTiOPO_4$, $RbTiOPO_4$, $TlTiOPO_4$ Crystals Determined from Mandelstamm-Brillouin Light Scattering Spectra,'' *Solid State Commun.* **69:**877–881 (1989).

109. Y. Tsay, B. Bendow, and S. S. Mitra, ''Theory of the Temperature Derivative of the Refractive Index in Transparent Crystals,'' *Phys. Rev. B* **5:**2688–2696 (1972).

110. L. W. Tilton, E. K. Plyler, and R. E. Stephens, ''Refractive Index of Silver Chloride for Visible and Infra-red Radiant Energy,'' *J. Opt. Soc. Am.* **40:**540–543 (1950).

111. G. C. Bhar, D. K. Ghosh, P. S. Ghosh, and D. Schmitt, ''Temperature Effects in $AgGaS_2$ Nonlinear Devices,'' *Appl. Opt.* **22:**2492–2494 (1983).

112. K. Vedam, J. L. Kirk, and B. N. N. Achar, ''Piezo- and Thermo-Optic Behavior of Spinel ($MgAl_2O_4$),'' *J. Solid State Chem.* **12:**213–218 (1975).

113. A. Feldman, D. Horowitz, R. M. Walker, and M. J. Dodge, ''Optical Materials Characterization Final Technical Report, February 1, 1978–September 30, 1978,'' NBS Technical Note 993, February 1979.

114. J. Tapping and M. L. Reilly, ''Index of Refraction of Sapphire Between 24 and 1060°C for Wavelengths of 633 and 799 nm,'' *J. Opt. Soc. Am. A* **3:**610–616 (1986).

115. C. H. Lange and D. D. Duncan, ''Temperature Coefficient of Refractive Index for Candidate Optical Windows,'' *SPIE Proc.* **1326:**71–78 (1990).

116. H. W. Newkirk, D. K. Smith, and J. S. Kahn, ''Synthetic Bromellite. III. Some Optical Properties,'' *Am. Mineralogist* **51:**141–151 (1966).

117. K. Vedam and P. Hennessey, ''Piezo- and Thermo-optical Properties of $Bi_{12}GeO_{20}$, II. Refractive Index,'' *J. Opt. Soc. Am.* **65:**442–445 (1975).

118. G. N. Ramachandran, ''Thermo-optic Behavior of Solids, I. Diamond,'' *Proc. Ind. Acad. Sci.* **A25:**266–279 (1947).

119. J. Fontanella, R. L. Johnston, J. H. Colwell, and C. Andeen, ''Temperature and Pressure Variation of the Refractive Index of Diamond,'' *Appl. Opt.* **16:**2949–2951 (1977).

120. I. H. Malitson, ''A Redetermination of Some Optical Properties of Calcium Fluoride,'' *Appl. Opt.* **2:**1103–1107 (1963).

121. M. J. Dodge, ''Refractive Index,'' in M. J. Weber (ed.), *Handbook of Laser Science and Technology, Volume IV, Optical Material: Part 2,* CRC Press, Boca Raton, 1986.

122. T. W. Houston, L. F. Johnson, P. Kisiuk, and D. J. Walsh, ''Temperature Dependence of the Refractive Index of Optical Maser Crystals,'' *J. Opt. Soc. Am.* **53:**1286–1291 (1963).

123. R. Weil and D. Neshmit, ''Temperature Coefficient of the Indices of Refraction and the Birefringence in Cadmium Sulfide,'' *J. Opt. Soc. Am.* **67:**190–195 (1977).

124. R. J. Harris, G. T. Johnson, G. A. Kepple, P. C, Krok, and H. Mukai, ''Infrared Thermooptic Coefficient Measurement of Polycrystalline ZnSe, ZnS, CdTe, CaF_2 and BaF_2, Single Crystal KCl, and TI-20 Glass,'' *Appl. Opt.* **16:**436–438 (1977).

125. H. H. Li, ''Refractive Index of Alkali Halides and Its Wavelength and Temperature Derivatives,'' *J. Phys. Chem. Ref. Data* **5:**329–528 (1976).

126. W. S. Rodney, ''Optical Properties of Cesium Iodide,'' *J. Opt. Soc. Am.* **45:**987–992 (1955).

127. G. D. Boyd, H. Kasper, and J. H. McFee, ''Linear and Nonlinear Optical Properties of $AgGaS_2$, $CuGaS_2$, and $CuInS_2$, and Theory of the Wedge Technique for the Measurement of Nonlinear Coefficients,'' *IEEE J. Quantum Electr.* **7:**563–573 (1971).

128. G. C. Bhar and G. Ghosh, ''Temperature-dependent Sellmeier Coefficients and Coherence Lengths for some Chalcopyrite Crystals,'' *J. Opt. Soc. Am.* **69:**730–733 (1979). [Also see G. C. Bhar, ''Refractive Index Dispersion of Chalcopyrite Crystals,'' *J. Phys. D* **13:**455–460 (1980).]

129. M. Bertolotti, V. Bogdanov, A. Ferrari, A. Jascow, N. Nazorova, A. Pikhtin, and L. Schirone, ''Temperature Dependence of the Refractive Index in Semiconductors,'' *J. Opt. Soc. Am. B* **7:**918–922 (1990).

130. D. A. Yas'kov and A. N. Pikhtin, ''Optical Properties of Gallium Phosphide Grown by Float Zone. I. Refractive Index and Reflection Coefficient,'' *Mat. Res. Bull.* **4:**781–788 (1969). [Also see D. A. Yas'kov and A. N. Pikhtin, ''Dispersion of the Index of Refraction of Gallium Phosphide,'' *Sov. Phys. Sol. State* **9:**107–110 (1967).]

131. H. H. Li, ''Refractive Index of Silicon and Germanium and Its Wavelength and Temperature Derivatives,'' *J. Phys. Chem. Ref. Data* **9:**561–658 (1980).

132. D. L. Wood, K. Nassau, T. Y. Kometani, and D. L. Nash, ''Optical Properties of Cubic Hafnia Stabilized with Yttria,'' *Appl. Opt.* **29:**604–607 (1990).

133. C. S. Hoefer, ''Thermal Variations of the Refractive Index in Optical Materials,'' *Proc. SPIE* **681:**135–142 (1986).

134. B. Zysset, I. Biaggio, and P. Günter, ''Refractive Indices of Orthorhombic $KNbO_3$. I. Dispersion and Temperature Dependence,'' *J. Opt. Soc. Am. B* **9:**380–386 (1992). [Also see Y. Uematsu, ''Nonlinear Optical Properties of $KNbO_3$ Single Crystal in the Orthorhombic Phase,'' *Jap. J. Appl. Phys.* **13:**1362–1368 (1974).]

135. J. D. Bierlein and H. Vanherzeele, ''Potassium Titanyl Phosphate: Properties and New Applications,'' *J. Opt. Soc. Am. B* **6:**622–633 (1989).

136. S. P. Velsko, M. Webb, L. Davis, and C. Huang, ''Phase-Matched Harmonic Generation in Lithium Triborate (LBO),'' *IEEE J. Quantum Electron.* **27:**2182–2192 (1991).

137. D. S. Smith, H. D. Riccius, and R. P. Edwin, ''Refractive Indices of Lithium Niobate,'' *Optics Commun.* **17:**332–335 (1976).

138. N. P. Barnes and D. J. Gettemy, ''Temperature Variation of the Refractive Indices of Yttrium Lithium Fluoride,'' *J. Opt. Soc. Am.* **70:**1244–1247 (1980).

139. R. E. Stephens and I. H. Malitson, ''Index of Refraction of Magnesium Oxide,'' *J. Nat. Bur. Stand.* **49:**249–252 (1952).

140. T. Radhakrishnan, ''Further Studies on the Temperature Variation of the Refractive Index of Crystals,'' *Proc. Indian Acad. Sci.* **A33:**22–34 (1951).

141. J. N. Zemel, J. D. Jensen, and R. B. Schoolar, ''Electrical and Optical Properties of Epitaxial Films of PbS, PbSe, PbTe, and SnTe,'' *Phys. Rev.* **140A:**330–342 (1965).

142. N. Uchida, ''Optical Properties of Single Crystal Paratellurite (TeO_2),'' *Phys. Rev. B* **4:**3736–3745 (1971).

143. J. R. DeVore, ''Refractive Index of Rutile and Sphalerite,'' *J. Opt. Soc. Am.* **41:**416–419 (1951).

144. M. D. Ewbank, P. R. Newman, N. L. Mota, S. M. Lee, W. L. Wolfe, A. G. DeBell, and W. A. Harrison, ''The Temperature Dependence of Optical and Mechanical Properties of Tl_3AsSe_3,'' *J. Appl. Phys.* **51:**3848–3852 (1980). [Also see J. D. Feichtner and G. W. Roland, ''Optical Properties of a New Nonlinear Optical Material: Tl_3AsSe_3,'' *Appl. Opt.* **11:**993–998 (1972).]

145. W. S. Rodney and I. H. Malitson, ''Refraction and Dispersion of Thallium Bromide Iodide,'' *J. Opt. Soc. Am.* **46:**956–961 (1956).

146. L. G. DeShazer, S. C. Rand, B. A. Wechsler, ''Laser Crystals,'' in M. J. Weber (ed.), *Handbook of Laser Science and Technology, Volume V, Optical Material: Part 3,* CRC Press, Boca Raton, 1986.

147. G. D. Boyd, E. Beuhler, and F. G. Storz, ''Linear and Nonlinear Optical Properties of $ZnGeP_2$ and CdSe,'' *Appl. Phys. Lett.* **18:**301–304 (1971).

148. D. L. Wood and K. Nassau, ''Refractive Index of Cubic Zirconia Stabilized with Yttria,'' *Appl. Opt.* **21:**2978–2981 (1982).

149. Schott Glass Technologies, Duryea, Pa.

150. Ohara Corporation, Somerville, N.J.

151. Hoya Optics, Inc., Fremont, Calif.

152. W. S. Rodney and R. J. Spindler, ''Index of Refraction of Fused-quartz Glass for Ultraviolet, Visible, and Infrared Wavelengths,'' *J. Res. Nat. Bur. Stand.* **53:**185–189 (1954). [Also see I. H. Malitson, ''Interspecimen Comparison of the Refractive Index of Fused Silica,'' *J. Opt. Soc. Am.* **55:**1205–1209 (1965).]

153. J. W. Fleming, ''Disperson in GeO_2–SiO_2 Glasses,'' *Appl. Opt.* **23:**4486–4493 (1984).

154. Barr & Stroud, Ltd., Glasgow, Scotland (UK).

155. Corning, Inc., Corning, N.Y. [Also see W. H. Dumbaugh, ''Infrared Transmitting Germanate Glasses,'' *Proc. SPIE* **297:**80–85 (1981).]

156. C. T. Moynihan, M. G. Drexhage, B. Bendow, M. S. Boulos, K. P. Quinlan, K. H. Chung, and E. Gbogi, ''Composition Dependence of Infrared Edge Absorption in ZrF_4 and HfF_4 Based Glasses,'' *Mat. Res. Bull.* **16:**25–30 (1981).

157. R. N. Brown, B. Bendow, M. G. Drexhage, and C. T. Moynihan, ''Ultraviolet Absorption Edge Studies of Fluorozirconate and Fluorohafnate Glass,'' *Appl. Opt.* **21:**361–363 (1982).

158. R. N. Brown and J. J. Hutta, ''Material Dispersion in High Optical Quality Heavy Metal Fluoride Glasses,'' *Appl. Opt.* **24:**4500–4503 (1985).

159. J. M. Jewell, C. Askins, and I. D. Aggarwal, ''Interferometric Method for Concurrent Measurement of Thermo-optic and Thermal Expansion Coefficients,'' *Appl. Opt.* **30:**3656–3660 (1991).

160. M. G. Drexhage, C. T. Moynihan, and M. Saleh, ''Infrared Transmitting Glasses Based on Hafnium Fluoride,'' *Mat. Res. Bull,* **15:**213–219 (1980).

161. B. Bendow, M. G. Drexhage, and H. G. Lipson, ''Infrared Absorption in Highly Transparent Fluorozirconate Glass,'' *J. Appl. Phys.* **52:**1460–1461 (1981).

162. M. G. Drexhage, O. H. El-Bayoumi, C. T. Moynihan, A. J. Bruce, K.-H. Chung, D. L. Gavin, and T. J. Loretz, ''Preparation and Properties of Heavy-Metal Fluoride Glasses Containing Ytterbium or Lutetium,'' *J. Am. Ceram. Soc.* **65:**C168–C171 (1982).

163. W. S. Rodney, I. H. Malitson, and T. A. King, ''Refractive Index of Arsenic Trisulfide,'' *J. Opt. Soc. Am.* **48:**633–636 (1958).

164. A. R. Hilton and C. E. Jones, ''The Thermal Change in the Nondispersive Infrared Refractive Index of Optical Materials,'' *Appl. Opt.* **6:**1513–1517 (1967).

165. Y. Ohmachi, ''Refractive Index of Vitreous As_2Se_3,'' *J. Opt. Soc. Am.* **63:**630–631 (1973).

166. J. A. Savage, ''Optical Properties of Chalcogenide Glasses,'' *J. Non-Cryst. Solids* **47:**101–116 (1982).

167. Amorphous Materials, Inc., Garland, Tex.

168. K. F. Hulme, O. Jones, P. H. Davies, and M. V. Hobden, ''Synthetic Proustite (Ag_3AsS_3): A New Crystal for Optical Mixing,'' *Appl. Phys. Lett.* **10:**133–135 (1967).

169. H. Schröter, ''On the Refractive Indices of Some Heavy-Metal Halides in the Visible and Calculation of Interpolation Formulas for Dispersion,'' *Z. Phys.* **67:**24–36 (1931) [in German].

170. G. C. Bhar, ''Refractive Index Interpolation in Phase-matching,'' *Appl. Opt.* **15:**305–307 (1976).

171. B. F. Levine, W. A. Nordland, and J. W. Silver, ''Nonlinear Optical Susceptibility of AgI,'' *IEEE J. Quantum Electron.* **QE-9:**468–470 (1973).

172. R. E. Fern and A. Onton, ''Refractive Index of AlAs,'' *J. Appl. Phys.* **42:**3499–3500 (1971).

173. J. Pastrňák and L. Roskovcová, ''Refractive Index Measurements on AlN Single Crystals,'' *Phys. Stat. Sol.* **14:**K5–K8 (1966). [Infrared term from D. A. Yas'kov and A. N. Pikhtin, ''Refractive Index and Birefringence or Semiconductors with the Wurtzite Structure,'' *Sov. Phys. Semicond.* **15:**8–12 (1981).]

174. I. H. Malitson and M. J. Dodge, ''Refractive Index and Birefringence of Synthetic Sapphire,'' *J. Opt. Soc. Am.* **62:**1405A (1972). [Also see M. J. Dodge, ''Refractive Index,'' in *Handbook of Laser Science and Technology, Volume IV, Optical Materials: Part 2,* CRC Press, Boca Raton, 1986, p. 30.]

175. W. J. Tropf and M. E. Thomas, "Aluminum Oxynitride (ALON) Spinel," in E. D. Palik (ed.), *Handbook of Optical Constants of Solids II,* Academic Press, Orlando, 1991, pp. 775–785.

176. I. H. Malitson, "Refractive Properties of Barium Fluoride," *J. Opt. Soc. Am.* **54:**628–632 (1964).

177. S. H. Wemple, M. Didomenico, and I. Camlibel, "Dielectric and Optical Properties of Melt-Grown $BaTiO_3$," *J. Phys. Chem. Solids* **29:**1797–1803 (1968).

178. D. F. Edwards and R. H. White, "Beryllium Oxide," in Palik (ed.), *Handbook of Optical Constants of Solids II,* Academic Press, Orlando, 1991, pp. 805–814. [Our fit to the dispersion data.]

179. R. E. Aldrich, S. O. Hou, and M. L. Harvill, "Electrical and Optical Properties of $Bi_{12}SiO_{20}$," *J. Appl. Phys.* **42:**493–494 (1971).

180. E. Burattini, G. Cappuccio, M. Grandolfo, P. Vecchia, and Sh. M. Efendiev, "Near-infrared Refractive Index of Bismuth Germanium Oxide ($Bi_{12}GeO_{20}$)," *J. Opt. Soc. Am.* **73:**495–497 (1983).

181. P. J. Gielisse, S. S. Mitra, J. N. Plendl, R. D. Griffis, L. C. Mansur, R. Marshall, and E. A. Oascoe, "Lattice Infrared Spectra of Boron Nitride and Boron Monophosphide," *Phys. Rev.* **155:**1039–1046 (1967).

182. F. Peter, "In Refractive Indices and Absorption Coefficients of Diamond between 644 and 226 Micrometers," *Z. Phys.* **15:**358–368 (1923) [In German].

183. W. L. Bond, "Measurement of the Refractive Index of Several Crystals," *J. Appl. Phys.* **36:**1674–1677 (1965). [Our fit to the dispersion data.]

184. A. G. DeBell, E. L. Dereniak, J. Harvey, J. Nissley, J. Palmer, A. Selvarajan, and W. L. Wolfe, "Cryogenic Refractive Indices and Temperature Coefficients of Cadmium Telluride from 6 μm to 22 μm," *Appl. Opt.* **18:**3114–3115 (1979).

185. W. S. Rodney and R. J. Spindler, "Refractive Index of Cesium Bromide for Ultraviolet, Visible, and Infrared Wavelengths," *J. Res. Nat. Bur. Stand.* **51:**123–126 (1953).

186. A. Feldman and D. Horowitz, "Refractive Index of Cuprous Chloride," *J. Opt. Soc. Am.* **59:**1406–1408 (1969).

187. A. H. Kachare, W. G. Spitzer, and J. E. Fredrickson, "Refractive Index of Ion-implanted GaAs," *J. Appl. Phys.* **47:**4209–4212 (1976).

188. A. S. Barker and M. Ilegems, "Infrared Lattice Vibrations and Free-electron Dispersion in GaN," *Phys. Rev. B* **7:**743–750 (1973).

189. D. F. Parsons and P. D. Coleman, "Far Infrared Optical Constants of Gallium Phosphide," *Appl. Opt.* **10:**1683–1685 (1971).

190. N. P. Barnes and M. S. Piltch, "Temperature-dependent Sellmeier Coefficients and Nonlinear Optics Average Power Limit for Germanium," *J. Opt. Soc. Am.* **69:**178–180 (1979). [Also see H. W. Icenogle, B. C. Platt, and W. L. Wolfe, "Refractive Indexes and Temperature Coefficients of Germanium and Silicon," *Appl. Opt.* **15:**2348–2351 (1976).]

191. O. G. Lorimor and W. G. Spitzer, "Infrared Refractive Index and Absorption of InAs and CdTe," *J. Appl. Phys.* **36:**1841–1844 (1965).

192. G. D. Pettit and W. J. Turner, "Refractive Index of InP," *J. Appl. Phys.* **36:**2081 (1965). [Infrared term comes from A. N. Pikhtin and A. D. Yas'kov, "Disperson of the Refractive Index of Semiconductors with Diamond and Zinc-blende Structures," *Sov. Phys. Semicond.* **12:**622–626 (1978).]

193. K. W. Kirby and L. G. DeShazer, "Refractive Indices of 14 Nonlinear Crystals Isomorphic to KH_2PO_4," *J. Opt. Soc. Am. B* **4:**1072–1078 (1987).

194. Y. Fujii and T. Sakudo, "Dielectric and Optical Properties of $KTaO_3$," *J. Phys. Soc. Japan* **41:**888–893 (1976).

195. T. Y. Fan, C. E. Huang, B. Q. Hu, R. C. Eckardt, Y. X. Fan, R. L. Byer, and R. S. Feigelson, "Second Harmonic Generation and Accurate Index of Refraction Measurements in Flux-grown $KTiOPO_4$," *Appl. Opt.* **26:**2390–2394 (1987). [Also see H. Y. Shen et al., "Second Harmonic Generation and Sum Frequency Mixing of Dual Wavelength Nd:$YALO_3$ Laser in Flux Grown $KTiOPO_4$ Crystal," *IEEE J. Quantum Electron.* **28:**48–51 (1992).]

196. R. Laiho and M. Lakkisto, "Investigation of the Refractive Indices of LaF_3, CeF_3, PrF_3, and NdF_3," *Phil. Mag. B* **48:**203–207 (1983).

197. F. Hanson and D. Dick, ''Blue Parametric Generation from Temperature-tuned LiB_3O_5,'' *Opt. Lett.* **16:**205–207 (1991). [Also see C. Chen, Y. Wu, A. Jiang, B. Wu, G. You, R. Li, and S. Lin, ''New Nonlinear-optical Crystal: LiB_3O_5,'' *J. Opt. Soc. Am. B* **6:**616–621 (1989), K. Kato, ''Tunable UV Generation to 0.2325 μm in LiB_3O_5,'' *IEEE J. Quantum Electron.* **QE-26:**1173–1175 (1990), and S. P. Velsko, M. Webb, L. Davis, and C. Huang, ''Phase-Matched Harmonic Generation in Lithium Triborate (LBO),'' *IEEE J. Quantum Electron.* **QE-27:**2182–2192 (1991).]

198. D. F. Nelson and R. M. Mikulyak, ''Refractive Indices of Congruently Melting Lithium Niobate,'' *J. Appl. Phys.* **45:**3688–3689 (1974).

199. W. J. Tropf and M. E. Thomas, ''Magnesium Aluminum Spinel ($MgAlO_4$), in E. D. Palik (ed.), *Handbook of Optical Constants of Solids II,* Academic Press, Orlando, 1991, pp. 881–895. [Improved fit with additional data.]

200. M. J. Dodge, ''Refractive Properties of Magnesium Fluoride,'' *Appl. Opt.* **23:**1980–1985 (1984).

201. M. J. Rosker, K. Cheng, and C. L. Tang, ''Practical Urea Optical Parametric Oscillator for Tunable Generation Throughout the Visible and Near-Infrared,'' *IEEE J. Quantum Electron.,* **QE-21:**1600–1606 (1985).

202. I. H. Malitson and M. J. Dodge, ''Refraction and Dispersion of Lead Fluoride,'' *J. Opt. Soc. Am.* **59:**500A (1969). [Also see M. J. Dodge, ''Refractive Index,'' in *Handbook of Laser Science and Technology, Volume IV, Optical Materials: Part 2*, CRC Press, Boca Raton, 1986, p. 31.]

203. I. H. Malitson, as quoted by W. L. Wolfe in W. G. Driscoll (ed.), *Handbook of Optics,* 1st ed., McGraw-Hill, New York, 1978. [Our fit to the dispersion data.]

204. F. Weiting and Y. Yixun, ''Temperature Effects on the Refractive Index of Lead Telluride and Zinc Sulfide,'' *Infrared Phys.* **30:**371–373 (1990).

205. S. Singh, J. P. Remeika, and J. R. Potopowicz, ''Nonlinear Optical Properties of Ferroelectric Lead Titanate,'' *Appl. Phys. Lett.* **20:**135–137 (1972).

206. L. Gample and F. M. Johnson, ''Index of Refraction of Single-crystal Selenium,'' *J. Opt. Soc. Am.* **59:**72–73 (1969).

207. P. T. B. Schaffer, ''Refractive Index, Dispersion, and Birefringence of Silicon Carbide Polytypes,'' *Appl. Opt.* **10:**1034–1036 (1971).

208. S. Singh, J. R. Potopowicz, L. G. Van Uitert, and S. H. Wemple, ''Nonlinear Optical Properties of Hexagonal Silicon Carbide,'' *Appl. Phys. Lett* **19:**53–56 (1971).

209. G. Hettner and G. Leisegang, ''Dispersion of the Mixed Crystals TlBr-TlI (KRS 5) and TlCl-TlBr (KRS-6) in the Infrared,'' *Optik* **3:**305–314 (1948). [In German] [Our fit to the dispersion data.]

210. Y. Nigara, ''Measurement of the Optical Constants of Yttrium Oxide,'' *Jap. J. Appl. Phys.* **7:**404–408 (1968).

211. T. M. Bieniewski and S. J. Czyzak, ''Refractive Indexes of Single Hexagonal ZnS and CdS Crystals,'' *J. Opt. Soc. Am.* **53:**496–497 (1963). [Our fit to the dispersion data.]

212. H. H. Li, ''Refractive Index of ZnS, ZnSe, and ZnTe and Its Wavelength and Temperature Derivatives,'' *J. Phys. Chem. Ref. Data* **13:**103–150 (1984).

213. B. Bendow, R. N. Brown, M. G. Drexhage, T. J. Loretz, and R. L. Kirk, ''Material Dispersion of Fluorozirconate-type Glasses,'' *Appl. Opt.* **20:**3688–3690 (1981).

214. P. Kloeck and L. Colombo, ''Index of Refraction, Dispersion, Bandgap and Light Scattering in GeSe and GeSbSe Glasses,'' *J. Non-Cryst. Solids* **93:**1–16 (1987).

215. Measurements made by R. J. Scheller of Schott Glass Technologies, Inc, Duryea, Pa.

216. S. A. Solin and A. K. Ramdas, ''Raman Spectrum of Diamond,'' *Phys. Rev. B* **1:**1687–1698 (1970). [Also see B. J. Parsons, ''Spectroscopic Mode Grüneisen Parameters for Diamond,'' *Proc. Royal Soc. Lond. A* **352:**397–417 (1977).]

217. B. A. Weinstein and G. J. Piermarini, ''Raman Scattering and Phonon Dispersion in Si and GaP at Very High Pressure,'' *Phys. Rev. B* **12:**1172–1186 (1975).

218. D. Olego and M. Cardona, ''Pressure Dependence of Raman Phonons of Ge and 3C-SiC,'' *Phys. Rev. B* **25:**1151–1160 (1982).

219. P. Vergnat, J. Claudel, A. Hadni, P. Strimer, and F. Vermillard, "Far Infrared Optical Constants of Cesium Halides at Low Temperatures," *J. Phys.* **30:**723–735 (1969) [in French].

220. H. Shimizu, Y. Ohbayashi, K. Yamamoto, K. Abe, M. Midorikawa, and Y. Ishibashi, "Far-infrared Reflection Spectra of CsCl Single Crystals," *J. Phys. Soc. Japan* **39:**448–450 (1975).

221. S. S. Mitra, "Infrared and Raman Spectra Due to Lattice Vibrations," in *Optical Properties of Solids,* Plenum Press, New York, 1969.

222. G. O. Jones, D. H. Martin, P. A. Mawer, and C. H. Perry, "Spectroscopy at Extreme Infra-red Wavelengths II. The Lattice Resonances of Ionic Crystals," *Proc. Royal Soc. A* **261:**10–27 (1961).

223. M. Galtier, A. Montaner, and G. Vidal, "Optical Phonons of CaO, SrO, BaO at the Center of the Brillouin Zone at 300 and 17 K," *J. Phys. Chem. Solids* **33:**2295–2302 (1972) [in French].

224. R. Ramnarine and W. F. Sherman, "The Far-infrared Investigation of the Mode Frequencies of Some Alkaline Earth Sulfides," *Infrared Phys.* **26:**17–21 (1986).

225. J. L. Jacobson and E. R. Nixon, "Infrared Dielectric Response and Lattice Vibrations of Calcium and Strontium Oxides," *J. Phys. Chem. Solids* **29:**967–976 (1968).

226. Z. V. Popović, G. Stanišić, D. Stojanović, and R. Kostić, "Infrared and Raman Spectral of CdO," *Phys. Stat. Sol.* (*b*) **165:**K109–K112 (1991).

227. J. R. Jasperse, A. Kahan, J. N. Plendl, and S. S. Mitra, "Temperature Dependence of Infrared Dispersion in Ionic Crystals LiF and MgO," *Phys. Rev.* **146:**526–542 (1966). [Also see A. Kachare, G. Andermann, and L. R. Brantley, "Reliability of Classical Dispersion Analysis of LiF and MgO Reflectance Data," *J. Phys. Chem. Solids* **33:**467–475 (1972).]

228. R. Geick, "Measurement and Analysis of the Fundamental Lattice Vibration Spectrum of PbS," *Phys. Lett.* **10:**51–52 (1964).

229. H. Birkhard, R. Geick, P. Kästner, and K.-H. Unkelback, "Lattice Vibrations and Free Carrier Dispersion in PbSe," *Phys. Stat. Sol.* (*b*) **63:**89–96 (1974).

230. E. G. Bylander and M. Hass, "Dielectric Constant and Fundamental Lattice Frequency of Lead Telluride," *Solid State Commun.* **4:**51–52 (1966).

231. M. Ilegems and G. L. Pearson, "Infrared Reflection Spectra of $Ga_{1-x}Al_xAs$ Mixed Crystals," *Phys. Rev. B* **1:**1576–1582 (1970).

232. A. Mooradian and G. B. Wright, "First Order Raman Effect in III-V Compounds," *Solid State Commun.* **4:**431–434 (1966). [Also see W. J. Turner and W. E. Reese, "Infrared Lattice Bands in AlSb," *Phys. Rev.* **127:**126–131 (1962).]

233. P. J. Gielisse, S. S. Mitra, J. N. Plendl, R. D. Griffis, L. C. Mansur, R. Marshall, and E. A. Pascoe, "Lattice Infrared Spectra of Boron Nitride and Boron Monophosphide," *Phys. Rev.* **155:**1039–1046 (1967).

234. J. A. Sanjurjo, E. López-Cruz, P. Vogl, and M. Cardona, "Dependence on Volume of the Phonon Frequencies and the IR Effective Charges of Several III-V Semiconductors," *Phys. Rev.* **B28:**4579–4584 (1983).

235. A. Manabe, A. Mitsuishi, and H. Yoshinga, "Infrared Lattice Reflection Spectra of II-VI Compounds," *Jap. J. Appl. Phys.* **6:**593–600 (1967).

236. G. R. Wilkenson, "Raman Spectra of Ionic, Covalent, and Metallic Crystals," in A. Anderson (ed.), *The Raman Effect, Vol. 2: Applications,* Marcel Dekker, New York, 1973.

237. A. S. Barker, "Dielectric Dispersion and Phonon Line Shape in Gallium Phosphide," *Phys. Rev.* **165:**917–922 (1968).

238. M. Hass and B. W. Henvis, "Infrared Lattice Reflection Spectra of III-V Compound Semiconductors," *J. Phys. Chem. Solids* **23:**1099–1104 (1962).

239. R. Carles, N. Saint-Cricq, J. B. Renucci, M. A. Renucci, and A. Zwick, "Second-order Raman Scattering in InAs," *Phys. Rev.* **B22:**4804–4815 (1980).

240. R. B. Sanderson, "Far Infrared Optical Properties of Indium Antimonide," *J. Phys. Chem. Solids* **26:**803–810 (1965).

241. L. Patrick and W. J. Choyke, "Lattice Absorption Bands in SiC," *Phys. Rev.* **123:**813–815 (1965).

242. W. G. Nilsen, ''Raman Spectrum of Cubic ZnS,'' *Phys. Rev.* **182:**838–850 (1969).

243. J. C. Irwin and J. LaCombe, ''Raman Scattering in ZnTe,'' *J. Appl. Phys.* **41:**1444–1450 (1970).

244. R. Shivastava, H. V. Lauer, L. L. Chase, and W. E. Bron, ''Raman Frequencies of Fluorite Crystals,'' *Phys. Lett.* **36A:**333–334 (1971).

245. W. Kaiser, W. G. Spitzer, R. H. Kaiser, and L. E. Howarth, ''Infrared Properties of CaF_2, SrF_2, and BaF_2,'' *Phys. Rev.* **127:**1950–1954 (1962).

246. I. Richman, ''Longitudinal Optical Phonons in CaF_2, SrF_2, and BaF_2,'' *J. Chem. Phys.* **41:**2836–2837 (1966).

247. D. R. Bosomworth, ''Far-infrared Optical Properties of CaF_2, SrF_2, BaF_2, and CdF_2,'' *Phys. Rev.* **157:**709–715 (1967).

248. J. D. Axe, J. W. Gaglianello, and J. E. Scardefield, ''Infrared Dielectric Properties of Cadmium Fluoride and Lead Fluoride,'' *Phys. Rev.* **139:**A1211–1215 (1965).

249. R. Droste and R. Geick, ''Investigation of the Infrared-Active Lattice Vibration in $SrCl_2$,'' *Phys. Stat. Sol.* (*b*) **62:**511–517 (1974).

250. A. Sadoc, F. Moussa, and G. Pepy, ''The Lattice Dynamics of $SrCl_2$,'' *J. Phys. Chem. Solids* **37:**197–199 (1976).

251. J. D. Axe and G. D. Pettit, ''Infrared Dielectric Dispersion and Lattice Dynamics of Uranium Dioxide and Thorium Dioxide,'' *Phys. Rev.* **151:**676–679 (1966).

252. P. G. Marlowe and J. P. Russell, ''Raman Scattering in Uranium Dioxide,'' *Phil. Mag.* **14:**409–410 (1966).

253. S. Shin and M. Ishigame, ''Defect-induced Hyper-Raman Spectra in Cubic Zirconia,'' *Phys. Rev. B* **34:**8875–8882 (1986).

254. S. P. S. Porto and R. S. Krishnan, ''Raman Effect of Corundum,'' *J. Chem. Phys.* **47:**1009–1012 (1967).

255. D. R. Renneke and D. W. Lynch, ''Infrared Lattice Vibrations and Dielectric Dispersion in Single-Crystal Cr_2O_3,'' *Phys. Rev.* **138:**A530–A533 (1965).

256. I. R. Beattle and T. R. Gibson, ''The Single-crystal Raman Spectra of Nearly Opaque Materials. Iron(III) Oxide and Chromium(III) Oxide,'' *J. Chem. Soc.* (*A*), 980–986 (1970).

257. S. Onari, T. Arai, and K. Kudo, ''Infrared Lattice Vibrations and Dielectric Dispersion in α-Fe_2O_3,'' *Phys. Rev. B* **16:**1717–1721 (1977).

258. G. L. Bottger and C. V. Damsgard, ''Raman Scattering in Wurtzite-Type AgI Crystals,'' *J. Chem Phys.* **57:**1215–1218 (1972).

259. A. T. Collins, E. C. Lightowlers, and P. J. Dean, ''Lattice Vibration Spectra of Aluminum Nitride,'' *Phys. Rev.* **158:**833–838 (1967).

260. E. Loh, ''Optical Phonons in BeO Crystals,'' *Phys. Rev.* **166:**673–678 (1967).

261. C. A. Arguello, D. L. Rousseau, and S. P. S. Porto, ''First-Order Raman Effect in Wurtzite-Type Crystals,'' *Phys. Rev.* **181:**1351–1363 (1969).

262. T. C. Damen, S. P. S. Porto, and B. Tell, ''Raman Effect in Zinc Oxide,'' *Phys. Rev.* **142:**570–574 (1966).

263. B. Tell, T. C. Damen, and S. P. S. Porto, ''Raman Effect in Cadmium Sulfide,'' *Phys. Rev.* **144:**771–774 (1966).

264. R. Geick, C. H. Perry, and S. S. Mitra, ''Lattice Vibrational Properties of Hexagonal CdSe,'' *J. Appl. Phys.* **137:**1994–1997 (1966).

265. D. D. Manchon, A. S. Barker, P. J. Dean, and R. B. Zetterstrom, ''Optical Studies of the Phonons and Electrons in Gallium Nitride,'' *Solid State Commun.* **8:**1227–1231 (1970).

266. D. W. Feldman, J. H. Parker, W. J. Choyee, and L. Patrick, ''Raman Scattering in 6*H* SiC,'' *Phys. Rev.* **170:**698–704 (1968).

267. R. Geick, U. Schröder, and J. Stuke, ''Lattice Vibrational Properties of Trigonal Selenium,'' *Phys. Stat. Sol.* **24:**99–108 (1967).

268. G. Locovsky, A. Mooradian, W. Taylor, G. B. Wright, and R. C. Keezer, ''Identification of the Fundamental Vibrational Modes of Trigonal, α-monoclinic and Amorphous Selenium,'' *Solid State Commun.* **5:**113–117 (1967).

269. E. D. Palik, "Tellurium (Te)," in E. D. Palik (ed.), *Handbook of Optical Constants of Solids II,* Academic Press, Orlando, 1991, pp. 709–723.

270. B. D. Saksena, "Analysis of the Raman and Infra-red Spectra of α-Quartz," *Proc. Ind. Acad. Sci.* **12A:**93–139 (1940).

271. J. F. Scott and S. P. S. Porto, "Longitudinal and Transverse Optical Lattice Vibrations in Quartz," *Phys. Rev.* **161:**903–910 (1967).

272. S. M. Shapiro and J. D. Axe, "Raman Scattering from Polar Phonons," *Phys. Rev. B* **6:**2420–2427 (1972).

273. J. F. Scott, "Raman Spectra of GeO_2," *Phys. Rev. B* **8:**3488–3493 (1970).

274. A. S. Barker and J. A. Detzenberger, "Infrared Lattice Vibrations in CoF_2," *Solid State Commun.* **3:**131–132 (1965).

275. M. Balkanski, P. Moch, and G. Parisot, "Infrared Lattice-Vibration Spectra in NiF_2, CoF_2, and FeF_2," *J. Chem Phys.* **44:**940–944 (1966).

276. R. M. Macfarlane and S. Ushioda, "Light Scattering from Phonons in CoF_2," *Solid State Commun.* **8:**1081–1083 (1970).

277. S. P. S. Porto, P. A. Fleury, and T. C. Damen, "Raman Spectra of TiO_2, MgF_2, ZnF_2, FeF_2, and MnF_2," *Phys. Rev.* **154:**522–526 (1967).

278. J. Giordano and C. Benoit, "Infrared Spectra of Iron, Zinc, and Magnesium Fluorides: I. Analysis of Results," *J. Phys. C* **21:**2749–2770 (1988). C. Benoit and J. Giordano, "Dynamical Properties of Crystals of MgF_2, ZnF_2, and FeF_2: II. Lattice Dynamics and Infrared Spectral," *J. Phys. C* **21:**5209–5227 (1988).

279. A. Kahan, J. W. Goodrum, R. S. Singh, and S. S. Mitra, "Polarized Reflectivity Spectra of Tegragonal GeO_2," *J. Appl. Phys.* **42:**4444–4446 (1971).

280. D. M. Roessler and W. A. Albers, "Infrared Reflectance of Single Crystal Tetragonal GeO_2," *J. Phys. Chem. Solids* **33:**293–296 (1972).

281. A. S. Barker, "Transverse and Longitudinal Optic Mode Study in MgF_2 and ZnF_2," *Phys. Rev.* **136:**A1290–A1295 (1964).

282. R. S. Krishnan and J. P. Russell, "The First-order Raman Spectrum of Magnesium Fluoride," *Brit. J. Appl. Phys.* **17:**501–503 (1966).

283. J. Giordano, "Temperature Dependence of IR Spectra of Zinc and Magnesium Fluoride," *J. Phys. C* **20:**1547–1562 (1987).

284. R. Summit, "Infrared Absorption in Single-crystal Stannic Oxide: Optical Lattice-vibration Modes," *J. Appl. Phys.* **39:**3762–3767 (1967).

285. J. F. Scott, "Raman Spectrum of SnO_2," *J. Chem. Phys.* **53:**852–853 (1970).

286. R. S. Katiyar, P. Dawson, M. M. Hargreave, and G. R. Wilkerson, "Dynamics of the Rutile Structure III. Lattice Dynamics, Infrared and Raman Spectra of SnO_2," *J. Phys. C* **4:**2421–2431 (1971).

287. R. S. Katiyar and R. S. Krishnan, "The Vibrational Spectrum of Rutile," *Phys. Lett.* **25A:**525–526 (1967).

288. A. S. Barker, "Infrared Lattice Vibrations in Calcium Tungstate and Calcium Molybdate," *Phys. Rev.* **135:**A742–A747 (1964).

289. P. Tarte and M. Liegeois-Duyckaerts, "Vibrational Studies of Molybdates, Tungstates and Related Compounds—I. New Infrared Data and Assignments for the Scheelite-type Compounds $X^{II}MoO_4$ and $X^{II}WO_4$," *Spectrochim. Acta* **28A:**2029–2036.

290. V. M. Nagiev, Sh. M. Efendiev, and V. M. Burlakov, "Vibrational Spectra of Crystals with Scheelite Structure and Solid Solutions on Their Basis," *Phys. Stat. Sol.* (*b*) **125:**467–475 (1984).

291. J. M. Stencel, E. Silberman, and J. Springer, "Temperature-dependent Reflectivity, Dispersion Parameters, and Optical Constants for $PbWO_4$," *Phys. Rev. B* **12:**5435–5441 (1976).

292. S. A. Miller, H. E. Rast, and H. H. Caspers, "Lattice Vibrations of $LiYF_4$," *J. Chem. Phys.* **53:**4172–4175 (1970).

293. E. Schultheiss, A. Scharmann, and D. Schwabe, "Lattice Vibrations in $BiLiF_4$ and $YLiF_4$," *Phys. Stat. Sol.* (*b*) **138:**465–475 (1986).

294. S. P. S. Porto and J. F. Scott, "Raman Spectra of $CaWO_4$, $SrWO_4$, $CaMoO_4$, and $SrMoO_4$," *Phys. Rev.* **157:**716–719 (1967).

295. S. Desgreniers, S. Jandl, and C. Carlone, "Temperature Dependence of the Raman Active Phonons in $CaWO_4$, $SrWO_4$, and $BaWO_4$," *J. Phys. Chem. Solids* **45:**1105–1109 (1984).

296. R. K. Khanna, W. S. Brower, B. R. Guscott, and E. R. Lippincott, "Laser Induced Raman Spectra of Some Tungstates and Molybdates," *J. Res. Nat. Bur. Std.* **72A:**81–84 (1968).

297. M. P. O'Horo, A. L. Frisillo, and W. B. White, "Lattice Vibrations of $MgAl_2O_4$ Spinel," *J. Phys. Chem. Solids* **34:**23–28 (1973).

298. M. E. Strifler and S. I. Boldish, "Transverse and Longitudinal Optic Mode Frequencies of Spinel $MgAl_2O_4$," *J. Phys. C* **11:**L237–L241 (1978).

299. K. Yamamoto, T. Murakawa, Y. Ohbayashi, H. Shimizu, and K. Abe, "Lattice Vibrations in $CdIn_2S_4$," *J. Phys. Soc. Japan* **35:**1258 (1973).

300. H. Shimizu, Y. Ohbayashi, K. Yamamoto, and K. Abe, "Lattice Vibrations in Spinel-type $CdIn_2S_4$," *J. Phys. Soc. Japan* **38:**750–754 (1975).

301. H. D. Lutz, B. Müller, and H. J. Steiner, "Lattice Vibration Spectra. LIX. Single Crystal Infrared and Raman Studies of Spinel Type Oxides," *J. Solid State Chem.* **90:**54–60 (1991).

302. H. D. Lutz, G. Wäschenbach, G. Kliche, and H. Haeuseler, "Lattice Vibrational Spectra, XXXIII: Far-Infrared Reflection Spectra, TO and LO Phonon Frequencies, Optical and Dielectric Constants, and Effective Changes of the Spinel-Type Compounds MCr_2S_4 (M = Mn, Fe, Co, Zn, Cd, Hg), MCr_2Se_4 (M = Zn, Cd, Hg), and $MInr_2S_4$ (M = Mn, Fe, Co, Zn, Cd, Hg)," *J. Solid State Chem.* **48:**196–208 (1983).

303. K. Wakamura, H. Iwatani, and K. Takarabe, "Vibrational Properties of One- and Two-Mode Behavior in Spinel Type Mixed Systems $Zn_{1-x}Cd_xCr_2S_4$," *J. Phys. Chem. Solids* **48:**857–861 (1987).

304. H. C. Gupta, G. Sood, A. Parashar, and B. B. Tripathi, "Long Wavelength Optical Lattice Vibrations in Mixed Chalcogenide Spinels $Zn_{1-x}Cd_xCr_2S_4$ and $CdCr_2(S_{1-x}Se_x)_4$," *J. Phys. Chem. Solids* **50:**925–929 (1989).

305. A. S. Barker and J. H. Hopfield, "Coupled-optical-phonon-mode Theory of the Infrared Dispersion in $BaTiO_3$, $SrTiO_3$, and $KTaO_3$," *Phys. Rev.* **135:**A1732–A1737 (1964).

306. A. S. Barker, "Temperature Dependence of the Transverse and Longitudinal Optic Mode Frequencies and Charges in $SrTiO_3$ and $BaTiO_3$," *Phys. Rev.* **145:**391–399 (1966).

307. J. L. Servoin, Y. Luspin, and F. Gervais, "Infrared Dispersion in $SrTiO_3$ at High Temperature," *Phys. Rev. B* **22:**5501–5506 (1980).

308. C. H. Perry and E. F. Young, "Infrared Studies of Some Perovskite Fluorides. I. Fundamental Lattice Vibrations," *J. Appl. Phys.* **38:**4616–4624 (1967).

309. A. Scalabrin, A. S. Chaves, D. S. Shim, and S. P. S. Porto, "Temperature Dependence of the A_1 and E Optical Phonons in $BaTiO_3$," *Phys. Stat. Sol.* (*b*) **79:**731–742 (1977).

310. J. L. Servoin, F. Gervais, A. M. Quittet, and Y. Luspin, "Infrared and Raman Responses in Ferroelectric Perovskite Crystals," *Phys. Rev. B* **21:**2038–2041 (1980).

311. G. Burns and B. A. Scott, "Lattice Modes in Ferroelectric Perovskites: PbTiO3," *Phys. Rev. B* **7:**3088–3101 (1973).

312. J. P. van der Ziel, A. E. Meixner, H. M. Kasper, and J. A. Ditzenberger, "Lattice Vibrations of $AgGaS_2$, $AgGaSe_2$, and $CuGaS_2$," *Phys. Rev. B* **9:**4286–4294 (1974).

313. W. H. Koschel and M. Bettini, "Zone-Centered Phonons in $A^IB^{III}S_2$ Chalcopyrites," *Phys. Stat. Sol.* (*b*) **72:**729–737 (1975).

314. L. Artus, J. Pascual, A. Goullet, and J. Camassel, "Polarized Infrared Spectra of $AgGaSe_2$," *Solid State Commun.* **69:**753–756 (1989).

315. G. D. Holah, A. Miller, W. D. Dunnett, and G. W. Isler, "Polarised Infrared Reflectivity of $CdGeAs_2$," *Solid State Commun.* **23:**75–78 (1977).

316. E. V. Antropova, A. V. Kopytov, and A. S. Poplavnoi, "Phonon Spectrum and IR Optical Properties of $CdGeAs_2$," *Opt. Spectrosc.* **64:**766–768 (1988).

317. A. Miller, G. D. Holah, and W. C. Clark, "Infrared Dielectric Dispersion of $ZnGeP_2$ and $CdGeP_2$," *J. Phys. Chem. Solids* **35:**685–693 (1974).

318. M. Bettini and A. Miller, "Optical Phonons and $ZnGeP_2$ and $CdGeP_2$," *Phys. Stat. Sol.* (*b*) **66:**579–586 (1974).

319. I. P. Kaminow, E. Buehler, and J. H. Wernick, "Vibrational Modes in $ZnSiP_2$," *Phys. Rev. B* **2:**960–966 (1970).

320. R. Zallen, M. L. Slade, and A. T. Ward, "Lattice Vibrations and Interlayer Interactions in Crystalline As_2S_3 and As_2Se_3," *Phys. Rev. B* **3:**4257–4273 (1971).

321. S. P. S. Porto, J. A. Giordmaine, and T. C. Damen, "Depolarization of Raman Scattering in Calcite," *Phys. Rev.* **147:**608–611 (1966).

322. K. H. Hellwege, W. Lesch, M. Plihal, and G. Schaack, "Two Phonon Absorption Spectra and Dispersion of Phonon Branches in Crystals of Calcite Structure," *Z. Physik* **232:**61–86 (1970). [Also see R. K. Vincent, "Emission Polarization Study on Quartz and Calcite," *Appl. Opt.* **11:**1942–1945 (1972).]

323. J. Q. Lu, G. X. Lan, B. Li, Y. Y. Yang, and H. F. Wang, "Raman Scattering Study of the Single Crystal β-BaB_2O_4 under High Pressure," *J. Phys. Chem. Solids* **49:**519–527 (1988).

324. W. Wojdowski, "Vibrational Modes in $Bi_{12}GeO_{20}$ and $Bi_{12}SiO_{20}$ Crystals," *Phys. Stat. Sol.* (*b*) **130:**121–130 (1985).

325. H. Vogt, T. Chattopadhyay, and H. J. Stolz, "Complete First-order Raman Spectra of the Pyrite Structure Compounds FeS_2, MnS_2, and SiP_2," *J. Phys. Chem. Solids* **44:**869–873 (1983).

326. H. D. Lutz, G. Schneider, and G. Kliche, "Far-infrared Reflection Spectra, TO- and LO-phonon Frequencies, Coupled and Decoupled Plasmon-phonon Modes, Dielectric Constants, and Effective Dynamical Charges of Manganese, Iron, and Platinum Group Pyrite Type Compounds," *J. Phys. Chem. Solids* **46:**437–443 (1985).

327. D. K. Agrawal and C. H. Perry, "The Temperature Dependent Raman Spectra of KDP, KD∗P, KDA, and ADP," in M. Balkanski (ed.), *Proceedings of the Second International Conference on Light Scattering in Solids,* Flammarion Sciences, Paris, 1971, pp. 429–435.

328. G. E. Kugel, F. Bréhat, B. Wyncke, M. D. Fontana, G. Marnier, C. Carabatos-Nedelec, and J. Mangin, "The Vibrational Spectrum of $KTiOPO_4$ Single Crystal Studied by Raman and Infrared Reflective Spectroscopy," *J. Phys. C* **21:**5565–5583 (1988).

329. R. P. Bauman and S. P. S. Porto, "Lattice Vibrations and Structure of Rare-earth Fluorides," *Phys. Rev.* **161:**842–847 (1967).

330. R. P. Lowndes, J. F. Parrish, and C. H. Perry, "Optical Phonons and Symmetry of Tysonite Lanthanide Fluorides," *Phys. Rev.* **182:**913–922 (1969).

331. E. Liarokapis, E. Anastassakis, and G. A. Kourouklis, "Raman Study of Phonon Anharmonicity in LaF_3," *Phys. Rev. B* **32:**8346–8355 (1985).

332. W. Otaguro, E. Weiner-Avnera, C. A. Arguello, and S. P. S. Porto, "Phonons, Polaritrons, and Oblique Phonons in $LiIO_3$ by Raman Scattering and Infrared Reflection," *Phys. Rev. B* **4:**4542–4551 (1971).

333. J. L. Duarte, J. A. Sanjurjo, and R. S. Katiyar, "Off-normal Infrared Reflectivity in Uniaxial Crystals: α-$LiIO_3$ and α-quartz," *Phys. Rev. B* **36:**3368–3372 (1987).

334. R. Claus, G. Borstel, E. Wiesendanger, and L. Steffan, "Directional Dispersion and Assignment of Optical Phonons in $LiNbO_3$," *Z. Naturforsch.* **27a:**1187–1192 (1972).

335. X. Yang, G. Lan, B. Li, and H. Wang, "Raman Spectra and Directional Dispersion in $LiNbO_3$ and $LiTaO_3$," *Phys. Stat. Sol.* (*b*) **141:**287–300 (1987).

336. D. G. Bozinis and J. P. Hurrell, "Optical Modes and Dielectric Properties of Ferroelectric Orthorhombic $KNbO_3$," *Phys. Rev. B* **13:**3109–3120 (1976).

337. A. S. Pine and G. Dresselhaus, "Raman Scattering in Paratellurite," *Phys. Rev. B* **5:**4087–4093 (1972).

338. D. M. Korn, A. S. Pine, G. Dresselhaus, and T. B. Reed, "Infrared Reflectivity of Paratellurite, TeO_2," *Phys. Rev. B* **8:**768–772 (1973).

339. W. J. Tropf and M. E. Thomas, ''Yttrium Oxide (Y_2O_3),'' in E. D. Palik (ed.), *Handbook of Optical Constants of Solids II,* Academic Press, Orlando, 1991, pp. 1081–1098.

340. M. Thirumavalavan, J. Kumar, F. D. Gnanam, and P. Ramasamy, ''Vibrational Spectra of $Y_3Al_5O_{12}$ Crystals Grown from Ba- and Pb-based Flux Systems,'' *Infrared Phys.* **26:**101–103 (1986).

341. G. A. Gledhill, P. M. Nikolić, A. Hamilton, S. Stojilković, V. Blagojević. P. Mihajlovic, and S. Djurić, ''FIR Optical Properties of Single Crystal $Y_3Al_5O_{12}$ (YAG),'' *Phys. Stat. Sol.* (*b*) **163:**K123–K128 (1991).

342. R. P. Lowndes, ''Anharmonicity in the Silver and Thallium Halides: Far-Infrared Dielectric Response,'' *Phys. Rev. B* **6:**1490–1498 (1972).

343. G. Lucovsky, ''Optic Modes in Amorphous As_2S_3 and As_2Se_3,'' *Phys. Rev. B* **6:**1480–1489 (1972).

344. W. G. Spitzer, R. C. Miller, D. A. Kleinman, and L. E. Howarth, ''Far Infrared Dielectric Dispersion in $BaTiO_3$, $SrTiO_3$, and TiO_2,'' *Phys. Rev.* **126:** 1710–1721 (1962).

345. E. J. Danielewicz and P. D. Coleman, ''Far Infrared Optical Properties of Selenium and Cadmium Telluride,'' *Appl. Opt.* **13:**1164–1170 (1974).

346. J. L. Verble and R. F. Wallis, ''Infrared Studies of the Lattice Vibrations in Iron Pyrite,'' *Phys. Rev.* **182:**783–789 (1969).

347. H. D. Lutz, G. Kliche, and H. Haeuseler, ''Lattice Vibrational Spectra XXIV: Far-infrared Reflection Spectra, Optical and Dielectric Constants, and Effective Charges of Pyrite Type Compounds FeS_2, MnS_2, $MnSe_2$, and $MnTe_2$,'' *Z. Naturforsch.* **86a:**184–190 (1981).

348. C. J. Johnson, G. H. Sherman, and R. Weil, ''Far Infrared Measurement of the Dielectric Properties of GaAs and CdTe at 300 K and 8 K,'' *Appl. Opt.* **8:**1667–1671 (1969).

349 D. A. Kleinman and W. G. Spitzer, ''Infrared Lattice Absorption of GaP,'' *Phys. Rev.* **118:**110–117 (1960).

350. A. Hadni, J. Claudel, D. Chanal, P. Strimer, and P. Vergnat, ''Optical Constants of Potassium Bromide in the Far Infrared,'' *Phys. Rev.* **163:**836–843 (1967).

351. A. Hadni, J. Claudel, G. Morlot, and P. Strimer, ''Transmission and Reflection Spectra of Pure and Doped Potassium Iodide at Low Temperature,'' *Appl. Opt.* **7:**161–165 (1968) [in French].

352. J. Zarembowitch, J. Gouteron, and A. M. Lejus, ''Raman Spectra of Lanthanide Sesquioxide Single Crystals with A-type Structure,'' *Phys. Stat. Sol.* (*b*) **94:**249–256 (1979).

353. A. S. Barker and R. Loudon, ''Dielectric Properties and Optical Phonons in $LiNbO_3$,'' *Phys. Rev.* **158:**433–445 (1967).

354. I. F. Chang and S. S. Mitra, ''Temperature Dependence of Long-Wavelength Optic Phonons of NaF Single Crystals,'' *Phys. Rev. B* **5:**4094–4100 (1972).

355. H. Burkhard, R. Geick, P. Kästner, and K.-H. Unkelbach, ''Lattice Vibrations and Free Carrier Dispersion in PbSe,'' *Phys. Stat. Sol.* (*b*) **63:**89–96 (1974).

356. W. G. Spitzer and D. A. Kleinman, ''Infrared Lattice Bands of Quartz,'' *Phys. Rev.* **121:**1324–1335 (1961).

357. B. Orel and V. Moissenko, ''A Vibrational Study of Piezoelectric TeO_2 Crystals,'' *Phys. Stat. Sol.* (*b*) **165:**K37–K41 (1991).

358. A. M. Hofmeister and K. R. Campbell, ''Infrared Spectroscopy of Yttrium Aluminum, Yttrium Gallium, and Yttrium Iron Garnets,'' *J. Appl. Phys.* **72:**638–646 (1992).

359. H. v. Campe, ''Fundamental Absorption of $AgGaS_2$ Single Crystals and Thin Polycrystalline Films,'' *J. Phys. Chem. Solids* **44:**1019–1023 (1983).

360. M. E. Thomas, W. J. Tropf, and S. L. Gilbert, ''Vacuum-Ultraviolet Characterization of Sapphire, ALON, and Spinel Near the Band Gap,'' to be published in *Opt. Eng.* **32:**1340–1343 (1993).

361. T. Tomiki and T. Miyata, ''Optical Studies of Alkali Fluorides and Alkaline Earth Fluorides in VUV Region,'' *J. Phys. Soc. Japan* **27:**658–678 (1969).

362. T. Toyada, H. Nakanishi, S. Endo, and T. Irie, "The Fitting Parameters of Exponential Optical Absorption $Bi_{12}SiO_{20}$," *J. Phys. C* **19:**L259–L263 (1986).

363. D. Dutton, "Fundamental Absorption Edge in Cadmium Sulfide," *Phys. Rev.* **112:**785–792 (1958).

364. R. Nitecki and J. A. Gaj, "On the Urbach Rule in CdSe," *Phys. Stat. Sol* (*b*) **62:**K17–K19 (1974).

365. R. T. Williams and S. E. Schnatterly, "Magnetic Circular Dichroism of the Urbach Edge in KI, CdTe, and TlCl," in S. S. Mitra and B. Bendow (eds.), *Optical Properties of Transparent Solids,* Plenum, New York, 1975, pp. 145–160.

366. Y. Takubo and T. Koda, "The Urbach Tail of Cuprous Halides," *J. Phys. Soc. Japan* **39:**715–719 (1975).

367. W. J. Turner, W. E. Reese, and G. D. Pettit, "Exciton Absorption and Emission in InP," *Phys. Rev.* **136A:**1467–1470 (1964).

368. T. Tomiki, T. Mayata, and H. Tsukamoto, "The Urbach Rule for the Sodium- and Potassium-Halides," *Z. Naturforsch.* **29A:**145–157 (1974).

369. D. Redfield and W. J. Burke, "Optical Absorption Edge of $LiNbO_3$," *J. Appl. Phys.* **45:**4566–4571 (1974).

370. M. I. Cohen and R. F. Blunt, "Optical Properties of $SrTiO_3$ in the Region of the Absorption Edge," *Phys. Rev.* **168:**929–933 (1968).

371. T. Takizawa, "Optical Absorption and Reflection Spectra of Paratellurite, TeO_2," *J. Phys. Soc. Japan* **48:**505–510 (1980).

372. S. Tutihasi, "Ultraviolet Absorption in Thallous Halides," *J. Phys. Chem. Solids* **12:**344–348 (1960).

373. T. Tomiki, F. Fukudome, M. Kaminao, M. Fujisawa, Y. Tanahara, and T. Futemma, "Optical Spectra of $Y_3Al_5O_{12}$ (YAG) Single Crystals in the Vacuum Ultraviolet," *J. Phys. Soc. Japan* **58:**1801–1810 (1989).

374. T. Tomiki, M. Kaminao, Y. Tanahara, T. Futemma, M. Fujisawa, and F. Fukudome, "Anisotropic Optical Spectra of $YAlO_3$ (YAP) Single Crystals in the Vacuum Ultraviolet Region," *J. Phys. Soc. Japan* **60:**1799–1813 (1991).

375. T. Tomiki, J. Tamashiro, Y. Tanahara, A. Yamada, H. Fututani, T. Miyahara, H. Kato, S. Shin, and M. Ishigame, "Optical Spectra of Y_2O_3 Single Crystals in VUV," *J. Phys. Soc. Japan* **55:**4543–4549 (1986).

376. M. V. Kurik, "Urbach Rule," *Phys. Stat. Sol.* (*a*) **8:**9–45 (1971).

377. M. E. Thomas, "Infrared Properties of the Extraordinary Ray Multiphonon Processes in Sapphire," *Appl. Opt.* **28:**3277–3278 (1989).

378. E. D. Palik, "Cadmium Telluride (CdTe)," in E. D. Palik (ed.), *Handbook of Optical Constants of Solids,* Academic Press, Orlando, 1985, pp. 409–427.

379. J. E. Eldridge, "Cesium Iodide (CsI)," in E. D. Palik (ed.), *Handbook of Optical Constants of Solids II,* Academic Press, Orlando, 1991, pp. 853–874.

380. E. D. Palik, "Gallium Arsenide (GaAs)," in E. D. Palik (ed.), *Handbook of Optical Constants of Solids,* Academic Press, Orlando, 1985, pp. 429–443.

381. L. L. Boyer, J. A. Harrington, M. Hass, and H. B. Rosenstock, "Multiphonon Absorption in Ionic Crystals," *Phys. Rev. B* **11:**1665–1680 (1975).

382. J. I. Berg and E. E. Bell, "Far-infrared Optical Constants of KI," *Phys. Rev.* **B4:**3572–3580 (1971).

383. D. M. Roessler and D. R. Huffman, "Magnesium Oxide (MgO)," in E. D. Palik (ed.), *Handbook of Optical Constants of Solids II,* Academic Press, Orlando, 1991, pp. 919–955.

384. T. Hidaka, T. Morikawa, and J. Shimada, "Spectroscopic Small Loss Measurements on Infrared Transparent Materials," *Appl. Opt.* **19:**3763–3766 (1980).

385. E. D. Palik and A. Addamiano, "Zinc Sulfide (ZnS)," in E. D. Palik (ed.), *Handbook of Optical Constants of Solids,* Academic Press, Orlando, 1985, pp. 597–619.

386. P. A. Miles, ''Temperature Dependence of Multiphonon Absorption in Zinc Selenide,'' *Appl. Opt.* **16:**2891–2986 (1977).

387. J. A. Cox, D. Greenlaw, G. Terry, K. McHenry, and L. Fielder, ''Comparative Study of Advanced IR Transmissive Materials,'' *Proc. SPIE* **683:**49–62 (1988).

388. B. Bendow, R. N. Brown, M. G. Drexhage, T. J. Loretz, and R. L. Kirk, ''Material Dispersion of Fluorozirconate-type Glasses,'' *Appl. Opt.* **20:**3688–3690 (1981).

389. D. J. Treacy, ''Arsenic Sulfide (As_2S_3),'' in E. D. Palik (ed.), *Handbook of Optical Constants of Solids,* Academic Press, Orlando, 1985, pp. 641–663.

390. D. J. Treacy, ''Arsenic Selenide (As_2Se_3),'' in E. D. Palik (ed.), *Handbook of Optical Constants of Solids,* Acadmic Press, Orlando, 1985, pp. 623–639.

391. A. R. Hilton, D. J. Hayes, and M. D. Rechtin, ''Infrared Absorption of Some High-purity Chalcogenide Glasses,'' *J. Non-Cryst. Solids* **17:**319–338 (1975).